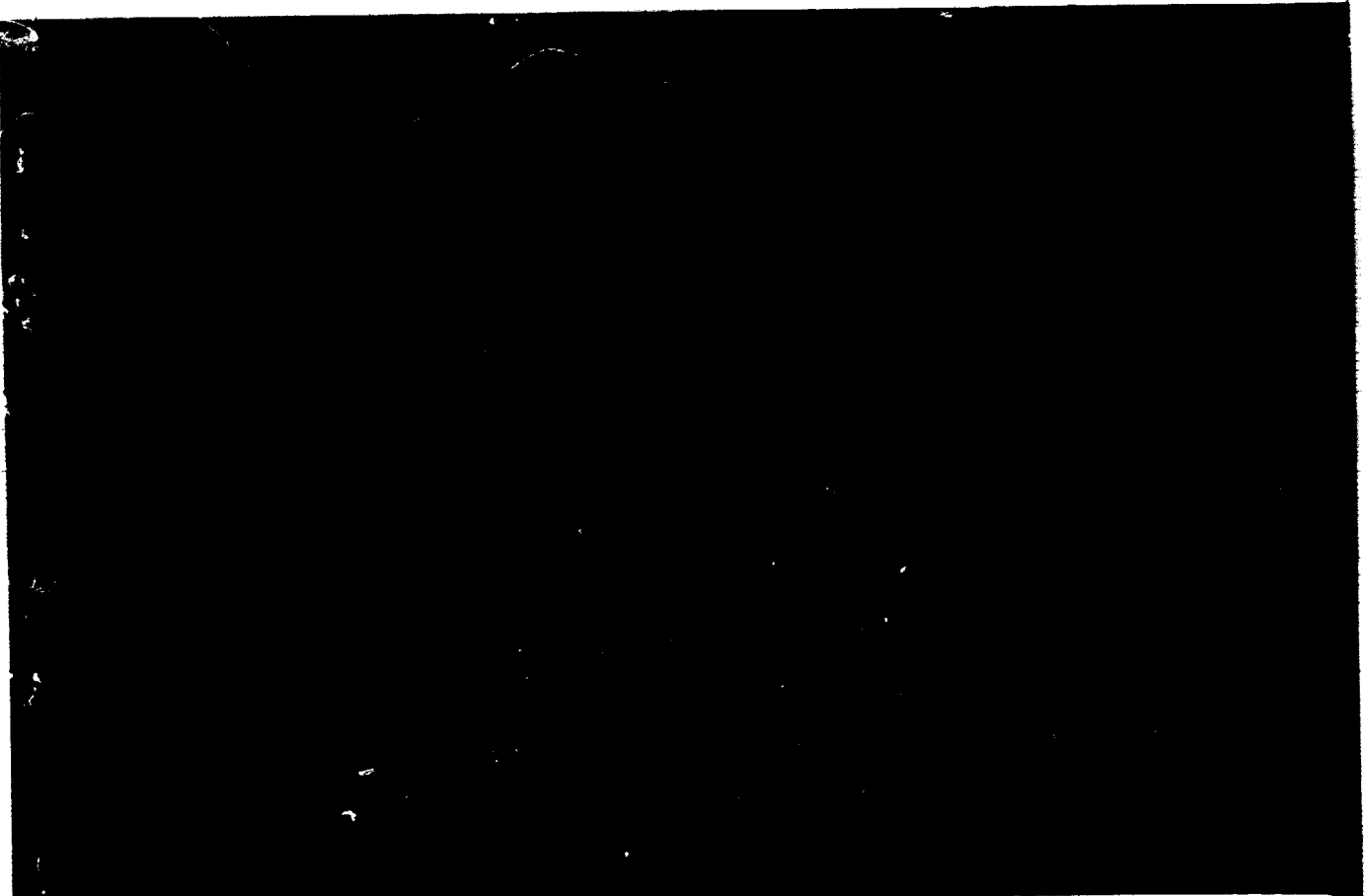


NASA CR-174975
Report No. MDC J3789

CALCULATION OF COMPRESSIBLE FLOW ABOUT THREE-DIMENSIONAL INLETS WITH AUXILIARY INLETS, SLATS AND VANES BY MEANS OF A PANEL METHOD

by

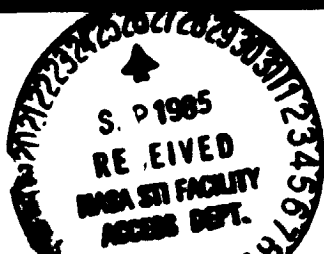
J. L. Hess, D. M. Friedman and R. W. Clark
Douglas Aircraft Company, Long Beach, California



(NASA-CR-174975) CALCULATION OF COMPRESSIBLE FLOW ABOUT THREE-DIMENSIONAL INLETS WITH AUXILIARY INLETS, SLATS AND VANES BY MEANS OF A PANEL METHOD Final Contractor Report, 17 Feb. (Douglas Aircraft 63/02 **885-35162**
Unclass 22236

June 1985

This work was completed under NASA Contract NAS3-22250 for



NASA
National Aeronautics and Space Administration
Lewis Research Center
Cleveland, Ohio 44135

Copy number

Report number

MDC J3789

CALCULATION OF COMPRESSIBLE FLOW ABOUT THREE-DIMENSIONAL
INLETS WITH AUXILIARY INLETS, SLATS AND VANES
BY MEANS OF A PANEL METHOD

Revision date

Revision letter

Issue date

June 1985

Contract number

NAS3-22250

Prepared by: J. L. Hess, D. M. Friedman and R. W. Ciark

Approved by:

Tuncer Cebeci

T. Cebeci
Staff Director
Research & Technology
Aircraft Configuration & Performance

DOUGLAS AIRCRAFT COMPANY

MCDONNELL DOUGLAS



CORPORATION

ABSTRACT

An efficient and user-oriented method has been constructed for calculating flow in and about complex inlet configurations. Efficiency is attained by: the use of a panel method, a technique of superposition for obtaining solutions at any inlet operating condition, and employment of an advanced matrix-iteration technique for solving large full systems of equations, including the nonlinear equations for the Kutta condition. User concerns are addressed by the provision of several novel graphical output options that, taken together, yield a more complete comprehension of the flowfield than had been possible previously. Examples of these features are presented for some complicated configurations.

TABLE OF CONTENTS

	<u>Page</u>
1.0 Introduction	1
2.0 The Higher-Order Panel Method	3
2.1 General Description	3
2.2 Consistency Analysis	5
2.3 Development of the Panels from Input Points	6
2.4 Velocities Induced by the Source Distribution on the Panels	8
2.5 The Source Derivative Terms. Assembly of the Matrix of Influence Coefficients	9
2.5.1 The Numerical Differentiation Procedure. Geometric Constants	9
2.5.2 Logic of the Assembly Procedure	11
2.6 Vorticity Influences of a Panel	13
2.6.1 Panel Vorticity and the Underlying Dipole Distribution	13
2.6.2 Edge Vortices	17
2.6.3 The Trailing Vortex Wake	17
2.6.4 Two Special Situations	20
2.6.5 Assembly of the Vorticity Onset Flows	22
2.7 The Kutta Condition	25
2.8 The Iterative Matrix Solution	26
2.8.1 Block Gauss-Siedel Iterative Scheme	28
2.8.2 Convergence Acceleration Scheme	30
3.0 The Inlet Procedure	34
3.1 General Description	35
3.2 The Fundamental Flow Solutions	35
3.3 The Combination Program	37
4.0 Calculated Results	39
5.0 Input Instructions for the Higher-Order Potential-Flow Program (DF12)	42
6.0 References	56

Appendices

A	Consistent Expansion for the Potential Induced by a Curved Source Panel at a Point in Space	A-1
B	Generation of Panel Geometric Quantities by Means of Bi-Cubic Splines	B-1
C	Area Moments of a Panel	C-1
D	Near-Field Source Formulas	D-1

E	Intermediate-Field Source Formulas	E-1
F	Far-Field Source Formulas	F-1
G	Some Special Near-Field Formulas	G-1
H	Calculation of Vorticity Induced Velocities in Terms of Source Induced Velocities	H-1
I	Near-Field Formulas for the Effect of a Line-Vortex Along a Streamwise Edge of a Panel	I-1
J	Far-Field Line-Vortex Formulas	J-1
K	Parabolic Chordwise Vorticity	K-1
L	B Derivatives at Section Edges	L-1
M	Iterative Matrix Solution	M-1
N	The Compressibility Correction	N-1
O	Options of the Combination Program	O-1
P	Organization of the Input Data	P-1

PRINCIPAL NOTATION

- A Matrix of induced normal velocities at the control points. Also flat panel area.
- b Subscripts 32, 41. Intercept on η axis of panel side.
- B Dipole derivative along an N-line. Subscripts F and S denote values on first and second N-lines of a panel, respectively. Subscript K denotes value associated with K-th lifting strip (Fig. 1).
- c Geometric constant for a panel designed to minimize dipole discontinuity along a lifting strip.
- $c_K^{(x)}, c_K^{(y)}$ Geometric constants expressing source derivative on a panel in terms of values of source density on surrounding panels.
- d Length of a side of a panel; used with subscripts to denote a particular side.
- h Geometric constant denoting arc length along an N-line from trailing edge to η -axis of a panel. Subscripts F and S denote first and second N-lines, respectively.
- i, j Integer subscripts denoting panel number.
- $\hat{i}, \hat{j}, \hat{k}$ Unit vectors along axis of Cartesian coordinate system. Subscript e denotes panel coordinate system.
- L Number of lifting strips.
- L(total) Total arc length of an N-line from trailing edge to leading edge and back again.
- m Subscripts 32, 41. Slope of a panel side.
- n_ξ, n_η, n_ζ Components of \vec{n} in panel coordinates.
- \vec{n} Unit normal vector to a panel.
- N Number of panels.
- N-line Curve along which input points are distributed. On lifting portions it defines a wing section (Fig. 1).
- P, Q, R Derivatives of panel shape at origin of panel coordinates
- r Magnitude of \vec{r}
- \vec{r} Vector between the two points in space.
- S Surface area of curved panel. Used with subscripts 32, 41 denotes cosine of slope angle of a panel side.

- t Maximum dimension of a panel.
- u, v Nonorthogonal coordinates used in parametric cubic surface representation.
- V Velocity. Used with various subscripts and superscripts.
- V_{ij} Velocity at i -th control point due to unit source density on j -th panel.
- V_i Final combined velocity at i -th control point.
- $\vec{V}_i^{(k)}$ Velocity at i -th control point due to unit dipole derivative on k -th lifting strip.
- w Width of a panel or lifting strip.
- x, y, z Cartesian coordinates.
- ξ, η, ζ Coordinates of a point of a panel in its own coordinate system.
- μ Underlying dipole distribution on a panel that defines the panel vorticity distribution. Subscripts x and y denote derivatives at the origin of panel coordinates.
- σ Source density on a panel. Subscripts x and y denote derivatives at the origin of panel coordinates. Integer subscripts denote value at origin of some particular panel.
- $\vec{\omega}$ Vector vorticity strength on a panel.

1.0 INTRODUCTION

The present work consists of the construction of a computer program for analyzing flow in and about very complicated three-dimensional inlet configurations. The basic calculational technique is a panel method, whose choice is dictated by considerations of numerical efficiency and geometric generality. Such a method can calculate flow about virtually any passive configuration in a routine fashion. An inlet, however, is active in the sense that it contains complicated internal machinery that controls the amount of fluid that enters. For the present purpose, it is not necessary or even desirable to analyze this machinery in detail. Instead, its effect is lumped into a single parameter, namely the mass flow through the inlet. This situation is seen most clearly in the static case where the inlet is at rest in an otherwise undisturbed fluid. Here the only fluid motion is that due to ingestion of fluid by the inlet. The difference between a method applicable to inlets and a method for passive bodies is that the former must contain a calculational device for controlling mass flow through the inlet. As will be seen, this requirement is equivalent to a calculational device for generating a static solution.

Reference 1 describes a method for calculating flow about simple three-dimensional inlets by means of a first-order panel method. Reference 2 presents a procedure applicable to inlets having auxiliary inlets which uses a higher-order panel method. The present program generalizes this last to the case of inlets having leading-edge slats. Thus this method must account for lifting effects, while that of Ref. 2 did not. This represents a considerable difference. Not only must the code contain formulas giving the effects of bound and trailing vorticity, but the iterative matrix solution must be altered radically to include the nonlinear Kutta condition. Moreover, the user must now bear the responsibility of specifying the location of the trailing vortex wake. As far as the code is concerned, the designation "leading-edge slat" may be interpreted very generally as a lifting portion of the configuration. Thus the program can consider an inlet mounted on a lifting wing-pylon configuration.

It should be pointed out that the rather elaborate scheme outlined here is made necessary by the requirement to simultaneously analyze flow outside and inside

the inlet. If only the exterior flow were of interest, the inlet entrance could be represented by panels on which an inflow velocity distribution is specified.

This inlet program is thus the latest in a series of panel-method programs, each of which depends on the previous ones. Two previous inlet programs, Refs. 1 and 2, have already been mentioned. The present code is based on the higher-order lifting panel method of Ref. 3, which in turn is based on the higher-order nonlifting panel method of Ref. 4, and both are extensions of the first-order lifting panel method of Ref. 5. Recent documents, notably Refs. 2 and 3, refer liberally to the earlier documents. Thus no one document contains all the necessary formulas and logic of the ensemble of programs that were developed up to this time. It was decided to remedy this situation by making the present report complete. All the panel-method formulas and inlet procedures that pertain to the present code are contained herein. The resulting reference manual is somewhat lengthy, but it is complete.

2.0 THE HIGHER-ORDER PANEL METHOD

2.1 General Description

The panel method here is a higher-order source method. In a source method the unknown value of source density on each panel is adjusted to satisfy the normal-velocity boundary condition at the panel control points, while dipole and/or vorticity is treated as an auxiliary singularity that is used to produce the lifting effects. In contrast to a first-order panel method (Ref. 5), which uses a constant source density on flat panels, the higher-order method (Ref. 3) accounts for source-derivative and surface-curvature effects. As examples will show, inclusion of these effects can be quite important for internal flows. The panel method of Ref. 3 is the only current method that accounts for local surface curvature despite analysis that indicates that a method is not truly higher order if these effects are ignored (see Section 2.2 below).

A three-dimensional lifting flow is characterized by the presence of a trailing vortex sheet that issues from the trailing edge of the lifting portion of the configuration, e.g. a wing or slat (see Figure 1). If more than one lifting device is present, such a sheet issues from every trailing edge. The location of the trailing vortex sheet is not known a priori. In the present panel method the location is simply input by the user based on his experience and physical intuition. In the case of a wing-fuselage, this issue is unimportant because the wake is relatively far from all parts of the wing and is weak near the body. In the inlet case, however, the wake of the slat is ingested and probably lies close to the inner surface of the inlet. The wake location could be important, and its estimation might be somewhat difficult, particularly at angle of attack.

A key issue in any lifting procedure is the method of applying the Kutta condition. Oddly most panel-method publications virtually ignore this question, presumably because the authors consider it unimportant. In fact, the Kutta condition is of first importance, because it determines the circulation distribution that drives the whole lifting flow. Classically, the Kutta condition is stated as the avoidance of an infinite velocity at the trailing edge. Clearly such a condition cannot be enforced numerically, and some other

criterion, which is a consequence of the Kutta condition, must be invoked. Physically, it is absolutely necessary that upper- and lower-surface pressures on the wing must approach a common value at the trailing edge. This is the form of the Kutta condition employed in the present panel method. Oddly no other panel method uses the equal-pressure Kutta condition. Instead, other derivative conditions are used. The reason for this is probably that the equal-pressure condition is nonlinear, while the alternate conditions are linear, which simplifies the numerical procedure. The price of linearity is high, however, because calculated results can be seriously in error. Figure 2 shows calculated results from Ref. 6. It can be seen that only the present panel method gives equal upper- and lower-surface trailing-edge pressures for this case. The other methods give a pressure mismatch of up to half of free-stream dynamic pressure.

Another important feature of the present panel method is its use of an iterative matrix solution. An inlet having a centerbody, an auxiliary inlet, and one or more slats is a very complicated configuration, which if mounted on a wing-pylon becomes much more complicated. Thus the cases to which the present method will be applied tend to have large panel numbers. For such cases an iterative solution of the linear equations that express the boundary condition is an order of magnitude faster computationally than a direct elimination solution. As is well known, the computational effort for an iterative solution is proportional to the square of the number of equations, i.e. to the panel number, while that of the direct solution is proportional to the cube. Thus the advantage of the former becomes greater as the panel number increases and as the computation time becomes a more important factor. For the iterative solution to realize this advantage, it must converge reliably in a relatively small number of iterations, say 10-20. As reported in Ref. 2, an accelerated block Gauss-Siedel achieved this efficiency in the nonlifting panel method. The addition of lift produces a major complication in that the values of bound vorticity must be included among the unknowns and the set of equations must contain those expressing the Kutta conditions at various span locations along the trailing edges. As mentioned above, these last are nonlinear. The standard "Newton-type" method for solving sets of nonlinear equations consists of successive linearizations followed by iteration. That is, in each iteration a set of linear equations is solved, but the coefficient matrix changes with

each iteration. This alternative type of iteration was incorporated into the basic block Gauss-Siedel scheme, and after a restructuring of the acceleration procedure, a reliable method was obtained. The number of iterations required for convergence is increased 30% compared to the nonlifting case.

2.2 Consistency Analysis

One of the distinguishing features of panel methods is that the velocity due to a panel singularity is computed analytically, as contrasted with other so-called "boundary-element" methods where numerical quadratures are employed. This feature is rendered necessary by the requirement faced by a practical panel method that panel dimensions are often larger than characteristic physical dimensions of the boundary. For example, in the midchord mid-semi-span region of a wing the spanwise dimension of panels is normally an order of magnitude larger than the local wing thickness (Fig. 1). The integrals over a panel giving the potentials and/or velocities due to various singularity distributions can be integrated analytically only if the panel is flat. Other panel methods have assumed flat panels from the beginning and then hypothesized singularity distributions that are two-variable polynomials of various degrees, usually ranging from constant to quadratic. Investigators who use the polynomials of higher degree tend to label their methods "higher-order" and thus to imply that the increase of accuracy with panel number of such a method is more rapid than that of a "lower order" method. Such an assertion has been proven false by direct comparisons of calculated results (Refs. 6 and 7). The reason is simply that successive refinement of an integrand (the singularity distribution) without simultaneous refinement of the integration region (the panel geometry) cannot lead to improved results, because the factors neglected are more important than the additional factors included.

An alternative approach is to expand the effect of a general panel about its tangent panel. All relevant quantities can be expanded in Taylor's series about the tangency point and the integral expressed as a sequence of terms each of "higher order" in panel dimension than the preceding terms. Since all integrals are over the flat tangent panel, they all can be evaluated analytically. But the expanded terms contain derivatives of both the singularity strength and the body shape. The analysis is done in detail in Appendix A for

the case of source singularity. It is shown there that a term of a given order contains derivatives of the surface shape that are one degree higher than the highest singularity derivative. Thus consistent combinations are: flat-panel/constant source, paraboloidal panel/linear source, cubic panel/quadratic source, etc. The same is true for vorticity, which reflects the fact that vorticity effects can be expressed in terms of source effects (see Appendix H). Dipole effects have a more complicated expansion due to the fact that a dipole distribution on a panel is equivalent to a vorticity distribution equal to its gradient (and thus a polynomial one degree lower) plus a concentrated vortex filament around the edges of the panel. The present approach uses panel vorticity and adds the appropriate edge vortices.

2.3 Development of the Panels from Input Points

As in all panel methods, the body surface and wake are input to the computer by specifying the coordinates of a number of points on the surface. These are associated in groups of four to form the quadrilateral surface panels (Fig. 1). This may be done in a variety of ways. In the present program the end result is a trapezoidal tangent panel (Fig. 3) and various geometric quantities (about 60) associated with it. This is a much smaller number of geometric quantities than many other panel methods require. The order of the input points is along certain curves called N-lines (Fig. 1). On lifting portions of the body the first and last points on the N-line are at the trailing edge. The set of panels formed from the points lying on two consecutive N-lines on a lifting portion is denoted a lifting strip of panels.

The initial step in generating the panel consists of using a "canned" routine for fitting surfaces by parametric bicubic splines. This is applied to each panel individually to generate the panel coordinate system, the coordinates of the four corners of the panel in this system, and the three second derivatives of the surface at the origin of panel coordinates. The panel coordinate origin is the point of tangency to the surface of the tangent panel and is also the control point where the normal-velocity boundary condition is applied. The procedure for doing this is described in Appendix B.

As shown in Fig. 3, the corner point coordinates are $\xi_K, \eta_K, K = 1, 2, 3, 4$.
The lengths of the parallel sides are:

$$d_{12} = d_F = \xi_2 - \xi_1, \quad d_{43} = d_S = \xi_3 - \xi_4 \quad (2.3.1)$$

The width of the panel is

$$w = \eta_1 - \eta_3 \quad (2.3.2)$$

The slanting sides are straight lines with equations of the form

$$\xi = m\eta + b \quad (2.3.3)$$

where

$$\begin{aligned} m_{32} &= \frac{\xi_2 - \xi_3}{w}, & m_{41} &= \frac{\xi_1 - \xi_4}{w} \\ b_{32} &= \frac{\xi_3\eta_2 - \xi_2\eta_3}{w}, & b_{41} &= \frac{\xi_4\eta_1 - \xi_1\eta_4}{w} \end{aligned} \quad (2.3.4)$$

The maximum diagonal of the panel is

$$t = \max \left\{ \begin{aligned} &\sqrt{(\xi_2 - \xi_4)^2 + (\eta_2 - \eta_4)^2} \\ &\sqrt{(\xi_3 - \xi_1)^2 + (\eta_3 - \eta_1)^2} \end{aligned} \right. \quad (2.3.5)$$

Further define

$$s_{32} = \sqrt{1 + m_{32}^2}, \quad s_{41} = \sqrt{1 + m_{41}^2} \quad (2.3.6)$$

The lengths of the slanting sides are

$$d_{32} = w s_{32}, \quad d_{41} = w s_{41} \quad (2.3.7)$$

Also needed for lifting panels are the total arc lengths along the N-lines from the trailing edge up to the η -axis of the panel in question. These are

$$h_F = \sum d_F - \epsilon_1, \quad h_S = \sum d_S - \epsilon_4 \quad (2.3.8)$$

where the sums are over the previous panels of the lifting strip.

Finally the normalized moments of the area of the panel are required. The method of calculating these is in Appendix C.

2.4 Velocities Induced by the Source Distribution on the Panels

Formulas for the velocity induced by an individual panel at a point in space are obtained from the expressions developed in Appendix A by differentiating and then performing the indicated integrations over the flat projected panel. Different procedures are called for depending on the distance of the point in question from the panel. For nearby points, the expressions of Appendix A are integrated exactly. This procedure is rather lengthy and details are omitted. Only the final formulas for this "near field" are presented (Appendix D) and these are the key to the present panel method. It is assumed that the point in question has been transformed into the panel coordinate system and all near-field formulas are given in terms of this coordinate system. For points further from the panel, the integrals of Appendix A are evaluated by a classic multipole expansion. The orders of the expansions are selected to be at least as high as the terms in question. This is a relatively simple procedure analytically, and the resulting "intermediate field" formulas require much less computing time than the near-field formulas (Appendix E). This computation also is carried out in panel coordinates. The velocities calculated by the near-field and intermediate-field formulas must be transformed into the reference coordinate system. For points even further away, a "far-field" approximation is used (Appendix F). This is obtained simply by retaining only the first terms in the multipole expansions. However, the far-field formulas have been put in vector form, and thus they can be evaluated directly in the so-called reference coordinate system in which the body is input. This eliminates the need for transformations and further reduces computing time. Some of the quantities in the near-field formulas lose numerical significance for certain ranges of values of the parameters, e.g. control point near the extension of a side or effect of a very long thin panel on adjacent control points. Most of these problems are due to the short word length used by IBM computers

and do not arise for CDC equipment. A variety of special formulas based on power series expansions have been developed for use in the troublesome situations. These are collected in Appendix G.

The source potential is given in Eqs. (A.31) through (A.35) of Appendix A. The velocity induced by the panel is obtained by taking the negative gradient to obtain

$$\vec{v} = \vec{v}^{(0)}\sigma_0 + [P\vec{v}^{(P)} + 2Q\vec{v}^{(Q)} + R\vec{v}^{(R)} + \vec{v}^{(1x)}\sigma_x + \vec{v}^{(1y)}\sigma_y] \quad (2.4.1)$$

where each individual velocity is the negative gradient of the corresponding potential.

2.5 The Source Derivative Terms. Assembly of the Matrix of Influence Coefficients

2.5.1 The Numerical Differential Procedure. Geometric Constants

As stated in Section 2.4, the basic source velocity formula (2.4.1) contains coefficients σ_x and σ_y , which are the derivatives of the source density with respect to the panel's coordinate directions. It is not intended that these be additional unknowns. Instead, they are expressed in terms of the unknown values of source density at the control points of the surrounding panels. Thus, ultimately the values of source density at the control points of the panels are the only unknowns. The source-derivative procedure is slightly different for the first and last panels of a strip and for panels of the first and last strips. However, the modifications are quite straightforward. In the initial discussion it is assumed that the panel on which source derivatives are being evaluated (the panel in question) has adjacent panels on all four sides as shown in Fig. 4. For the purposes of the present discussion only, the control points of the adjacent panels are numbered $K = 0, 1, 2, 3, 4$ as shown in Fig. 4, where 0 denotes the element in question. These control points are transformed into the coordinate system of the panel in question. Let the ξ and η coordinates of these control points be ξ_{0K}, η_{0K} , $K = 0, 1, \dots, 4$ and the values of source density at the control points be σ_K , $K = 0, 1, \dots, 4$ (evidently $\xi_{00} = \eta_{00} = 0$). The differentiation process expresses

the source derivatives on the panel in question in terms of the unknown values of source density on the adjacent panels in the form

$$\sigma_x = \sum_{K=0}^M c_K^{(x)} \sigma_K \quad (2.5.1)$$

$$\sigma_y = \sum_{K=0}^M c_K^{(y)} \sigma_K$$

where M represents the number of adjacent panels. It is 4 for interior panels, 3 for panels on the edge of a section, and 2 for panels in a corner of a section.

The essentials of the numerical process are that it calculates one-dimensional derivatives in the u and v directions of the parametric-cubic coordinate system of Appendix A and then expresses the derivatives with respect to the panel coordinates in terms of these.

For each panel, calculate the geometric quantities

$$\Delta \bar{\xi} = \frac{1}{2} [\xi_1 + \xi_2 - \xi_3 - \xi_4], \quad a = \sqrt{(\Delta \bar{\xi})^2 + w^2} \quad (2.5.2)$$

$$u = \Delta \bar{\xi} / a, \quad \bar{v} = w / a, \quad \bar{d} = \frac{1}{2} (d_F + d_S)$$

For the purpose of one-dimensional differentiation, define the coordinates

$$\begin{aligned} x_1 &= -\frac{1}{2} (\bar{d}_0 + \bar{d}_1), & x_2 &= \frac{1}{2} (\bar{d}_0 + \bar{d}_2) \\ t_3 &= \frac{1}{2} (a_0 + a_3), & t_4 &= -\frac{1}{2} (a_0 + a_4) \end{aligned} \quad (2.5.3)$$

where the subscripts are panel designations of Fig. 4. Then centered 3-point differentiation, which is appropriate in the interior of a section, gives

$$\sigma_x = \frac{x_2}{x_1(x_2 - x_1)} \sigma_1 - \frac{x_1 + x_2}{x_1 x_2} \sigma_0 - \frac{x_1}{x_2(x_2 - x_1)} \sigma_2 \quad (2.5.4)$$

$$\sigma_t = \frac{t_3}{t_4(t_3 - t_4)} \sigma_4 - \frac{t_3 + t_4}{t_4 t_3} \sigma_0 - \frac{t_4}{t_3(t_3 - t_4)} \sigma_3$$

The first of Eqs. (2.5.4) already gives the first of Eqs. (2.5.1). Thus

$$c_0^{(x)} = -\frac{x_1 + x_2}{x_1 x_2}, \quad c_1^{(x)} = \frac{x_2}{x_1(x_2 - x_1)}, \quad c_2^{(x)} = \frac{x_1}{x_2(x_2 - x_1)} \quad (2.5.5)$$

$$c_3^{(x)} = c_4^{(x)} = 0$$

By analogy the second of Eqs. (2.5.4) gives t-derivative coefficients

$$c_4^{(t)} = \frac{t_3}{t_4(t_3 - t_4)}, \quad c_0^{(t)} = \frac{t_3 + t_4}{t_3 t_4}, \quad c_3^{(t)} = -\frac{t_4}{t_3(t_3 - t_4)} \quad (2.5.6)$$

$$c_1^{(t)} = c_2^{(t)} = 0$$

By the chain rule

$$\sigma_t = \sigma_x u + \sigma_y v \quad (2.5.7)$$

Thus

$$\sigma_y = \frac{1}{v} (\sigma_t - \sigma_x u) = \sum_K \frac{1}{v} (c_K^{(t)} - u c_K^{(x)}) \sigma_K \quad (2.5.8)$$

and finally

$$c_K^{(y)} = \frac{1}{v} (c_K^{(t)} - u c_K^{(x)}), \quad K = 0, 1, \dots, 4 \quad (2.5.9)$$

For panels on the edge of sections, the centered 3-point formulas (2.5.4) must be replaced by 2-point one-sided formulas in the direction (or directions) where a third value does not exist.

2.5.2 Logic of the Assembly Procedure

In the first-order method the velocity induced by a panel depends only on the source density on that panel and thus the "influence coefficients" for that panel are calculated solely from that panel's geometry. The essentially new feature of the source derivative procedure is that the velocity induced by a panel depends on the value of source density at the control point of that panel and also on the values of source density at the control points of adjacent elements. Similarly, the velocities induced by adjacent elements depend on the source density on the panel in question. Thus the "influence coefficients" for

a panel depend not only on the geometry of that panel but also on the geometry of adjacent panels and the assembly of the influence coefficient matrix is more complicated.

Let the panels be numbered consecutively in the order they have been formed. Thus, reference is made to the i -th panel and to the j -th panel where both i and j range from 1 to N . Another way of stating the essentially new feature above is that a distinction must be made between the effect of the j -th panel and the effect of the j -th value of source density, whereas these two effects are identical in the first-order method. Let \vec{V}_{ij}^* be the velocity induced at the i -th control point by the j -th panel and \vec{V}_{ij} be the velocity induced at that point by the j -th value of source density. Then in the notation of Section 2.4 and the present section,

$$\vec{V}_{ij}^* = [\vec{V}^{(0)} + \vec{V}^{(P)}_P + 2\vec{V}^{(Q)}_Q + \vec{V}^{(R)}_R + C_0^{(x)}\vec{V}^{(1x)} + C_0^{(y)}\vec{V}^{(1y)}]_{\sigma_0} + \sum_{K=1}^M [C_K^{(x)}\vec{V}^{(1x)} + C_K^{(y)}\vec{V}^{(1y)}]_{\sigma_K} \quad (2.5.10)$$

Notice that subscripts i and j are omitted on the right side of Eq. (2.5.10) for simplicity. In the overall numbering scheme, σ_0 in (2.5.10) is σ_j and $\sigma_1, \sigma_2, \sigma_3$ and σ_4 have subscripts near j . All velocities in (2.5.10) depend only on the geometry of the j -th panel. The curvatures P, Q, R and the coefficients $C_K^{(x)}$ and $C_K^{(y)}$ depend on the surrounding panels, but once calculated they can be associated with the j -th panel only.

Consider now the i -th row of the matrix \vec{V}_{ij}^* , which expresses the effects of the various values of source density at the i -th control point. The first bracketed term in (2.5.10) is an effect of σ_j and is added to the j -th location of the row. The four terms in the summation of (2.5.10) represent effects of other values of σ and must be added to other locations. Referring to Fig. 4, it can be seen that the panels numbered 1 and 2 are on the same strip as the panel in question and thus represent effects of the preceding and succeeding values of σ . In particular, value 1 is associated with σ_{j-1} and value 2 with σ_{j+1} and the relevant terms of Eq. (2.5.10) are added to those locations. Panels 3 and 4, however, are on adjacent strips. Suppose there are E

panels on each strip. Then value 3 is associated with σ_{j-E} and value 4 with σ_{j+E} , and the relevant terms of Eq. (2.5.10) are added to these locations of the row.

2.6 Vorticity Influence of a Panel

2.6.1 Panel Vorticity and the Underlying Dipole Distribution

The effect of a vorticity distribution on a panel cannot be expressed in terms of a potential, as mentioned above. The velocity induced by the panel of Fig. 8 at a point (x,y,z) is

$$\vec{V}_\omega = \iint_S \frac{\vec{\omega} \times \vec{r}}{r^3} dS \quad (2.6.1)$$

where $\vec{\omega}$ is the vector vorticity strength and

$$\vec{r} = (x - \xi)\vec{i} + (y - \eta)\vec{j} + (z - \zeta)\vec{k} \quad (2.6.2)$$

The distance r has its usual meaning, which is also equal to $|\vec{r}|$, and the integral is over the true panel. To insure that the vorticity satisfies the usual vorticity conservation theorems over the panel, it is convenient to express $\vec{\omega}$ in terms of equivalent dipole distribution μ . As shown in Ref. 5, the relation is

$$\vec{\omega} = -\vec{n} \times \text{grad}\mu \quad (2.6.3)$$

where \vec{n} is the unit normal vector, whose components n_ξ, n_η, n_ζ are given by Eqs. (A.8) through (A.10). In Appendix A, $\vec{i}, \vec{j}, \vec{k}$ were used as unit vectors along the axes of the panel coordinate system, because no other coordinate system entered the discussion. Here, to avoid any possible confusion, these unit vectors will be written $\vec{i}_e, \vec{j}_e, \vec{k}_e$ (Appendix B) to specify that they are indeed unit vectors of the panel system. To be compatible with the source density and panel-geometry expansions, μ is taken to be a quadratic function of panel coordinates ξ and η in

$$\mu = \mu_0 + \mu_x \xi + \mu_y \eta + \mu_{xx} \xi^2 + \mu_{xy} \xi \eta + \mu_{yy} \eta^2 \quad (2.6.4)$$

so that the components of $\vec{\omega}$ vary linearly over the panel. Furthermore, since a two-term expansion of the source potential is all that appears feasible, only a two-term expansion of Eq. (2.6.1) is required. Evidently

$$\frac{\partial \mu}{\partial \xi} = \mu_x + 2(\mu_{xx}\xi + \mu_{xy}\eta) \quad (2.6.5)$$

$$\frac{\partial \mu}{\partial \eta} = \mu_y + 2(\mu_{xy}\xi + \mu_{yy}\eta)$$

are two-term expansions of the components of $\text{grad}\mu$. Then Eq. (2.6.3) gives

$$\vec{\omega} = (n_z \frac{\partial \mu}{\partial \eta}) \vec{i}_e - (n_z \frac{\partial \mu}{\partial \xi}) \vec{j}_e + (n_n \frac{\partial \mu}{\partial \xi} - n_\xi \frac{\partial \mu}{\partial \eta}) \vec{k}_e \quad (2.6.6)$$

Two-term expansions of the \vec{i}_e and \vec{j}_e components of (2.6.6) contain zeroth and first-order terms. Since the leading term of the \vec{k}_e component is linear, only that one term is required. The two-term expansion of Eq. (2.6.6) is

$$\vec{\omega} = [\mu_y + 2(\mu_{xy}\xi + \mu_{yy}\eta)] \vec{i}_e - [\mu_x + 2(\mu_{xx}\xi + \mu_{xy}\eta)] \vec{j}_e + [-c_{2\eta}\mu_x + c_{2\xi}\mu_y] \vec{k}_e \quad (2.6.7)$$

Now using Eq. (2.6.7), a two-term expansion of Eq. (2.6.1) may be carried out, and the resulting velocity put in terms of source influences. This development is carried out in Appendix H.

The dipole strength is required to vary linearly over the N-lines bounding the panel. In particular

$$\mu = B_F(\xi + h_F) \quad \text{on} \quad \eta = \eta_1 \quad (2.6.8)$$

$$\mu = B_S(\xi + h_S) \quad \text{on} \quad \eta = \eta_3$$

when these are applied to Eq. (2.6.4), it turns out that μ must have the form

$$\begin{aligned} \mu = & \frac{1}{W} [\xi\eta + h_F\eta - \eta_3\xi - \eta_3h_F + c_W(\eta - \eta_3)(\eta - \eta_1)] B_F \\ & - \frac{1}{W} [\xi\eta + h_S\eta - \eta_1\xi - \eta_1h_S + c_W(\eta - \eta_3)(\eta - \eta_1)] B_S \end{aligned} \quad (2.6.9)$$

Notice that μ is expressed as the sum of two dipole distributions: one multiplying B_F that is zero for $\eta = \eta_3$ and one multiplying B_S that is zero for $\eta = \eta_1$. Thus, one dipole distribution is associated with each N-line. The logic of the calculation keeps these two separate until a later stage of the calculation. The constants B_F and B_S are essentially bound vorticity strengths that are determined by the Kutta condition. It is the distribution multiplying each that is important at this stage, so in effect the B's are set equal to unity. The constants in the underlying dipole distributions are

μ -derivative	First N-line	Second N-line	
μ_x	$\frac{\eta_1}{w}$	$-\frac{\eta_3}{w}$	
μ_y	$\frac{h_F}{w} - c(\eta_1 + \eta_3)$	$-\frac{h_S}{w} + c(\eta_1 + \eta_3)$	
μ_{xx}	0	0	(2.6.10)
μ_{xy}	$\frac{1}{2w}$	$-\frac{1}{2w}$	
μ_{yy}	c	-c	

The foregoing are on-body formulas. For wake panels set

$$\mu_x = \mu_{xx} = \mu_{xy} = 0 \tag{2.6.11}$$

$$h_F = L_F \text{ (total)}, \quad h_S = L_S \text{ (total)}$$

where L (total) is the total arc length of an N-line from trailing edge to trailing edge. Equation (2.6.11) reflects the fact that the underlying dipole strength is constant along N-lines in the wake.

All constants in Eq. (2.6.10) are known except c . It is determined to make the dipole strength as continuous as possible from one panel to the next along a lifting strip. Clearly nothing enforces continuity if there is a physical gap between the panels, so c is determined assuming that adjacent panels on a lifting strip share a common side. This seems the best that can be done.

Consider the dipole strength along the "top" side of the panel between the points (ξ_3, η_3) and (ξ_2, η_2) (Fig. 3). It is obtained by setting $\xi = m_{32}\eta + b_{32}$ in Eq. (2.6.9). The result is

$$\mu(32) = \mu(\text{linear}) + (B_F - B_S)(cw^2 + wm_{32}) \left[\frac{s}{L} \left(\frac{s}{L} - 1 \right) \right] \quad (2.6.12)$$

In the square bracket s denotes arc length along the side and L the total length of the side ($L = d_{32}$ in the notation of Section 2.3). The function $\mu(\text{linear})$ is a linear function that varies from the value of μ at the point (ξ_3, η_3) to the value of μ at the point (ξ_2, η_2) . On the adjacent element, the "bottom" side that lies between the points (ξ_4, η_4) and (ξ_1, η_1) is the one that lies along the side discussed above. The dipole strength along this side is

$$\mu(41) = \mu(\text{linear}) + (B_F - B_S)(cw^2 + wm_{41}) \left[\frac{s}{L} \left(\frac{s}{L} - 1 \right) \right] \quad (2.6.13)$$

Ignoring any small gaps between elements, the quantities $\mu(\text{linear})$, s , and L are identical in Eqs. (2.6.10) and (2.6.11), as are B_F and B_S . The only quantities that are different are those in the curly brackets. Here c and w correspond to different elements, while the slopes m_{32} and m_{41} correspond to different sides of different elements. Thus continuity between panels i and $i + 1$ of a strip is obtained if

$$w^{(i)} [c^{(i)} w^{(i)} + m_{32}^{(i)}] = w^{(i+1)} [c^{(i+1)} w^{(i+1)} + m_{41}^{(i+1)}] \quad (2.6.14)$$

where w is panel width (usually the same for all panels of a strip), m_{32} is the slope of the upper panel edge and m_{41} the slope of the lower panel edge. Eq. (2.6.14) is solved for successive values of $c^{(i)}$ beginning with

$$c^{(1)} = 0 \quad (2.6.15)$$

and proceeding over all on-body panels of the strip. The choice, Eq. (2.6.15), is arbitrary and expresses the fact that Eq. (2.6.14) has a nonunique solution.

2.6.2 Edge Vortices

The fundamental development of Ref. 5 shows that the velocity induced at a point in space by a dipole distribution μ over a panel is identical to the sum of the velocity induced by a vorticity distribution $\vec{\omega}$, as given by Eq. (2.6.3), and the velocity due to a concentrated line vortex around the perimeter of the panel whose variable strength equals the local value of dipole strength. While the velocity due to the dipole distribution is inherently a potential flow (zero curl), neither of the other two velocities are; only their sum is potential. Using $\vec{\omega}$ in the form of Eq. (2.6.3) satisfies the vorticity conservation theorems over the surface of the panel but not at its edges. Thus to the vorticity velocity of Appendix H must be added the effects of line vortices on the edges of the panel with strength equal to the local value of the underlying dipole distribution. Since an actual body obviously does not have line vortices in its surface, in the absence of numerical approximation the edge vortices of adjacent panels would cancel exactly. Thus it might be hoped that the panel edge vortices could be ignored away from physical edges such as wing tips. It turns out that this is true for spanwise panel edges but not for streamwise panel edges. That is, referring to Fig. 1, the edge vortices of adjacent panels on the same lifting strip cancel to a good approximation (especially when the continuity algorithm of Section 2.6.1 is employed) and thus may be ignored. However, the edge vortices that lie along an N-line in general do not cancel with those of panels of the adjacent lifting strip to a degree that justifies their omission.

There are several ways of accounting for the effect of the edge vortex, all of which are theoretically equivalent to some order of accuracy. The approach used here is the analogy of that used throughout the higher-order development. A vortex lying along the edge of a curved panel is projected into the tangent plane. The relevant formulas are developed in Appendices I and J.

2.6.3 The Trailing Vortex Wake

The wake is input to the program by specifying points along N-lines just as for on-body points. The option exists of making the last panel on each wake

strip semi-infinite. In many cases, such as a clean wing, the location of the wake has very little effect on the solution. In such cases, the wake may be taken as semi-infinite right from the trailing edge, and no wake points need be specified. This optional wake may have the direction of either the trailing-edge bisector or the x-axis.

Wake panels have vorticity but no source density. However, because of the way in which vorticity effects are calculated in the present program, essentially the same induced-velocity formulas must be evaluated as for on-body panels. Of course, no boundary conditions are applied on wake panels, and their presence does not affect the order of the matrix of the linear equations for the source density.

For finite wake panels, the basic influence formulas are unchanged, but the constants defining the underlying dipole distribution and the edge vortex formulas are modified as described in the previous sections. Also modified are the values of c that improve dipole continuity between panels of a lifting strip (Section 2.6.1). Let superscript (1) denote quantities associated with the first on-body element of a lifting strip and superscript u denote quantities associated with the last on-body element of the strip. Similarly, the superscripts $w1, w2$, etc. denote the first wake element, second wake element, etc. of the same lifting strip. The important value of c is $c^{(w1)}$, i.e., the one for the first wake element. It is computed from

$$c^{(w1)} = \frac{w^{(u)} [w^{(u)} c^{(u)} + m_{32}^{(u)}] - w^{(1)} [w^{(1)} c^{(1)} + m_{41}^{(1)}]}{[w^{(w1)}]^2} \quad (2.6.15)$$

where the quantities w, m_{32}, m_{41} have their usual meaning (usually $c^{(1)} = 0$). Values of c for the remaining wake elements are obtained from

$$c^{(w1)} [w^{(w1)}]^2 = c^{(w2)} [w^{(w2)}]^2 = c^{(w3)} [w^{(w3)}]^2 = \dots \quad (2.6.16)$$

In most cases of interest, the trailing vortex wake extends to infinity. To facilitate accounting for this condition, provision has been made for considering the last element of the wake to be semi-infinite. A finite element of the sort shown in Fig. 3 is formed at the end of the wake, including all the geometric quantities of Section 2.3. The induced velocity calculation for this

element is performed using the origin of coordinates appropriate to the finite element, but the formulas used to calculate induced velocities are appropriate for the semi-infinite element. Naturally, all points in space are in the "near field" with respect to a semi-infinite element, so it is the formulas of Appendix D that apply. These formulas are modified by setting

$$m_{32} = 0 \quad (2.6.17)$$

$$\xi_2 \rightarrow \infty \quad \xi_3 \rightarrow \infty$$

This yields immediately

$$\begin{aligned} \alpha_1, \beta_1, \gamma_1, \alpha_4, \beta_4, \gamma_4 & \text{ unchanged} & (2.6.18) \\ \alpha_3 = \alpha_2 = -1, & \quad \beta_3 = \beta_2 = \gamma_3 = \gamma_4 = 0 \end{aligned}$$

The log functions, Eq. (D.3), and their derivatives, Eq. (D.6) are replaced by

$$L^{(41)} = \text{unchanged, all derivatives unchanged} \quad (2.6.19)$$

$$L^{(32)} = 0, \quad \text{all derivatives equal zero}$$

$$-L^{(12)} + L^{(34)} = \log \frac{r_4 - (x - \xi_4)}{r_1 - (x - \xi_1)} \quad (2.6.20)$$

$$\begin{aligned} \frac{\partial L^{(34)}}{\partial x} &= \frac{\alpha_4 - 1}{r_4 - (x - \xi_4)} & \frac{\partial L^{(12)}}{\partial x} &= \frac{\alpha_1 - 1}{r_1 - (x - \xi_1)} \\ \frac{\partial L^{(34)}}{\partial y} &= \frac{\beta_4}{r_4 - (x - \xi_4)} & \frac{\partial L^{(12)}}{\partial y} &= \frac{\beta_1}{r_1 - (x - \xi_1)} \\ \frac{\partial L^{(34)}}{\partial z} &= \frac{\gamma_4}{r_4 - (x - \xi_4)} & \frac{\partial L^{(12)}}{\partial z} &= \frac{\gamma_1}{r_1 - (x - \xi_1)} \end{aligned} \quad (2.6.21)$$

The inverse tangent functions, Eqs. (D.4), and their derivatives, Eqs. (D.5), are replaced by

$$T_K^{(32)} = \tan^{-1} \left(\frac{y - \eta_k}{z} \right) \quad k = 3 \text{ or } 2 \quad (2.6.22)$$

$$T_K^{(41)} = \text{unchanged}, \quad k = 4 \text{ or } 1$$

$$\frac{\partial T_k^{(32)}}{\partial x} = 0$$

$$\frac{\partial T_k^{(32)}}{\partial y} = \frac{z}{z^2 + (y - \eta_k)^2}, \quad \eta_2 = \eta_1 \quad k = 3 \text{ or } 2$$

$$\frac{\partial T_k^{(32)}}{\partial z} = \frac{-(y - \eta_k)}{z^2 + (y - \eta_k)^2} \quad (2.6.23)$$

$$\frac{\partial T_k^{(41)}}{\partial x} = \text{unchanged}$$

$$\frac{\partial T_k^{(41)}}{\partial y} = \text{unchanged} \quad k = 4 \text{ or } 1$$

$$\frac{\partial T_k^{(41)}}{\partial z} = \text{unchanged}$$

All of the quantities of Appendix D are now recalculated using these modified values, except that H_{02} is replaced by

$$H_{02} = m_{41} \frac{r_4 - r_1}{1 + m_{41}^2} - \frac{x - m_{41}y - b_{41}}{(1 + m_{41}^2)^{3/2}} L^{(41)} + w \quad (2.6.24)$$

The induced velocities from the last wake element are added to the other dipole velocities of the lifting strip in the ordinary way.

2.6.4 Some Special Situations

Two special situations exist where panels must be placed inside the body surface. No normal-velocity boundary condition can be applied at such elements

and no source density should be applied to them. However, they do have vorticity and this must be accounted for.

The first situation occurs when a portion of the body intersects a lifting portion at a finite angle (often nearly normal) without breaking the continuity of the trailing edge. An example is provided by the wing-pylon intersection shown in Fig. 5. A certain portion of the lifting body surface is "inside" the pylon. However, the underlying dipole distribution should be continuous through this region to avoid numerical difficulties. Thus, as far as vorticity calculations are concerned, the "inside" panels are normal members of the lifting strips to which they belong. But they are ignored as far as source calculations or boundary conditions are concerned. Such panels are designated "ignored panels." They usually comprise only part of a lifting strip.

The second situation occurs when a lifting portion of the body intersects another portion at a finite angle (often nearly normal). The important case of this is the wing-fuselage intersection, as illustrated in Fig. 6. As is well-known, the local "section lift coefficient" on the wing does not fall to zero at the fuselage intersection. Thus, the underlying dipole strength on the N-line lying along the intersection is not zero. However, the lifting section cannot simply be terminated, because that would result in a concentrated edge vortex filament right on the surface. Accordingly, an additional or "extra" lifting strip is added to the lifting section (see Fig. 6). It is either the first or the last strip of the lifting section. The extra strip lies inside the other body and is a complete lifting strip including wake. No source densities or normal-velocity boundary conditions are applied to the panels of the extra strip. The underlying dipole strength is taken constant in the "spanwise" direction across the extra strip. The value of the dipole strength on the extra strip has nonzero dipole strength and may lead to a concentrated edge vortex in the streamwise direction. For example, as shown in Fig. 5, the vortex may lie along the fuselage centerline and its downstream extension. If the lifting configuration has a right-and-left symmetry, e.g., a fuselage with both wings, and if the flow is also symmetric, e.g. zero yaw, the extra strips for the right and left sides have the same strengths on their interior edges. Thus, in this case the edge vortices cancel. If, however, the lift is not

symmetric, there will be an edge vortex. This is unavoidable because it is physically real. An example is the hub vortex of a propeller. This also occurs at a tip tank, which is essentially a small fuselage with only one wing.

2.6.5 Assembly of the Vorticity Onset Flows

As described in Sections (2.6.1) and (2.6.2), the velocity induced by the vorticity on a panel and the associated edge vortices fall naturally into two parts - one proportional to the value of B on the first N-line and one proportional to the value of B on the second N-line. These are summed over the lifting strip to yield two vorticity onset flows for each lifting strip. In general, each onset flow has three components at every control point. Specifically,

$$\begin{aligned} \mathbf{V}_{ik}^{(F)} &= \sum_j^{\text{strip } k} \mathbf{V}_{ij}^{(F)} \\ \mathbf{V}_{ik}^{(S)} &= \sum_j^{\text{strip } k} \mathbf{V}_{ij}^{(S)} \end{aligned} \quad k = 1, 2, \dots, L \quad (2.6.25)$$

where L is the number of lifting strips. The summations of Eq. (2.6.25) are over a complete lifting strip including the wake elements. If a lifting section begins with an "extra strip" (Section 2.6.4), both velocities $\mathbf{V}_{ik}^{(F)}$ and $\mathbf{V}_{ik}^{(S)}$ for the extra strip are added to the velocity $\mathbf{V}_{ik}^{(F)}$ corresponding to the first ordinary strip of the section. Similarly, if the last strip of a lifting section is an extra strip, both velocities for the extra strip are added to the $\mathbf{V}_{ik}^{(S)}$ of the last ordinary lifting strip of the section. (This gives an underlying dipole strength on the extra strip that is constant at a value equal to that attained on the adjacent lifting strip along the common N-line of the two strips.) Thus, the calculation of Eq. (2.6.25) gives an N x L matrix of velocities at the control points, where L refers to ordinary lifting strips only. Since L is small compared to N, these matrices are small compared to the source-velocity matrices. Each of the velocities, Eq. (2.6.25), represents the velocity due to an underlying dipole distribution of the strip that has slope unity on one N-line and zero on the other with a linear "spanwise" variation in between.

The characteristic onset flow velocities due to a strip are

$$\begin{aligned} \vec{v}_{ik}^{(0)} &= \vec{v}_{ik}^{(S)} + \vec{v}_{ik}^{(F)} \\ \vec{v}_{ik}^{(1)} &= \frac{1}{Z} [\vec{v}_{ik}^{(S)} - \vec{v}_{ik}^{(F)}] \end{aligned} \quad (2.6.26)$$

The first velocity of Eq. (2.6.26) is that due to an underlying dipole distribution on the strip that is constant in the "spanwise" direction. The second velocity is that due to a dipole distribution that varies linearly in the "spanwise" direction and has zero value at "midspan." These velocities are used to form the basic circulatory onset flows $\vec{v}_i^{(k)}$.

If the "step function" option for bound vorticity is used, the proper form of the dipole distribution is simply constant in the "spanwise" direction over a lifting strip, and the velocity $\vec{v}_{ik}^{(0)}$ is precisely the onset flow. Thus, for this option, the vorticity onset flows are

$$\vec{v}_i^{(k)} = \vec{v}_{ik}^{(0)}, \quad k = 1, 2, \dots, L \quad (2.6.27)$$

The above yields L onset flows, each of which corresponds to a unit value of the "streamwise" dipole derivative B on one lifting strip and zero values of B on all other lifting strips.

The machinery for the "piecewise linear" option for bound vorticity is somewhat more complicated. The "spanwise" variation of the "streamwise" dipole derivative B (bound vorticity) is linear in the "spanwise" direction across a lifting strip. Thus, the velocity at the i-th point (control point or off-body point) due to the k-th strip is

$$\vec{v}_i \text{ (strip } k) = \vec{v}_{ik}^{(0)} B_k + w_k \vec{v}_{ik}^{(1)} B'_k \quad (2.6.28)$$

where w_k is the "spanwise" width of the strip. B' is the "spanwise" derivative of B, and subscripts k denote quantities associated with the k-th lifting strip. The derivative B'_k is evaluated by a parabolic fit through B_{k-1} , B_k and B_{k+1} . Specifically, define

$$\begin{aligned}
 D_k &= - \frac{w_k}{w_k + 1/2(w_{k-1} + w_{k+1})} \left[\frac{w_k + w_{k+1}}{w_k + w_{k-1}} \right] \\
 E_k &= \frac{w_k}{w_k + 1/2(w_{k-1} + w_{k+1})} \left[\frac{w_k + w_{k+1}}{w_k + w_{k-1}} - \frac{w_k + w_{k-1}}{w_k + w_{k+1}} \right] \\
 F_k &= \frac{w_k}{w_k + 1/2(w_{k-1} + w_{k+1})} \left[\frac{w_k + w_{k-1}}{w_k + w_{k+1}} \right]
 \end{aligned} \tag{2.6.29}$$

Then Eq. (2.6.28) is approximated numerically by

$$\vec{V}_i \text{ (strip } k) = \vec{V}_{ik}^{(0)} B_k + \vec{V}_{ik}^{(1)} [D_k B_{k-1} + E_k B_k + F_k B_{k+1}] \tag{2.6.30}$$

The velocity Eq. (2.6.30) contains values of the "streamwise" dipole derivative B for three consecutive strips. However, a proper circulation onset flow is proportional to the value of B on a single strip. Since each B_k enters \vec{V}_i (strip k) for three consecutive strips, its three contributions may be summed to give the basic vorticity onset flow.

$$\vec{V}_i^{(k)} = \vec{V}_{ik}^{(0)} + \vec{V}_{i,k-1}^{(1)} F_{k-1} + \vec{V}_{ik}^{(1)} E_k + \vec{V}_{i,k+1}^{(1)} D_{k+1} \tag{2.6.31}$$

In performing the above parabolic fit Eq. (2.6.30), the values of the function B to be fit are, of course, the values of bound vorticity on the strips. Each of these has been associated with an abscissa or "independent variable" that expresses the spanwise position of each strip. Differences of these abscissas appear as combinations of the widths w_k . Calculation of the w_k is not obvious, because in general the "span" or width of each strip is not constant but varies in the "chordwise" direction. An average width is calculated for each strip and used in the calculation above.

The calculational machinery of the program insures that the underlying dipole strength varies linearly in arc length along an N -line, i.e. that dipole strength equals $B\ell$, where B is a constant to be determined and ℓ is arc length measured from the lower surface trailing edge. In particular, at the upper surface trailing edge, the dipole strength is BL (total). This is the circulation about the N -line and the value of vorticity that carries into the wake. The machinery above fits the spanwise distribution of dipole derivative

B, but it makes better sense physically to fit the circulation distribution BL (total). This is a smoother function because it is independent of planform breaks.

The code has the option of fitting either B or BL (total). While the above concept is somewhat complicated to explain, its numerical implementation is simplicity itself. All that is necessary is to divide the vorticity onset flows associated with each N-line by the corresponding values of L (total). Then, the values of "B" that are solved for will really be values of BL (total). Thus in Eq. (2.6.26)

$$\frac{\bar{v}_{ik}^{(F)}}{L_F(\text{total})} \quad \text{replaces} \quad \bar{v}_{ik}^{(F)} \quad (2.6.32)$$

$$\frac{\bar{v}_{ik}^{(S)}}{L_S(\text{total})} \quad \text{replaces} \quad \bar{v}_{ik}^{(S)}$$

No other changes are necessary. These are added to produce a single dipole onset flow per strip and a complete flow solution obtained for it.

2.7 The Kutta Condition

The Kutta condition is applied as a condition of pressure equality on the upper and lower surfaces of the trailing edge, which amounts to a condition of equal velocity magnitude. As a numerical approximation, the Kutta condition may be applied by equating pressures at the control points of the two panels adjacent to the trailing edge on the upper and lower surfaces of the wing. Alternatively, velocities at the upper surface control points of the few panels nearest the trailing edge can be extrapolated to obtain velocity components "at" the trailing-edge upper surface, and the same could be done for the lower surface. This last allows application of the Kutta condition more nearly at the trailing edge, and the analogy of this procedure yields considerable improvement in accuracy in two-dimensional cases. This is the option used in the present method.

However the point of application of the Kutta condition is chosen, the logic of the calculation is the same. In particular, a velocity vector can be calculated at the upper and at the lower trailing-edge point for each strip of panels (Fig. 1). From the discussion of Sections 2.5 and 2.6.5 it is clear that the velocity vector at the i -th control point is given by

$$\vec{V}_i = \sum_{j=1}^N \vec{V}_{ij} \sigma_j + \sum_{k=1}^L \vec{V}_i^{(k)} B_k + \vec{V}_\infty \quad (2.7.1)$$

where \vec{V}_∞ is the onset flow (usually a uniform stream). Initially, the σ_j and B_k are unknown, but it can be seen that \vec{V}_i depends on them linearly. If velocities are extrapolated to the trailing edge, this linear dependence remains. Let superscripts U and L denote velocities at the upper and lower trailing edge, respectively. Further let subscript $m = 1, 2, \dots, L$ denote conditions on the m -th lifting strip of panels. Thus $\vec{V}_m^{(U)}$ and $\vec{V}_m^{(L)}$ are the velocity vectors at the upper and lower trailing edge, respectively, of the m -th lifting strip. The condition that these two velocity vectors have equal magnitudes may be written in terms of dot products as

$$\vec{V}_m^{(U)} \cdot [\vec{V}_m^{(U)} + \vec{V}_m^{(L)}] = \vec{V}_m^{(L)} \cdot [\vec{V}_m^{(U)} + \vec{V}_m^{(L)}] \quad (2.7.2)$$

Applying Eq. (2.7.2) at the trailing edge of each lifting strip yields L quadratic equations in the $(N + L)$ unknowns σ_j and B_k .

2.8 Iterative Matrix Solution

The velocity induced at the i -th control point by the source and vortex singularities is given in Eq. (2.7.1). Taking the scalar products of these velocity vectors with the unit normal vector \vec{n}_i of each control point gives an $N \times N$ matrix of source influence coefficients and an $N \times L$ matrix of vortex influence coefficients defining the normal-velocity influence of each elementary singularity distribution at every control point. If we define the solution vector X whose entries are the source strengths σ_j , ($j = 1, N$) followed by the vortex strengths B_k , ($k = 1, L$), the condition of zero normal velocity on the body can be written in the form

$$AX = R \quad (2.8.1)$$

where A is the N x (N+L) matrix of source and vortex normal velocity influence coefficients, and the right side in Eq. (2.8.1) is the negative of the normal component of the freestream velocity. It is important to note that A is purely geometric and does not depend on the onset flow, which enters only the right side.

Equation (2.8.1) defines a system of N linear equations in the (N+L) unknown singularity strengths. A further set of L equations therefore are required to complete the formulation of the problem. These equations are provided by the Kutta condition, whose derivation is outlined in the previous section. This condition ensures that the computed upper and lower surface pressures match at the trailing edge. The resulting equation, (2.7.2), can be written in the form

$$(\bar{v}^{(U)} - \bar{v}^{(L)}) \cdot \bar{v}_{av} = 0 \quad (2.8.2)$$

where $\bar{v}^{(U)}$ and $\bar{v}^{(L)}$ are the upper and lower surface trailing edge velocities while \bar{v}_{av} is the average of these two velocities.

One Kutta condition is applied for each lifting strip, giving a set of N linear and L nonlinear equations to be solved for the N+L unknowns. For complex configurations, N can be large, up to 2000 in the current version of the code, while L is typically between one and two orders of magnitude less.

The computing time required for the solution of the linear equations by a direct solution is proportional to N^3 , while that required for an iterative matrix solution is proportional to N^2 per iteration. Therefore, provided that the number of iterations required to obtain a converged solutions is relatively small (compared with the number of unknowns), there is a large benefit to be obtained through the use of an iterative matrix solution. The scheme adopted here is an accelerated block Gauss-Seidel iterative procedure which has been shown to give rapidly convergent solutions for a wide range of geometries (Ref. 8). This section will outline the details of this iterative scheme, and Appendix M will present the details of the acceleration scheme which has been

adopted in order to improve the speed and the stability of the convergence procedure.

As pointed out above, the Kutta condition to be applied is nonlinear, and so it must be linearized in some manner consistent with the iterative solution procedure which is to be applied. If we introduce the subscript K to denote quantities evaluated after the K-th iteration, Eq. (2.8.2) can be written as

$$(\vec{v}^{(U)} - \vec{v}^{(L)})_K - (\vec{v}_{av})_{K-1} = 0 \quad (2.8.3)$$

so that the average velocity from the previous iteration is used. For the first iteration, \vec{v}_{av} is replaced by a vector along the local trailing-edge bisector, which ensures that the physically meaningful root to the Kutta condition is selected in which both the upper and lower surface velocities leave the body at the trailing edge.

2.8.1 Block Gauss-Siedel Iterative Scheme

It was shown by Hess (Ref. 9) that the Gauss-Siedel iterative matrix solution scheme converges very rapidly for simple external flow problems. This approach, which is described by Varga (Ref. 10), relies on solving a succession of lower triangular matrix equations of the form

$$A_L X_K = R - A_U X_{K-1} \quad (2.8.4)$$

where X_K is the K-th approximation to the solution. The matrix A_L represents the diagonal and lower triangular part of A, while A_U represents the upper triangular part.

For lifting flow problems there is a strong coupling between the source and dipole strengths for a given lifting strip. Therefore, in order to maintain the diagonal dominance of the matrix, it is necessary to adopt a block Gauss-Siedel scheme. The particular approach used here takes the source strengths and the associated dipole strength for each lifting strip as separate blocks in the solution vector. In this way the normal velocity conditions for a given lifting strip are satisfied simultaneously along with the Kutta condition before

proceeding with the solution for the next block. This is not the only way in which the block structure could be implemented. Reference 11, for instance, groups all of the dipole unknowns together as a single block in the matrix. However, for the nonlinear Kutta condition, the approach adopted here is more convenient. For nonlifting sections of a configuration, the choice of the block structure is less crucial. As the block size for such panels is increased, the computational effort is increased but the rate of convergence is also increased. The use of a block size of 50 has been found to give a good compromise.

This iterative scheme is equivalent to solving a series of quasi-two-dimensional problems corresponding to each block in the matrix. The onset flow for each of these calculations includes the current effects of all the other panels on the body. Therefore, as the solution converges, a fully consistent three-dimensional solution is obtained.

The iterative solution procedure can be broken down into two steps, the first of which involves the calculation of the right-hand side of Eq. (2.8.4) based on the previous solution,

$$\text{RHS}_{K-1} = R - A_u X_{K-1} \quad (2.8.5)$$

The second step is the calculation of the new approximation

$$A_l X_K = \text{RHS}_{K-1} \quad (2.8.6)$$

Each of these steps is performed successively for each block of unknown source strengths, each of which involves the direct solution of a small set of simultaneous equations. In addition, for lifting strips, the dipole strength is computed by satisfying the Kutta condition for that particular strip.

At this stage, it should be pointed out that, for large matrix equations, the whole coefficient matrix A cannot be stored in the computer memory at one time. The order in which the matrix is formed and stored on disc will therefore

influence the way in which the matrix solution scheme is formulated. In general, the Gauss-Siedel iteration scheme is more naturally suited to a matrix which is stored by rows. However, when formulated, as outlined in Eqs. (2.8.5) and (2.8.6), the scheme can be applied to matrices stored either by rows or by columns. The matrix multiplication operations involved in both Eqs. (2.8.5) and (2.8.6) can be accomplished for either row or column stored matrices. The only difference arises from the order in which the multiplication loops are nested.

2.8.2 Convergence Acceleration Scheme

The previous section describes the implementation of the block Gauss-Siedel iteration scheme in a three-dimensional panel method calculation. For many external flow problems, such as the flow past wing-body configurations, this procedure converges very rapidly and significant savings in computer time can be achieved for large panel numbers by comparison with a direct matrix solution. However, for more complicated configurations, such as three-dimensional high-lift systems or wing/pylon/nacelle configurations, the convergence of this scheme becomes worse, and in some cases it can fail to converge entirely. Traditional convergence acceleration techniques are based on the extrapolation of the solution making use of the asymptotic convergence rate. Reference 12 gives a discussion of several iterative schemes, recommending a composite method which combines overrelaxation to accelerate the convergence and underrelaxation to damp out any oscillations in the convergence history. However, for complex configurations, different sections of the matrix will, in general, converge at different rates which makes the use of global convergence factors unsuitable. A new convergence acceleration scheme has therefore been developed which can be applied after each iteration without the need to establish asymptotic convergence rates. This scheme has been found to give improved convergence in all the cases considered while also enabling converged solutions to be obtained for cases which are well outside the normal range of convergence of the basic Gauss-Siedel iterative scheme.

The scheme adopted is a relaxation method in which, after each iteration, an improved solution is defined as a linear combination of the earlier approximations. However, the relaxation coefficients are computed after each iteration in such a way that the residual error of the new approximation is minimized.

To implement the scheme described in the previous paragraph, it is necessary to define the residual vector after each iteration. For the linear normal velocity equations, this residual is defined by

$$\text{RES}_K = R - AX_K \quad (2.8.7)$$

It is clearly undesirable to have to evaluate this expression after each iteration since this would involve (N^2) operations which is equivalent to an additional iteration. However, by separating the matrix A into its triangular parts, and applying Eqs. (2.8.5) and (2.8.6), the residual vector is given by

$$\text{RES}_K = \text{RHS}_K - \text{RHS}_{K-1} \quad (2.8.8)$$

and this expression can be easily evaluated at the end of each iteration. The residual for the Kutta conditions can be evaluated by computing the trailing-edge velocities after each iteration. Substitution in Eq. (2.8.3) then gives a value for the Kutta residual for each unknown dipole strength.

Apart from the calculation of the residual vector, defined by Eq. (2.8.7), the convergence acceleration scheme presented here does not depend in any way on the details of the Gauss-Siedel iteration. The schemes are applied as two independent steps of the overall iterative procedure. In the following outline we will define RES_K to be the residual vector, including both the normal velocity and the Kutta condition residuals after the K-th iteration corresponding to the solution vector X_K , which also includes both the source and the dipole unknowns.

Given a set of approximations to the solution, X_0, X_1, \dots, X_K , we can define a new approximation by

$$X' = \sum_{i=0}^K X_i f_i \quad (2.8.9)$$

where f_0, f_1, \dots, f_k are the acceleration coefficients which are yet to be determined. In general, the first approximation, X_0 , which is the starting solution to the iterative procedure, is taken to be the zero vector. Therefore, Eq. (2.8.9) defines a set of K independent approximations to the solution vector, and so it is convenient to constrain the acceleration coefficients so that

$$\sum_{i=0}^K f_i = 1 \quad (2.8.10)$$

It now follows from Eq. (2.8.7) that the new residual vector is given by

$$RES' = \sum_{i=0}^K RES_i f_i \quad (2.8.11)$$

It should be noted that, while this equation is exact for the normal velocity residuals which satisfy a linear equation, it is only approximate for the nonlinear Kutta residuals. However, this approximation is consistent with the linearization applied in the solution of the Kutta condition, and it is a good approximation for this application.

As the coefficients f_i vary, Eq. (2.8.9) defines a family of approximations to the solution of both Eqs. (2.8.1) and (2.8.2) for which the corresponding residual is given by Eq. (2.8.11). In order to minimize the error for this new solution, a single scalar measure of the error is required. The sum of the squares of the components of the residual vector provides a suitable error measure. In matrix notation this quantity can be evaluated in terms of the norm of the residual vector which is defined by

$$||RES'||^2 = [RES']^T RES' \quad (2.8.12)$$

where $[RES']^T$ is the matrix transpose of RES' .

This equation defines a quadratic function of each of the variables f_i . Since this function is non-negative, it follows that its minimum value must occur at the point at which

$$\partial ||RES'||^2 / \partial f_i = 0 \quad \text{for } i = 0, 1, \dots, K-1 \quad (2.8.13)$$

This provides a set of K linear equations which, together with Eq. (2.8.10), can be used to determine the acceleration coefficients completely.

Full details of the derivation of this set of equations and their solution are given in Appendix M.

This acceleration scheme involves two principal computational tasks. The first is the calculation of the acceleration coefficients, which in turn involves the calculation of the scalar products between every pair of residual vectors. The second is the application of these coefficients to the calculation of an improved solution and its corresponding residual vector. Both of these tasks will involve on the order of (KN) operations while each iteration requires N^2 operations. Therefore, since K , the number of previous solutions, is very much less than N , the additional computation introduced by the acceleration scheme is small. However, it has been found to have a significant effect on the rate of convergence of the scheme, while also giving an improved stability enabling converged solutions to be obtained for cases which are well outside the normal range of convergence of the basic Gauss-Siedel iterative scheme.

3.0 THE INLET PROCEDURE

3.1 General Description

The inlet procedure employs the above-described panel method to calculate fundamental flow solutions for the inlet which are then linearly combined to obtain the flow at any desired operating condition. Specifically, solutions may be obtained for any angle of attack or yaw, Mach number, and mass flow rate. The computational effort required to perform the combination for a particular operating condition is a small fraction of that required for the initial calculation of the fundamental solutions. Thus, solutions for any number of operating conditions may be obtained inexpensively, as needed, at any time after the fundamental solutions have been calculated.

The numerical efficiency of this inlet procedure is realized because the fundamental solutions are obtained for incompressible flow, and then combined and corrected for compressibility effects. A key element in this approach is an accurate and general compressibility correction that may be applied to the incompressible flow about the same inlet, as opposed to the standard Goethert procedure which requires a Mach-number-dependent stretched version of the inlet. The compressibility correction used is the Lieblein and Stockman method, Ref. 13, which is described in Appendix N. This procedure has been well verified by comparison with experimental data, Refs. 13-15. For internal flows it is effective even for supersonic flow without shocks, and it has been generalized to external flow about wings, Ref. 16.

From the beginning (Ref. 1) this work has had two principal aims: computational efficiency for arbitrary geometries, which is discussed above, and user orientation, which has been obtained principally by including a number of graphical output features. The main capabilities of the programs of Refs. 1 and 2 are surface streamline tracing and isoplotting of various flow quantities both on the surface and over cross sections. Both of these have been improved by providing the capability of drawing curves across section boundaries. That is, the panels may be grouped into logically independent but physically contiguous sections or networks, and the plotting routine can draw streamlines or

isocurves across these boundaries. A major new graphical feature is the portrayal of the surface or off-body velocity field by means of a set of vectors having the velocity magnitude and direction at all points. This type of picture has proven very useful in applications.

3.2 The Fundamental Flow Solutions

First, the definition of a flow solution must be described. In the present context these are incompressible flows. Every flow solution corresponds to a certain "onset flow" which is the flow incident to the body. In general the onset flow satisfies neither the normal-velocity boundary conditions nor the Kutta conditions. The source densities σ_j and the dipole derivatives B_k (bound vorticity strengths) are adjusted to satisfy these conditions. The most common onset flow is a uniform stream, but as will be seen, other onset flows are also necessary. For this reason, the onset flow vector at the panel control points is written \vec{V}_{oi} to show that it may vary from point to point. Then the velocity at the i -th control point is

$$\vec{V}_i = \sum_{j=1}^N \vec{V}_{ij} \sigma_j + \sum_{k=1}^L \vec{V}_i^{(k)} B_k + \vec{V}_{oi} \quad (3.2.1)$$

This replaces Eq. (2.7.1), and the method of Section 2.7 and Section 2.8 give the values of σ_j and B_k corresponding to that particular onset flow. When these values are inserted into Eq. (3.2.1) and the indicated summations performed, the resulting set of \vec{V}_i is designated a flow solution.

The set of fundamental flow solutions that are superposed by the combination program to obtain flow about the inlet at arbitrarily prescribed operating conditions may be described most easily in terms of two types of flow. The first is flow about the inlet due to a unit freestream at prescribed angle of attack and yaw with no effort to control mass flow through the inlet. In the nonlifting methods of Refs. 1 and 2, there were always three such flows: zero angle of attack and yaw, 90° angle of attack, and 90° angle of yaw. In lifting cases, however, the latter two flows make no sense. If the inlet has a leading-edge slot, for some circumferential locations, the trailing edge is the upstream point of the airfoil section. The result can be nonconvergence

of the iterative solution. In the present program a number of angle-of-attack/yaw combinations are input by the user. It is preferable to choose these combinations in the range where the user's interest ultimately will lie. The other type of solution is the static, for which the inlet ingests fluid and the flow is quiescent at infinity. The inlet methods of Refs. 1 and 2 use different mathematical devices to produce the static solution. Reference 1 uses a constant vorticity distribution over the inlet surface, as illustrated in Fig. 7a. This has some features in common with the surface vorticity used on the slats to generate lift, but is also has several differences. No Kutta condition is applied on the inlet, and no distribution of vorticity is solved for. Instead a single parameter, total vorticity strength, is adjusted to satisfy a single condition, mass flow through the inlet. If auxiliary inlets are present, the topology of the configuration does not permit use of surface vorticity. Accordingly, in the method of Ref. 2, the mechanism of the static solution is a single ring vortex located well downstream in the inlet, as shown in Fig. 7b. The strip vorticity option of Fig. 7a gives a superior static solution, and it is used in all cases except for the infrequently occurring one where an auxiliary inlet is present. In the very infrequent case where there are two independent mass flow rates, e.g. an "inlet within an inlet," the above mechanisms have to be applied to each inlet separately.

Because of the wide variety of cases to which the present method may be applied, some flexibility is necessary in the choice of fundamental flow solutions. For example, while the static solution has a sensible Kutta condition for an inlet with leading-edge slat, the same probably cannot be said for an inlet on a wing, where the static flow near the wing trailing edge is more-or-less parallel to it. Similarly, the high inclination angles at which a slatted inlet can operate at high mass flow rates lead to the above-described difficulty for 90° if no mass flow control is exercised. Thus, in general the fundamental flow solutions should all contain combinations of an inclined freestream and a static condition. This is perfectly permissible as long as the flow solutions contain all the independent possibilities, e.g. at least two angles of attack, yaw, and mass flow rate.

3.3 The Combination Program

The fundamental flow solutions and the body geometry are accessed by the combination program. At this stage also are input any off-body points and inlet cross-sections where the flow output is desired. A cross section is a panel network extending across the interior of the inlet. Flow quantities are computed at panel centers and a total mass flux for the cross section as a whole is evaluated. One cross section is designated the control station, and it is there that the mass flow condition is applied. In preparation for this, the average velocity at the control station V is computed for each fundamental solution.

The flow condition input to the combination program consists of flow conditions at infinity and at the control station. The various possibilities are presented in Appendix 0. The key quantity in the combination is the equivalent incompressible velocity, which is denoted with a prime. In particular, V_{∞}' is the equivalent incompressible freestream velocity (Eq. (0.13)) and V_c' is the equivalent incompressible average velocity at the control station (Eq. (0.20)). In all cases V' equals V multiplied by the local static-to-total density ratio, and the flow direction is unchanged.

In order to compute the combined flow for a given set of flow conditions, a number of the fundamental flows are combined linearly. In general, three linearly independent fundamental flows are required to satisfy the conditions at infinity while an additional static solution is required for each independent mass-flow condition. However, for flows without yaw, the number of fundamental flows required is reduced by one. In the fundamental solution mode, a number of user-specified fundamental solutions are obtained including at least one yaw solution if combined solutions with yaw will be required. The range of angles of attack and yaw specified should preferably span the complete range of combined solutions which will be required. When the combination program is run, the code will automatically select the closest linearly independent solutions to be used for the combination. This procedure is required by the nonlinearity in the potential flow solution which is introduced by the Kutta condition.

To illustrate the combination procedure, consider the case in which four fundamental solutions have been selected by the code. Let these individual solutions be denoted by the superscript m , and let a_m represent the unknown combination constants. The equivalent incompressible velocity for the combined flow is

$$\vec{V}_i' = \sum_{m=1}^4 a_m \vec{V}_i^{(m)} \quad (3.3.1)$$

where the combination constants a_m are initially unknown. Meeting the prescribed flow conditions at infinity and at the control station requires

$$\sum_{m=1}^4 a_m \vec{V}_\infty^{(m)} = \vec{V}_\infty' \quad (3.3.2)$$

$$\sum_{m=1}^4 a_m \bar{V}^{(m)} = \bar{V}_c'$$

This defines four equations (one vector, one scalar) for the four unknown a_m . Once computed they are inserted in Eq. (3.3.1) to obtain \vec{V}_i' , which is used in the compressibility correction (Appendix H).

4.0 CALCULATED RESULTS

The method described here will be illustrated using three separate geometrical configurations. The first two cases represent complex three-dimensional flows involving inlets with lifting slats on the leading edge of the cowl. The third configuration is a simple nonlifting axisymmetric inlet which illustrates some improvement in the computed results, as compared with the nonlifting method presented in Ref. 2.

The first geometry discussed is an axisymmetric inlet with a centerbody and leading-edge slat shown in Fig. 9. The cross-section shown in Fig. 9b illustrates the relationship of the leading-edge slat to the cowl. The ability of colored shaded graphics to portray complex three-dimensional bodies is illustrated in Figs. 9c and 9d. Figure 10 shows a comparison of the current method with the axisymmetric method of Ref. 18 for a combined flow along the axis of the inlet with an average velocity on the fan face, $x = 2.63$, of twice the freestream. A surface vorticity distribution on the cowl was used to generate the static solution in both the axisymmetric and the three-dimensional calculations. The pressure distributions on the cowl and the centerbody, shown in Fig. 10a, agree very closely while Fig. 10b shows that on the slat there is a small difference in the leading-edge pressure peak when compared with the axisymmetric result.

The remaining results for this configuration are presented for three incompressible flow conditions. The first is a pure static flow with no flow at infinity, and the second is a "pure freestream" solution at zero angles of attack and yaw, with no surface vorticity on the cowl. The third solution is a combined flow at 40° angle of attack, zero yaw and an average fan face velocity twice the freestream velocity. Figures 11-13 illustrate the flowfield across the inlet for these three flow conditions, the vectors drawn being proportional to the local flow velocity. The flowfield velocity vectors are computed in the plane through the inlet axis tilted 15° from the center plane of the inlet. The boundary lines shown on these figures represent the boundaries of the off-body flowfield rakes used to compute the flowfield rather than the exact aerodynamic surfaces. For clarity, the approximate body locations are shaded.

The static case shown in Fig. 11 illustrates the rapid decrease in velocity magnitude ahead of the inlet, while the expanded view of the slat region reveals a local flow environment similar to that of a conventional flap with the upstream stagnation point occurring in the vicinity of the slat leading edge. The axisymmetric freestream condition shown in Fig. 12 gives a more unconventional flowfield. In this case the "upstream" attachment line on the slat occurs on the forward-facing surface of the slat closer to the trailing edge than the leading edge, while the attachment line on the cowl occurs virtually under the leading edge of the slat. Figure 13 illustrates a combined flow in which the freestream is at 40° to the inlet axis while the internal velocity is twice the freestream. In this case the flow ahead of the inlet and on the centerbody is very different than that shown in Fig. 12. However, in the vicinity of the slat, the flowfield is qualitatively the same.

Figures 14-16 present the computed flowfield isobars for the same three flow conditions in the same off-body plane. Figure 14 again shows the conventional nature of the slat flowfield in the static case with the rapid pressure variation occurring as the flow goes around the inner lip of the cowl. On the other hand, Figs. 15 and 16 show the extreme pressure gradients occurring on the slat where the flow turns around the leading edge.

The second configuration considered is essentially the previous configuration but further complicated by the addition of another leading-edge slat, this time only a part-circumference slat, however. A section through the lower half of the configuration is shown in Fig. 17. Results are presented for this configuration at a combined solution of zero yaw, 40° angle of attack and fan face velocity of twice freestream.

Figure 18 compares the computed pressure distribution, plotted against radial distance, on the main slat at three different circumferential locations with the corresponding results computed for the single slat configuration. Near the top of the inlet the presence of the auxiliary slat does not have a large effect on the pressure. However, in the $z = 0$ plane there is a significant reduction in the leading-edge pressure peak, while close to the bottom of the inlet the second slat greatly reduces both the leading and trailing edge

pressure peaks on the main slat. Figure 19 shows the surface velocity distribution on both the inner and outer cowl surfaces for the same flow conditions. It can be seen from Fig. 19b that the nonaxial nature of the flow persists throughout even the interior of the inlet. This is presumably due to the presence of the ingested tip vortices trailing from each end of the part-circumferential slat which will induce some swirl into the internal flow.

The third configuration considered is a simple 72-panel (on the "half-body") round inlet, as shown in Fig. 20. This simple geometry was used to demonstrate the improvement gained in the new source derivative fitting algorithm in use in the present code. Figures 21a and b present the variation in peak C_p versus theta (measured circumferentially), and the variation in C_p versus axial distance at a fixed theta value ($\theta = 75^\circ$), respectively. The results are compared with those obtained by the method described in Ref. 2 in which a "least-squares" fitting procedure was used to compute the source derivative effects. The present approach, described in Section 2.5.1, demonstrates the improved level of axisymmetry which is obtained by the new formulation.

5.0 INPUT INSTRUCTIONS FOR THE HIGHER-ORDER POTENTIAL FLOW PROGRAM (DF12)

5.1 Introduction to the System

The computer code is actually a collection of pre- and post-processing programs grouped around the potential-flow program. It can be thought of as a system of programs designed to "talk" to each other via saved datasets. These programs are:

1. PRE-PROCESSOR: parametric cubics patch fitting of 3-D coordinate data.
2. FUNDAMENTAL POTENTIAL FLOW SOLVER: (DF12: Mode 1).
3. COMBINATION OF FUNDAMENTAL FLOWS (DF12: Mode 2).
4. POST-PROCESSOR: ISOPLLOT - plots iso-contours (on- or off-body).
5. POST-PROCESSOR: VECPLOT - plots velocity vectors (on- or off-body).
6. POST-PROCESSOR: TRACE-ON - calculates streamlines (on-body only).

Operation of these codes is facilitated by a set of interactive "submit CLISTS" and associated FORTRAN programs. A single CLIST controls the operation of programs 1, 2 and 3; separate CLISTS exist for each of programs 4, 5 and 6. While all these CLISTS have been designed for an IBM mainframe running TSO in an MVS/XA environment, similar interactive submittal procedures can easily be written for other systems to accomplish the same purpose, viz. simplify the user's job of running cases and enhance his ability to investigate both the quality and significance of the computed results.

5.2 Discussion of the Individual Programs

Since several of the programs can "communicate" with each other via saved datasets, a great deal of flexibility exists concerning the sequence in which the programs may be executed. For example, Program 1 can talk to either Programs 2 or 3, but is not always required to run Programs 2 or 3. Programs 4, 5 and 6 can talk to Programs 2 or 3, but only if the appropriate dataset from 2 or 3

was saved. To understand the possible interactions between programs, it is best to consider each one separately, first.

5.2.1 The PRE-PROCESSOR: PC-PATCH

This program is designed to take a user-defined set of 3-D Cartesian coordinates and fit a set of parametric bi-cubic patches to the implied surface. The input consists of a formatted "card-image" (i.e. 80-column, fixed block) dataset which contains the corner points of panels distributed on the surface of the body about which the flow is to be calculated (see Appendix P). The format of this data is:

cc 1-10	X	
cc 11-20	Y	Cartesian coordinates
cc 21-30	Z	
cc 31	ISTAT	0 = this point is on the same M-line as previous point 1 = this point starts a new M-line 2 = this point starts a new section
cc 32	LABEL	0 = this is an MLIF (nonlifting) section 1 = this is a LIFT (lifting) section (i.e. has Kutta condition) (Note: all LIFT sections, if any, must precede all other section types.) 2 = this is a WAKE section (all WAKE sections, if any, must come last on the input geometry dataset, after all other LABEL=0,1,3 and 4 sections) 3 = this is a DBLT (doublet) section 4 = this is a SRFV (surface vorticity) section (Note: may not use both DBLT and SRFV sections at the same time in a Mode 1 case.) 5 = this is a FLUX section (allowed as input to Mode 2 cases only)
cc 33	MCURV	0 = automatic M-line curvature selection (curved unless LABEL=1) 1 = M-lines are all curved (even if LABEL=1)

Note that LABEL and MCURV only apply to ISTAT=2 points, i.e. they need be entered only once on a section. (For a discussion of the limits on the numbers of points, panels, etc., see Section 6.2.4, Program Limits.)

These panel coordinate data are "fit" with parametric cubic patches (see Appendix B) and written to an output dataset hereafter referred to as a "PCU"-dataset (Parametric Cubics Unformatted). The PCU dataset serves as a true

surface definition for the higher-order potential-flow solver, but it is not required that the pre-processor supplied with this system be used to generate that PCU-dataset: any "PC"-fitting program may be used, as long as the following PCU-"format" is observed:

Record #1:	IFORM	A single integer (use "1") specifying the PCU-format
Record #2:	NSECT NPATT NTYPE(6) HEAD(9)	Number of SECTIONS (see Section 2.3) of data Total number of patches on the entire dataset 6 integers indicating the number of each type of SECTION in the following order: #NLIF, #LIFT, #WAKE, #DBLT, #SRFV, #FLUX 9-word (4 bytes/word) alphanumeric title

NSECT sets:

Record #3:	ISECT NPAT NU NV HEAD(15)	Running SECTION counter Number of PC-patches on this section (=NU x NV) Number of patches in the "N-line" direction Number of patches in the "M-line" direction 15-word (4 bytes/word) alphanumeric section title
Record #4:	TMAT(12)	12 double-precision word (8 bytes/word) transformation matrix (not presently used)
Record #5:	P(48)	48 double-precision word (8 bytes/word) PC-patch coefficients in GEOMETRIC form; repeated for all NPAT patches on this SECTION
.	.	.
.	.	.
Record #(4+NPAT)		

Note that the PRE-PROCESSOR program may be used to generate the PCU input dataset for both the on-body data (used in Mode 1, described below) and the flux-section data (optionally used in Mode 2, also described below). The PCU dataset created by this PRE-PROCESSOR is relatively inexpensive to create and is therefore normally discarded by the potential flow solver. This is true unless the potential flow solution is being saved for a Mode 2 case; in the latter situation, the PCU dataset is copied into the saved fundamental solution dataset created by Mode 1 to ensure that Mode 2 is operating on a consistent geometry base.

5.2.2 DF12, Mode 1: FUNDAMENTAL POTENTIAL FLOW SOLVER

This program forms the heart of the system in that the fundamental flows are generally the most complex and expensive part of the solution and form the

basis from which any combined solutions are obtained. The input to this program consists of a PCU-dataset (described above, in Section 5.2.1) on unit 1, and a formatted card-image dataset which contains some simple control flags on unit 5. The format of the control flags dataset is:

Record #1:

cc 1-72 TITLE(I), I=1,18 Alphanumeric run description
cc 73 MODE A single integer indicating the mode (1)

Remaining records (as needed) in NAMELIST/Z/ format:

AREF Reference area (use semi-area if NSYM=1) (default: 1.0)
BOV2 Reference semispan (default: 1.0)
CREF Reference chord length (default: 1.0)
ORIGIN(3) Moment reference center (X,Y, and Z; default: 0.,0.,0.)
IAUTOW 0 = user-input wake
 1 = automatic trailing-edge bisectors
 2 = automatic parallel to x-axis
 (default: 1)
ICOMBO 0 = do not save data for a possible Mode 2 combination case
 1 = yes, save data
 (default: 0)
IDEBUG 0 = print standard set of input flags
 1 = print expanded set of input flags (for debugging purposes)
 (default: 0)
IFUNDP 0 = no fundamental solution printout
 1 = minimum fundamental solution printout
 2 = full fundamental solution printout
 (default: 2)
IPCV 0 = constant chordwise vorticity distribution
 1 = parabolic chordwise vorticity distribution
 (default: 0)
IPR132 0 = small print size (164 columns, 89 lines per page)
 1 = large print size (132 columns, 60 lines per page)
 (default: 0)
IPV 0 = do not save P/V (pressure/velocity) dataset
 1 = save P/V dataset for possible use by ISOPLOT, VECPLOT
 and/or TRACE-ON
 (default: 0)
IQWIK 0 = do not save "QWIKPLOT"-type output dataset
 1 = save "QWIKPLOT" dataset (see below)
 (default: 0)

QWIKPLOT output dataset is similar to a P/V dataset in that the data is compacted into unformatted (binary) form. ISOPLOT, VECPLOT, and TRACE-ON all require a P/V dataset to execute; the QWIKPLOT dataset is organized around the concept of "strings" of data, where every record was created in the form: WRITE(IUNIT)VNAME,N,(Q(I),I=1,N), where VNAME is a double precision alphanumeric string identifier (8 bytes) and Q(I) is the string of data. An inhouse plotting program (called, not surprisingly, "QWIKPLOT") was written to read QWIKPLOT datasets allowing rapid and easy comparisons of results of many CFD codes, and/or test data.

LO 0 = higher-order solution
 1 = lower-order simulation
 (default: 0)

NSYM 0 = no symmetry
 1 = symmetric about Y=0 plane
 (default: 1)

ALPHA Freestream angle-of-attack, degrees (no default; may have up to 20 values)

BETA Freestream angle-of-yaw (default: 0; must have a value for each ALPHA value specified)
 (Warning: Cannot use nonzero BETA if NSYM=1.)

IEXTRA Strip numbers of "extra-strips" (see Section 2.6.4), if any; these count consecutive strips of LIFT sections only, which, as mentioned earlier, if present, must be the first sections of the input geometry dataset.

The 72-panel, simple round inlet half-body, drawn with its image in Fig. 20, is supplied along with the program source code as a check case. The coordinates for this case are shown in Fig. 22. A sample execution of the interactive submit program for a Mode 1 execution of this check case is shown in Fig. 23. If the submit program is not used, an input dataset of the form shown in Fig. 24(a) must be created by the user. The JCL produced by the submit program to execute this Mode 1 check case is shown in Fig. 24(b).

The output from the MODE 1 execution of this test case is shown in Fig. 25. It is basically self-explanatory with the following exceptions:

P,Q,R the curvature quantities as used in the paraboloidal panel definition: $\zeta = P\xi^2 + 2Q\xi\eta + R\eta^2$

SIGMA the source density value at the control point of the panel

- VN the net normal velocity on a panel
- VT the total velocity magnitude: $V_T = \sqrt{V_x^2 + V_y^2 + V_z^2}$
- CP the pressure coefficient:
 INCOMPRESSIBLE: $C_p = 1 - (V_T/V_{ref})^2$
 COMPRESSIBLE: $C_p = (p - p_{ref})/q_{ref}$
- CL the "lift coefficient": L/qA_{ref}
- CD the "drag coefficient": D/qA_{ref}
- CSF the "sideforce coefficient": F_y/qA_{ref}
 (Note: F_y is the force in the Y-direction)
- CPITCH the "pitching moment coefficient": $M_y/qA_{ref}C_{ref}$
- CROLL the "rolling moment coefficient": $M_x/qA_{ref}b_{ref}$
- CYAW the "yawing moment coefficient": $M_z/qA_{ref}b_{ref}$

where

- A_{ref} the user-input reference area (which should be the "half-area" if NSYM=1)
- b_{ref} the user-input reference span (which should be the semispan if NSYM=1)
- C_{ref} the user-input reference chord length
- q the dynamic pressure, $\rho V_{ref}^2/2$
- L and D measured in the lift and drag direction
- $F_x, F_y, F_z, M_x, M_y, M_z$ the forces and moments (integrated over the input panels, only, i.e. not over image panels created if NSYM=1) along and about the Cartesian axes.
- ETA Y/b_{ref} , where Y is taken as that of the first control point on the strip
- ASTRIP projected (into the X-Y plane) planform area of a lifting strip
- SECTCL, SECTCD local strip values of L/qA_{strip} and D/qA_{strip}
- CIRCULTN the computed circulation value of the lifting strip used to satisfy the Kutta condition.

5.2.3 DF12, Mode 2: COMBINATION OF FUNDAMENTAL FLOWS

This program permits the user to combine the fundamental flows (from a MODE 1 execution) to obtain desired mass flow values (typically within an inlet). The combination constants required to obtain the user-defined mass flow values are obtained automatically by the program when the user supplies a "FLUX" section at the place where the mass flow rates are specified. The cost of generating the automatic combination constants varies linearly with the number of panels the user has on his FLUX-section dataset, and therefore may equal or even exceed the cost of the Mode 1 solution, although this is typically not the case. Optionally, the user may simply input these combination constants himself, and thus define his own combination case (perhaps using combination constants obtained from an earlier Mode 2 run).

Since the fundamental flow solver was designed to handle geometries which contain lifting leading-edge devices, such as those shown in Figs. 9 and 17, the program logic which satisfies the Kutta condition made it necessary to have the freestream fundamental flows include some suction effects as part of the standard set of freestream onset fundamental flows. As a result, in order for the user to obtain pure freestream onset flows (i.e. without any suction effects), a $CC = -1.0$ may be used. Note also that up to 5 suction fundamental flows may be generated in a Mode 1 case, requiring, therefore, an equal number of flux-setting and/or CC-values to be specified in Mode 2. Furthermore, the number of flux-setting conditions specified may not exceed the number of FLUX sections that are input, although the number of FLUX sections may indeed exceed the number of suction solutions available from Mode 1; this latter case is the typical one wherein a number of additional FLUX sections are included in order to use VECPLOT and/or ISOPLOT to survey the off-body flowfield.

Since the compressibility correction employed by the present program is the Lieblein-Stockman correction which is an "after-the-fact" type of correction (unlike, say, the more common Goethert correction which solves a different potential-flow problem for each freestream Mach number), multiple Mach number results may be obtained from a single Mode 1 set of fundamental solutions.

Input for Mode 2 consists of the saved fundamental solution dataset from a Mode 1 case (created when ICOMBO=1), plus a PCU-dataset containing FLUX sections (if any), plus a card-image flags dataset, which differs according to

whether COMPRS=0 or 1. Consider first an incompressible Mode 2 case (i.e. COMPRS=0):

Record #1:

cc 1-72: TITLE(I), I=1, 18 Alphanumeric run description
cc 73: MODE A single integer indicating the mode (2)
(no default)

Remaining records (as needed) in NAMELIST/Y/ format:

COMPRS 0 = incompressible flow
1 = compressible flow (Lieblein-Stockman correction)
(default = 0)

I OFF 0 = no off-body points
1 = off-body points input on a separate dataset X,Y,Z 3F10.
(Do not confuse this with FLUX sections which are M x N
grids of points which produce (M-1) x (N-1) panels;
off-body points need have no organization into M x N
grids).
(default = 0)

IPR132 0 = small print size (164 columns, 89 lines per page)
1 = large print size (132 columns, 60 lines per page)
(default = 0)

IPV 0 = do not save on-body P/V dataset
1 = save on-body P/V dataset for optional later use by
ISOPLOT, VECPLOT, and/or TRACE-ON
(default = 0)

JPV 0 = do not save FLUX-section P/V dataset
1 = save FLUX-section P/V dataset for optional later use by
ISOPLOT, VECPLOT, and/or TRACE-ON
(default = 0)

IQWIK 0 = do not save "QWIKPLOT"-type output dataset
1 = save "QWIKPLOT"-type output dataset
(default = 0)
(For explanation of format, see Section 5.2.2 on "IQWIK".)

NCOMB Number of combination cases to be calculated NCOMB values of
ALPHAC, BETAC, VINP, VREF, etc. must be specified.
(<20; default: 1)

ALPHAC, Requested net "combined" angles of attack and yaw (in degrees)
to be
BETAC achieved.
(Note: The program automatically selects appropriate combinations of the available fundamental flows; however, the user cannot request "impossible" combinations, e.g. if all fundamental flows were run with BETA=0, then all BETAC values must also be 0.)
(defaults: ALPHAC has none, BETAC defaults to 0)

VINF Freestream speed (default: 1.0)

VREF Reference speed for C_p calculation. If COMPRS=1; then VREF is used for the Mach number correction. (default: VINF but, if VINF=0 also, then VREF is set to 1.)

VC(ICOMB,I) Requested average normal flux velocity, referring to the I-th flux-section, for combination solution number ICOMB (of NCOMB). (no default; for COMPRS=0, either VC or CC must be input for each suction fundamental flow generated in Mode 1)

CC(ICOMB,I) Designated combination constant for the I-th SUCTION fundamental solution. (default: see VC, above)

A sample execution of the interactive TSO submit program for a MODE 2 incompressible case is shown in Fig. 26. If the submit program is not used, an input dataset such as that shown in Fig. 27(a) is required to accomplish the same program execution. The JCL produced by the submit program to execute this Mode 2 check case is shown in Fig. 27(b).

The output from MODE 2, shown for the 72-panel inlet case in Fig. 28, was designed to be self-explanatory and differs significantly from that of MODE 1 in only two areas:

1. The page titled "FLOCMB. FLOW COMBINATION MATRIX DATA" contains the details of the automatic computation of the combination constants, which are labeled "CC."
2. For compressible cases (COMPRS=1), an extra column of the local Mach number, labeled MACH, is also shown on the output sheets.

The input flags for the compressible case (COMPRS=1) differ only slightly from the incompressible case. In particular, the freestream pressure (total or static) and freestream temperature (total or static) must be supplied. In

addition, the user is given the option of specifying either the freestream speed (VINFL) or the freestream Mach number (MINFL). The number of options for specifying the flux is expanded to include average flux Mach number (MFL) or average weight flow rate (WFL). Finally, the Lieblein-Stockman correction also makes use of an incompressible reference velocity (VIBAR) which the user may optionally control.

5.2.4 DF12 Program Limits

The following program limits and guidelines must be met by the user for Mode 1:

1. Maximum total # panels: 2000
(this includes WAKE panels, extra-strip panels (if any), etc.)
2. Maximum total # sections: 100
(includes WAKE sections, etc.)
3. Maximum total # strips: 300
(includes all sections)
4. Maximum # lifting strips: 100
(includes only LIFT and SRFV strips, and "extra" strips (if any))
5. Maximum # DBLT sections: 5 (see also 11 below)
6. Maximum # SRFV sections: 5 (see also 11 below)
7. All LIFT sections (if any) must precede all other sections in the input geometry dataset.
8. All WAKE sections (if any) must follow all other sections in the input geometry dataset.
9. The order of WAKE sections (if any) must coincide with the order of LIFT sections to which the WAKE sections correspond.
10. No N-line on any LIFT section may be of zero length.
11. DBLT and SRFV sections may not both be input at the same time.
12. Nonzero BETA cannot be requested if NSYM=1.

For Mode 2:

13. Only FLUX sections and/or off-body points may be input (along with the control flags, of course).
14. Maximum total # FLUX panels plus off-body points: 2000

15. The maximum total # FLUX sections: 20
16. Total # of (VC+MC+WC+CC) conditions specified \leq (#DBLT + #SRFV) sections that were input for Mode 1.
17. "Impossible" flow combinations should not be requested, e.g. if Mode 1 was run with only one angle of attack, then Mode 2 cannot possibly "combine" the Mode 1 fundamental flows to achieve any other angle of attack except the one specified in Mode 1.

5.2.5 Post-Processing Program: VECPLOT

Input to the velocity vector plotting program, VECPLOT, consists of: (1) an unformatted P/V (pressure/velocity) dataset (either on-body or off-body, i.e. FLUX), and (2) a unit 5 card-image dataset. The "format" of the P/V dataset (which is created automatically for on-body results of MODE 1 (if IPV=1), and either on-body (if IPV=1) and/or FLUX sections (if JPV=1) for MODE 2) is shown in Fig. 30.

The unit 5 card image dataset for VECPLOT is in NAMELIST /INPUT/ format:

IDEBUG	0 = (default) normal execution 1 = generate debug print
VREF	Value used to scale velocities before plotting vectors (0.0 → draw all vectors with unit length)
RYLENG	Length of a unit vector in rasters (note that page width, for example, is always 4000 rasters)
NVIIEWS	Number of "user-defined" views (default: NVIIEWS=0)
KVIIEWS(I)	Where KVIIEWS define up to 10 "standard-views" 1 = side view 2 = top 3 = bottom 4 = inside 5 = front 6 = rear 7 = lower outside front 45° 8 = upper outside front 45° 9 = lower outside rear 45° 10 = upper outside rear 45° If KVIIEWS(I)=0, then all 10 views are drawn (default: KVIIEWS(I)=0)

KSECT Section numbers for which plots will be drawn. Up to 40 sections can be selected. If no values specified, then all sections will be drawn.

If **NVIEWS**>0, then **NVIEWS** additional cards are required:

PSI(I), THET(I), PHI(I) (3F10.6)

defining rotation angles (see explanation in TSO submit procedure, Fig. 26) for each "user-defined" view.

A sample execution of the interactive **VECPLOT** submit CLIST is shown as part of the **DF12 Mode 2 TSO** submit in Fig. 26. The **JCL** stream that was produced is shown in Fig. 27(c). A sample output of **VECPLOT** is shown in Fig. 29.

5.2.6 Post-Processing Program: **ISOPLLOT**

Input to the isogram plotting program **ISOPLLOT**, consists of: (1) an unformatted **P/V** (pressure/velocity) dataset from **MODE 1** or **MODE 2**, and (2) a unit 5 card-image dataset containing control flags written in **NAMELIST/INPUT/** format:

IDEBUG 0 = (default) normal execution
1 = generate debug print

ISCAL Scale definition used to set **Cp** minimum and increment values:

ISCAL	Cp_{min}	ΔCp
1	-1.0	0.02
2	-3.0	0.05
3	-7.0	0.10
4	-15.0	0.20
5	No limit	Automatic

(default: 5)

IPLOTS Plot selection flag:
0 = generate all plots
1 = **Cp** plots only
2 = delta-star plots only
3 = skin-friction plots only

NVIEWS Number of "user-defined" views (up to 9 views can be defined)
(default: **NVIEWS**=0)

KVIEWS(I) Define up to 10 "standard-views"
 1 = side view
 2 = top
 3 = bottom
 4 = inside
 5 = front
 6 = rear
 7 = lower outside front 45°
 8 = upper outside front 45°
 9 = lower outside rear 45°
 10 = upper outside rear 45°
 If KVIEWS(1) = 0, then all 10 views are drawn
 (default: KVIEWS(1)=0)

KSECT Section numbers for which plots will be drawn. Up to 40 sections can be selected. If no values specified, then all sections will be drawn.

If NVIEW>0, then NVIEW additional cards are required:

PSI(I), THET(I), PHI(I) (3F10.6)

defining rotation angles for each "user-defined" view.

A sample execution of the interactive ISOPLLOT submit CLIST is shown as part of the DF12 Mode 2 TSO submit in Fig. 26. The JCL stream that was produced is shown in Fig. 27(d). A sample output of the ISOPLLOT program is shown in Fig. 29.

5.2.7 Post-Processing Program: TRACE-ON

Unlike VECPLOT and ISOPLLOT, this is an interactive (on TSO) surface streamline calculating program which requires as input a P/V (pressure/velocity) dataset from MODE 1 or MODE 2 and user responses to the interactive questions. In using this program, one area which the user must understand is the method of telling the program where to "start" streamlines. For the purposes of TRACE-ON, the body surface is assumed to consist of a number of SECTIONS, each of which consists of an NU by NV grid of data, where NU and NV represent the number of points along N-lines of data, and M-lines of data, respectively, of a given SECTION. Note that both MODE 1 and MODE 2 extrapolate the computed potential flow velocity data to the edges of the input SECTIONS. This means that there are more data values in the P/V dataset than panels printed on the MODE 1 and MODE 2 output sheets. For example, say the user inputs a section

with M "chordwise" points on each of N N-lines (see Fig. 31); the number of panels produced in the potential flow program is $(M-1) \times (N-1)$. But the number of data points on the P/V dataset is $(M+1) \times (N+1)$ since the data is extrapolated "chordwise" (i.e. in the N-line direction) at the beginning and end of the strip of panels, and "spanwise" to the "inboard" and "outboard" edges of the section. All the data points may therefore be described by parametric variables in the N-line and M-line directions; these are referred to, herein, by U and V, respectively. Thus the first control point of the potential flow program is called U=2., V=2., (not 1.,1. since 1.,1. would refer to the corner of the section). The second control point (along the same strip of panels in the section) would be U=3., V=2., and so on, as shown in the figure.

A sample execution of the TRACE-ON program is shown in Fig. 32, and a plot of the calculated streamlines are shown in Fig. 33.

6.0 REFERENCES

1. Hess, J.L. and Stockman, N.O.: An Efficient User-Oriented Method for Calculating Compressible Flow about Three-Dimensional Inlets. AIAA Paper No. 79-0081, Jan. 1979.
2. Hess, J.L. and Friedman, D.M.: Analysis of Complex Inlet Configurations Using a Higher-Order Panel Method. AIAA Paper No. 83-1823, Jul. 1983.
3. Hess, J.L. and Friedman, D.M.: An Improved Higher-Order Panel Method for Three-Dimensional Lifting Flow. Rept. No. NADC-79277-60, Dec. 1981.
4. Hess, J.L.: A Higher-Order Method for Three-Dimensional Potential Flow. Rept. No. NADC 77166-30, Jun. 1979.
5. Hess, J.L.: Calculation of Potential Flow About Arbitrary Lifting Bodies. McDonnell Douglas Rept. No. J5671, Oct. 1972.
6. Margason, R.J., et al: Subsonic Panel Methods - A Comparison of Several Production Codes. AIAA Paper No. 85-280, Jan. 1985.
7. Maskew, B.: Prediction of Subsonic Characteristics - A Case for Low-Order Panel Methods. AIAA Paper No. 81-0252, Jan. 1981.
8. Clark, R.W.: A New Iterative Matrix Solution Procedure for Three-Dimensional Panel Methods. AIAA Paper No. 85-0176, Jan. 1985.
9. Hess, J. L. and Smith, A.M.O.: Calculation of Potential Flow About Arbitrary Bodies. Progress in Aeronautical Sciences, Vol. 8, Pergamon Press, New York, 1966.
10. Varga, R.S.: Matrix Interactive Analysis. Academic Press, New York, 1961.

11. Labrujere, T.E., Loeve, W. and Slooff, J.W.: An Approximate Method for the Calculation of the Pressure Distribution of Wing-Body Combinations at Subcritical Speeds. AGARD Conference Proceedings No. 71, Aerodynamic Interference, Wash. D.C., Sept. 1971.
12. Bratkovich, A. and Marshall, F.A.: Iterative Techniques for the Solution of Large Linear Systems in Computational Aerodynamics. J. Aircraft, Vol. 12, No. 2, Feb. 1975.
13. Lieblein, S. and Stockman, N.O.: Compressibility Correction for Internal Flow Solutions. J. of Acft, Vol. 9, No. 4, Apr. 1972.
14. Albers, J.A. and Stockman, N.O.: Calculation Procedures for Potential and Viscous Flow Solutions for Engine Inlets. Trans. of ASME, J. of Engg. Power, Jan. 1975.
15. Albers, J.A.: Theoretical and Experimental Internal Flow Characteristics of a 13.97-Centimeter-Diameter Inlet at STOL Takeoff and Approach Conditions. NASA TN D-7185, Mar. 1973.
16. Dietrich, D.A., Oehler, S.L. and Stockman, N.O.: Compressible Flow Analysis About Three-Dimensional Wing Surfaces Using a Combination Technique. AIAA Paper No. 83-0183, Jan. 1983.
17. Hess, J.L.: Higher-Order Numerical Solution of the Integral Equation for the Two-Dimensional Neumann Problem. Computer Methods in Applied Mechanics and Engineering, Vol. 2, No. 1, Feb. 1973.
18. Hess, J.L.: Improved Solution for Potential Flow About Arbitrary Axisymmetric Bodies by Use of a Higher-Order Surface-Source Method. Computer Methods in Applied Mechanics and Engineering, Vol. 5, No. 3, May 1975.
19. Peters, G.J.: Interactive Computer Graphics Application of the Parametric Bicubic Surface to Engineering Design Problems. Computer Aided Geometric Design (Eds.: Barnhill, R.E. and Reisenfeld, R.F.), Academic Press, New York, 1974.

20. Struik, D.J.: *Differential Geometry*. Addison-Wesley, Cambridge, 1950.
21. Semple, W.G.: *A Note on the Relationship of the Influences of Sources and Vortices in Incompressible and Linearized Compressible Flow*. British Aircraft Corp. (Military Aircraft Division) Rept. No. Ae/A/541, Oct. 1977.

ORIGINAL PAGE IS
OF POOR QUALITY

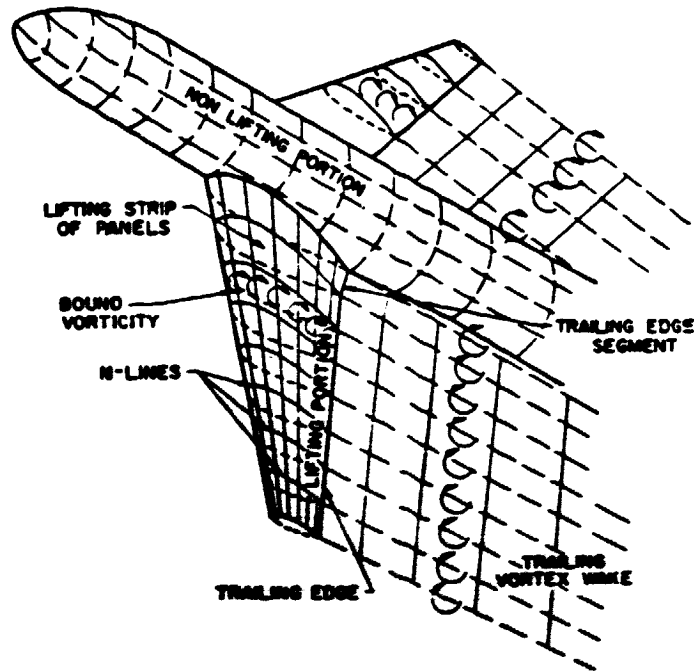


Figure 1. Representation of a three-dimensional lifting configuration.

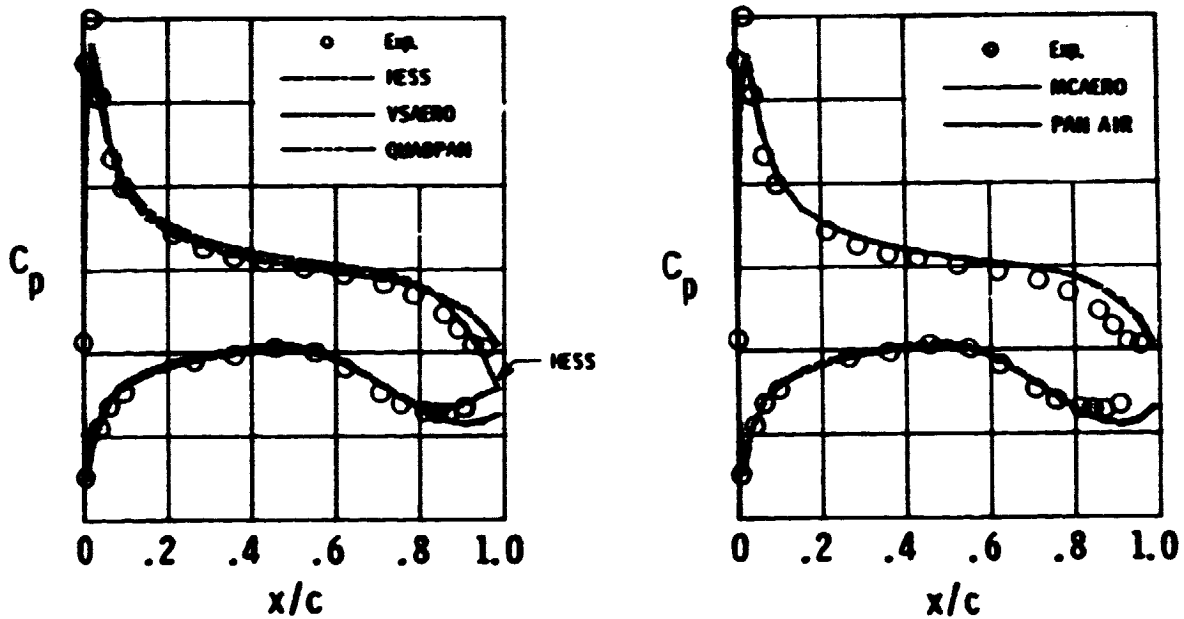


Figure 2. Chordwise pressure distribution for the EET configuration, $\alpha = 0.55$, $\eta = 4.31^\circ$, (a) low order methods, (b) high-order methods.

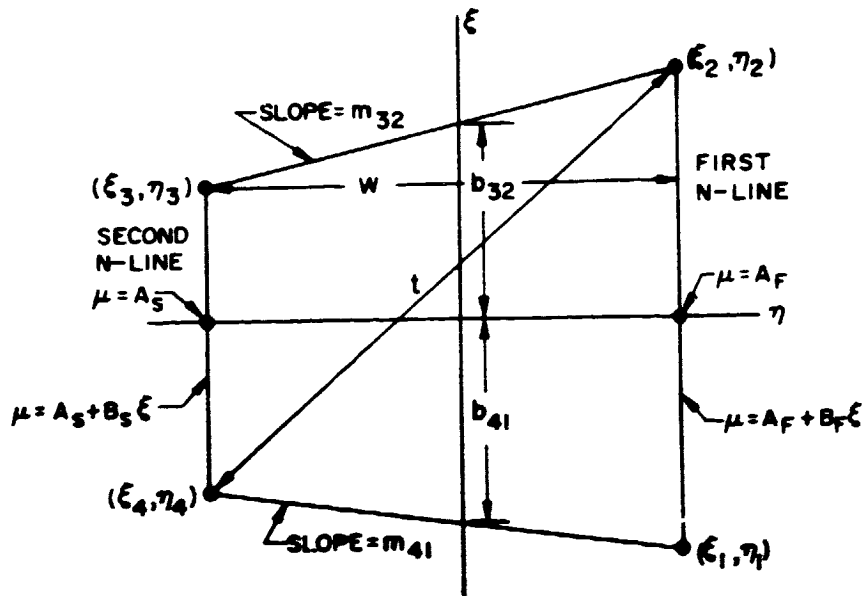


Figure 3. A plane trapezoidal panel.

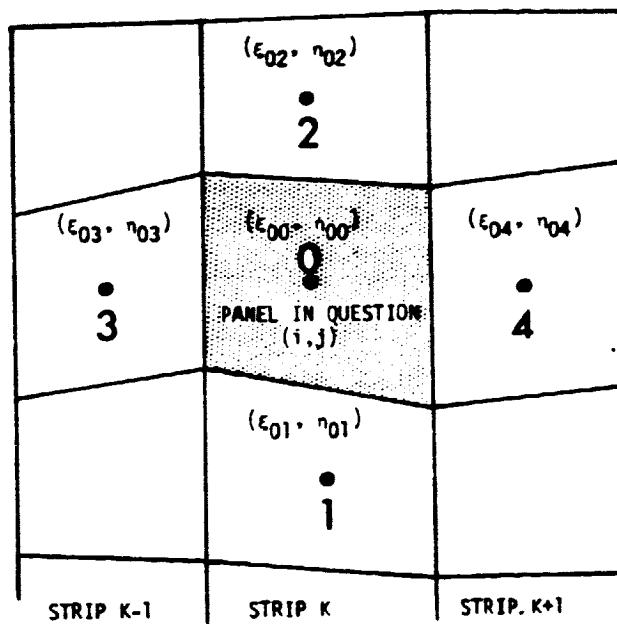


Figure 4. Adjacent panels used in numerical source density derivatives.

ORIGINAL PAGE IS
OF POOR QUALITY

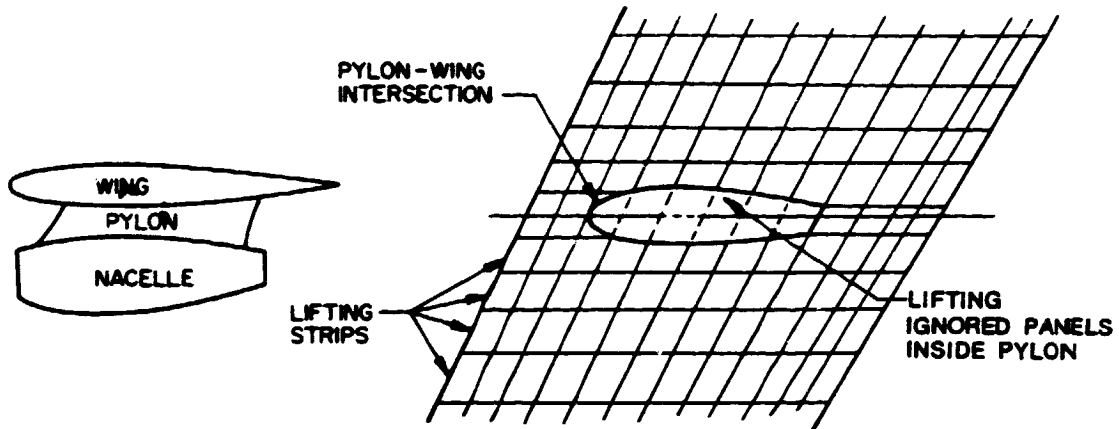


Figure 5. Use of ignored panels.

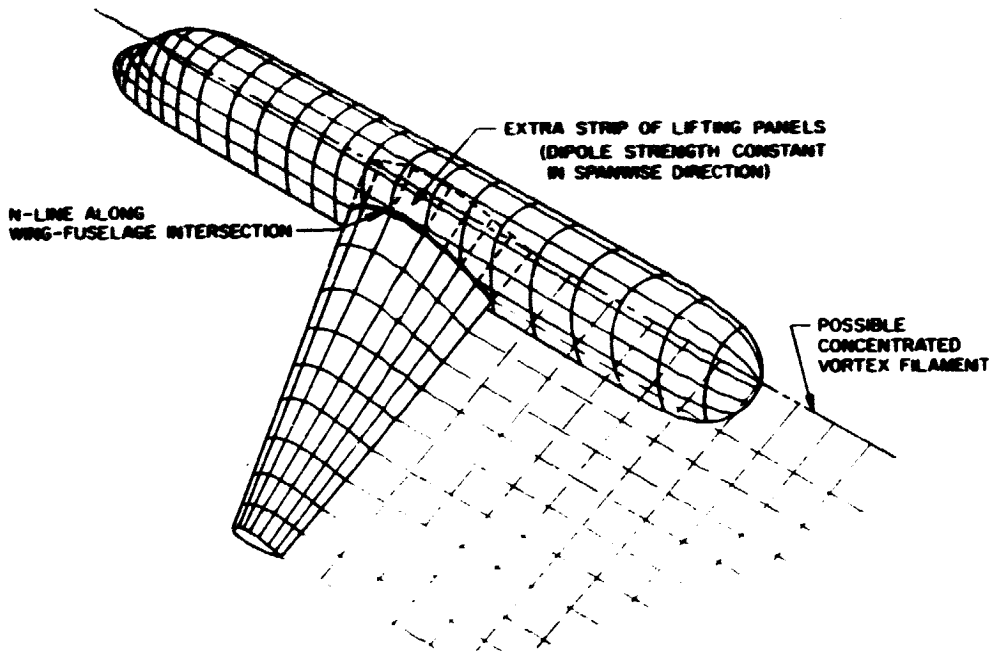
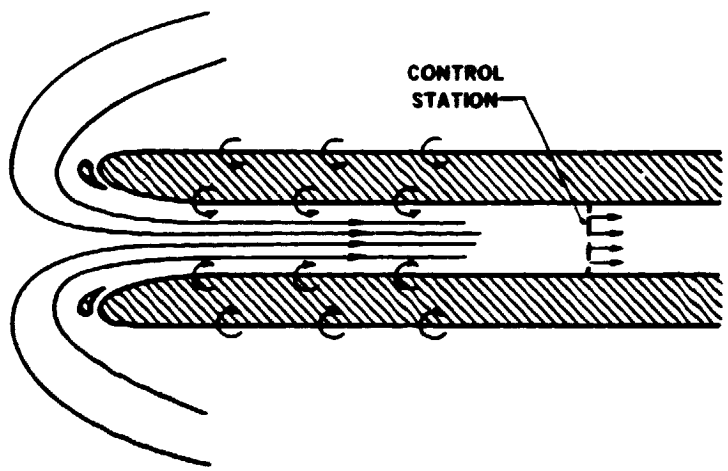
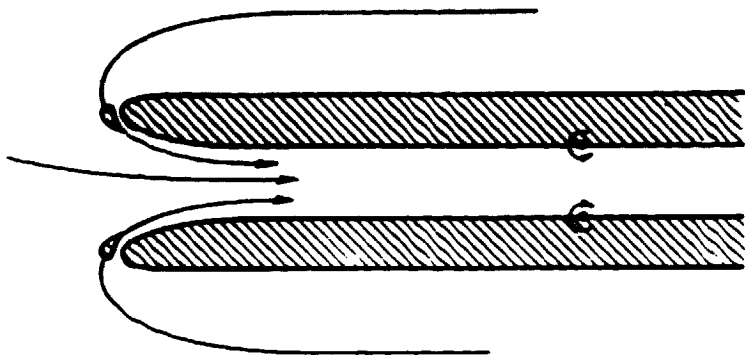


Figure 6. Use of an extra strip.



(a)



(b)

Figure 7. Two methods for obtaining the static fundamental solution, (a) surface vorticity, (b) ring vortex.

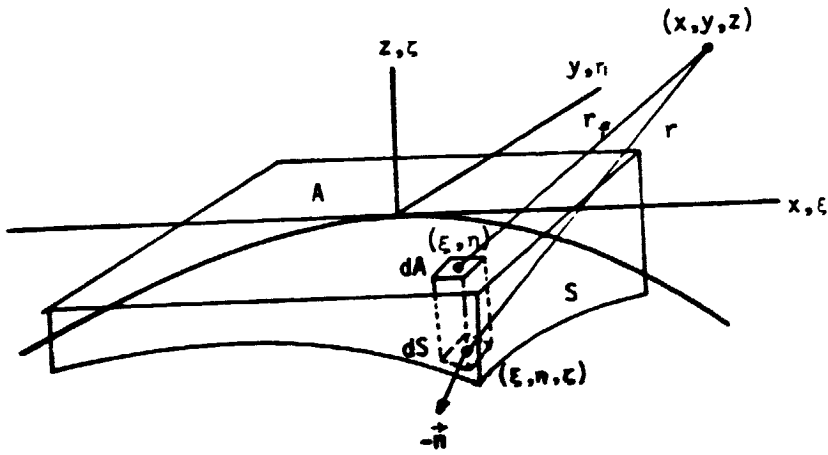
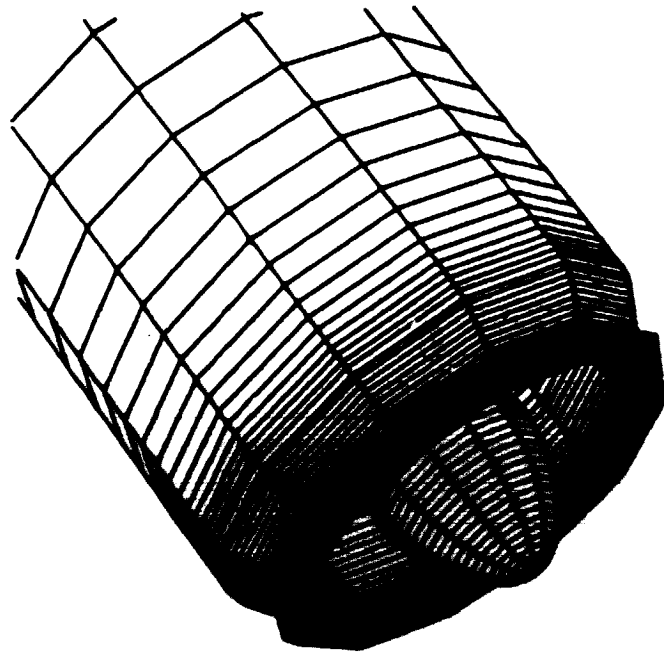
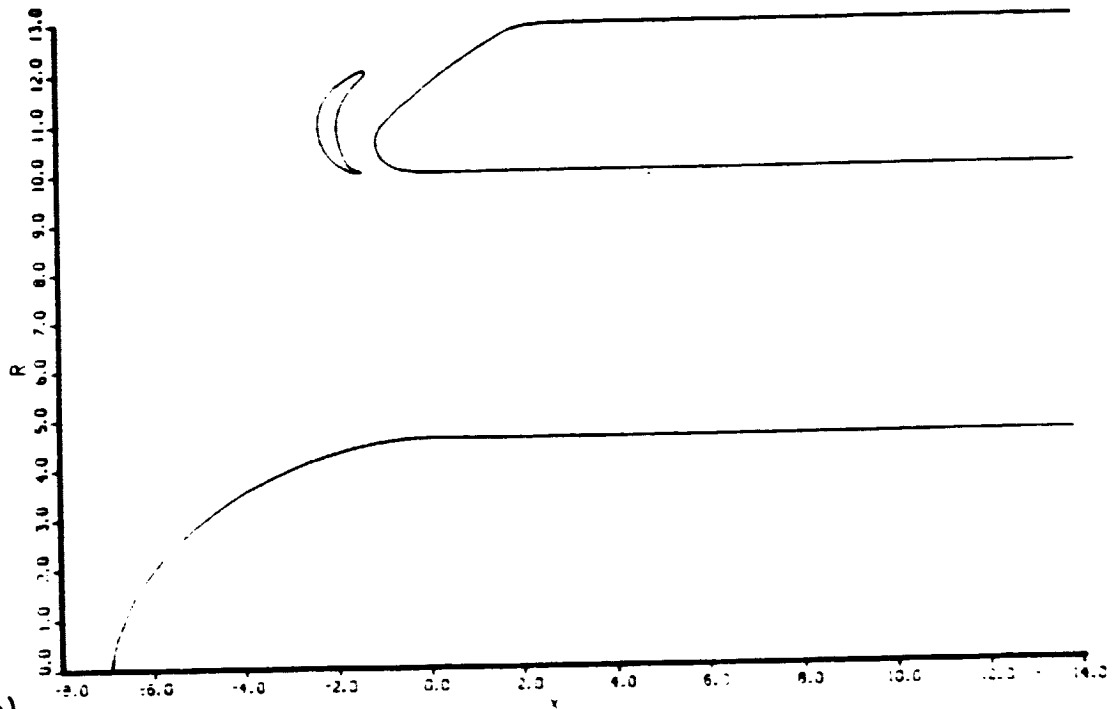


Figure 8. A general curved surface panel and its projection in the tangent plane.



(a)



(b)

Figure 9. Circular Inlet with Leading-Edge Slat and Centerbody. (a) Front View. (b) Cross-Section through Upper Half of Inlet.

ORIGINAL PAGE IS
OF POOR QUALITY



Figure 9. (c) "Faceted" Solid Rendering of Single-Slat Case.

ORIGINAL PAGE IS
OF POOR QUALITY

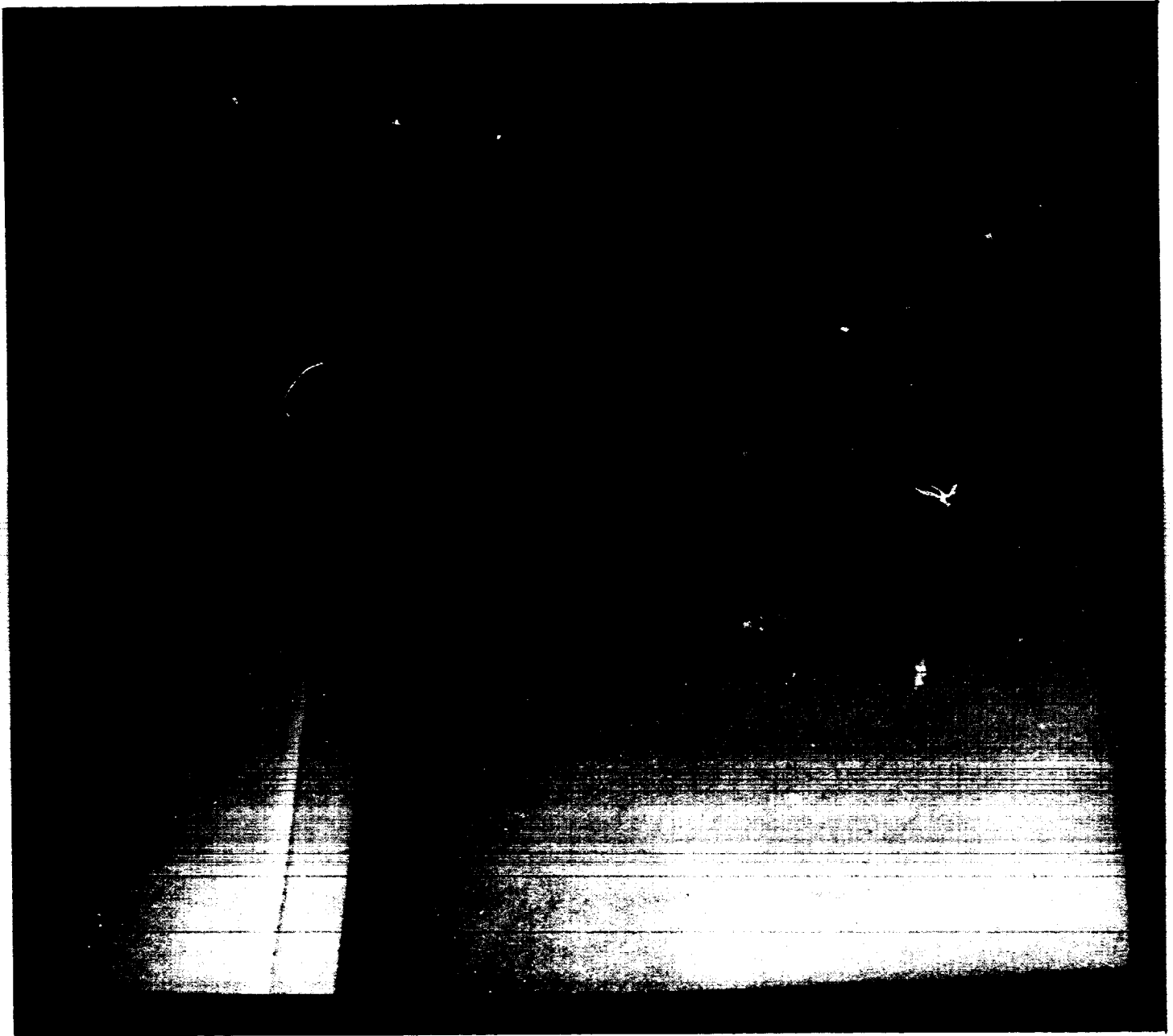
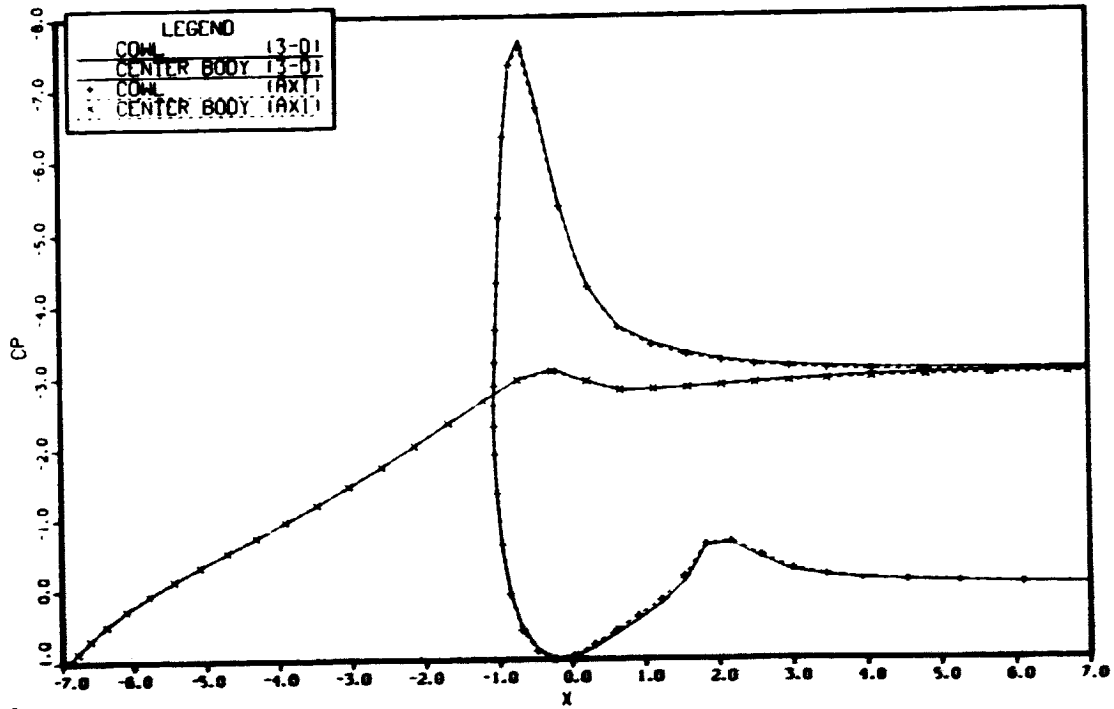
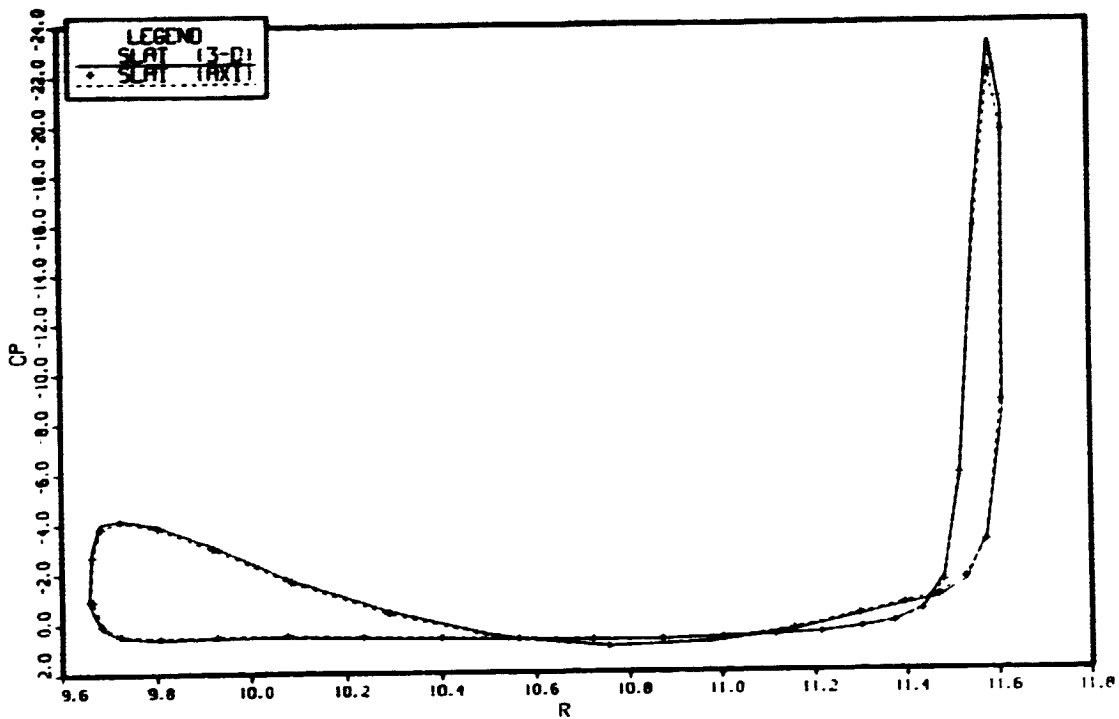


Figure 9. (d) "Smooth-Shaded" Solid Rendering of Side-View Closeup of Single-Slat Case.



(a)



(b)

Figure 10. Comparison Between Axisymmetric and Three-Dimensional Methods for Single Slat Inlet. (a) Pressure Distribution on Cowl and Centerbody. (b) Pressure Distribution on Slat.

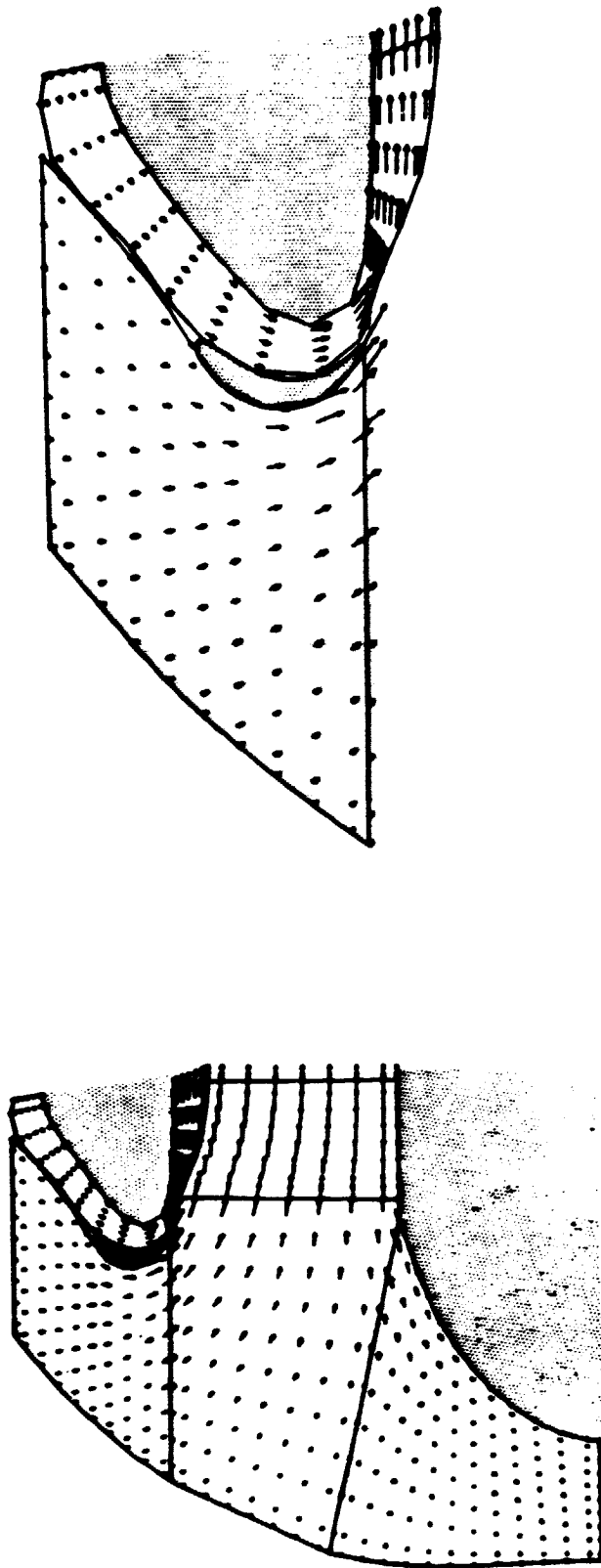


Figure 11. Flowfield for inlet with single slit. Static Solution.

ORIGINAL PAGE IS
OF POOR QUALITY

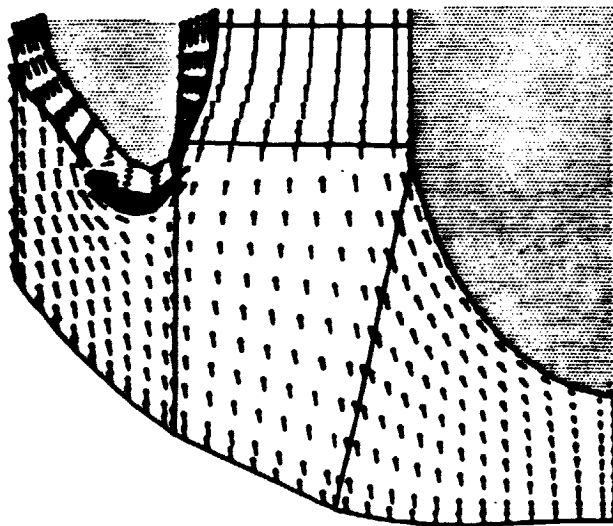
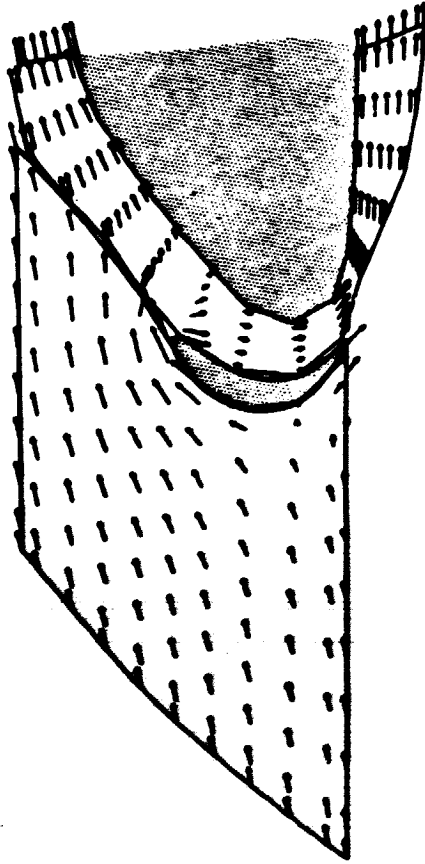


Figure 12. Flowfield for Inlet with Single Slat. Zero Angles of Attack and Yaw. No Added Suction.

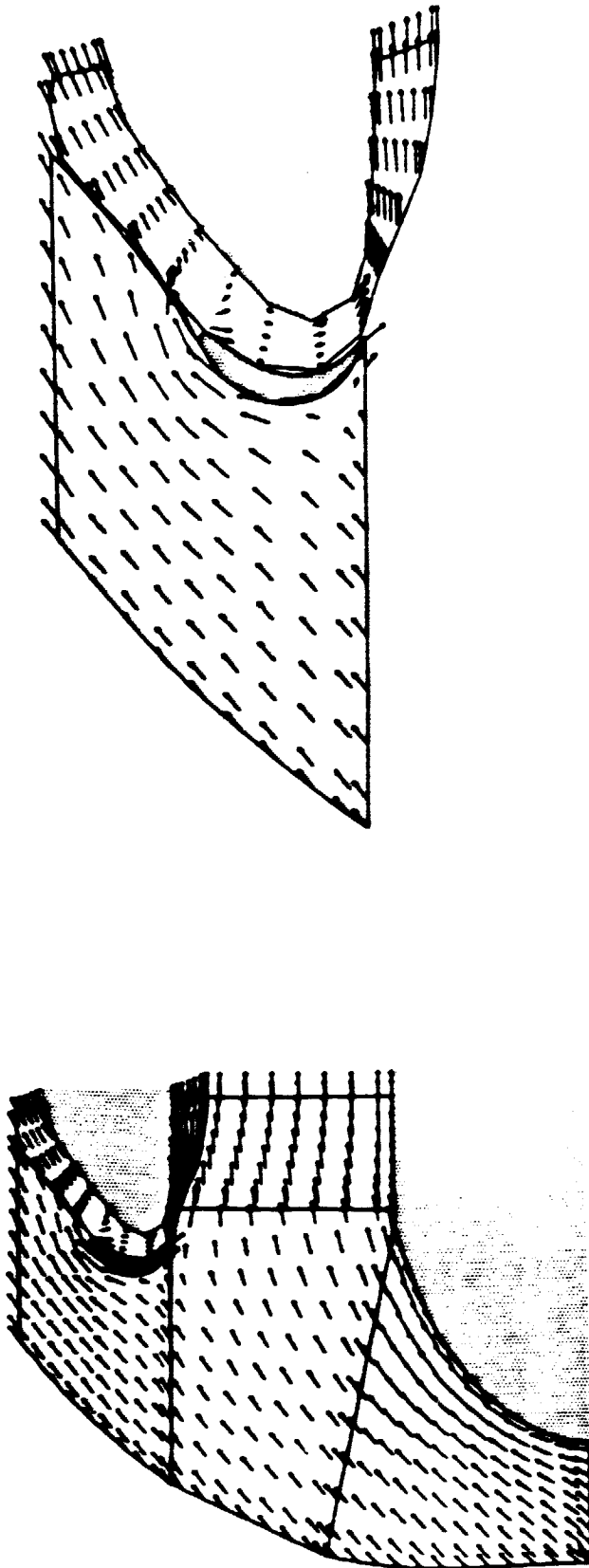


Figure 13. Flowfield for Inlet with Single Slat. Combined Solution, 40° Angle of Attack, Zero Yaw, Fan Face Velocity Twice Freestream.

ORIGINAL PAGE IS
OF POOR QUALITY

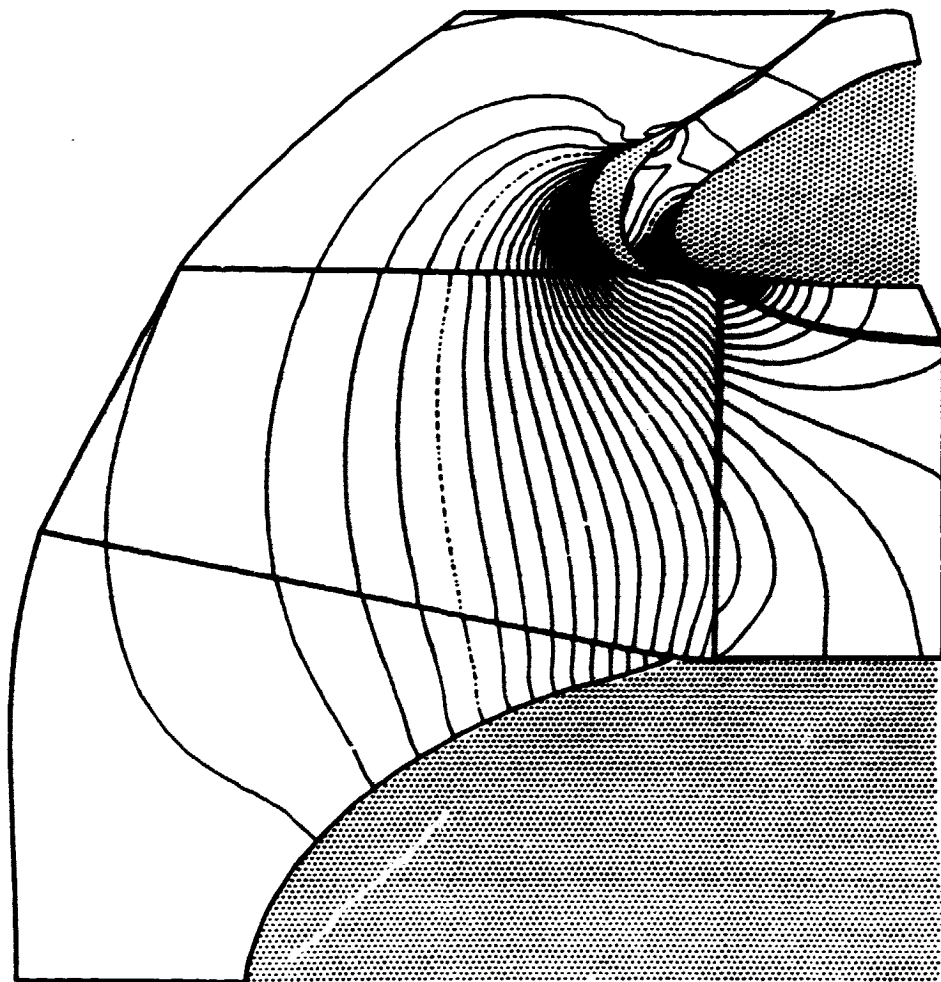


Figure 14. Off-Body Isobars for Inlet with Single Slat. Static Solution.

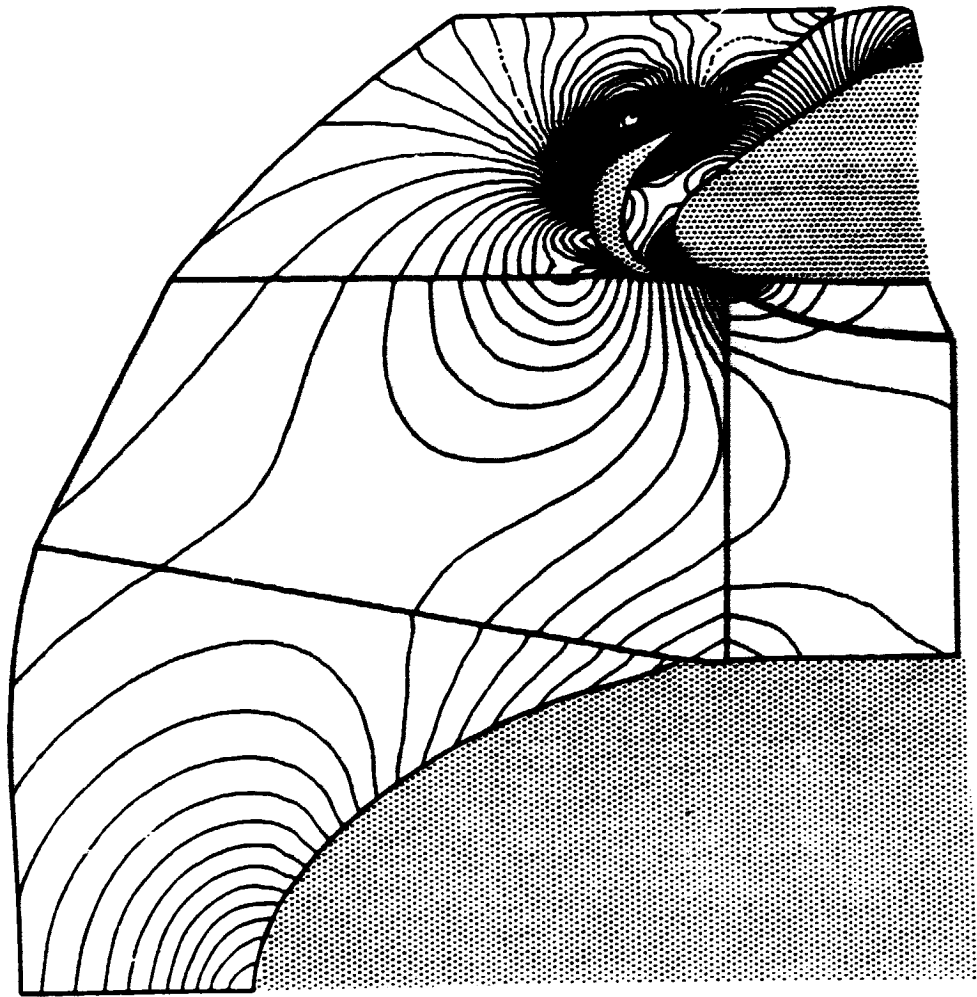


Figure 15. Off-Body Isobars for Inlet with Single Slat. Zero Angles of Attack and Yaw. No Added Suction.

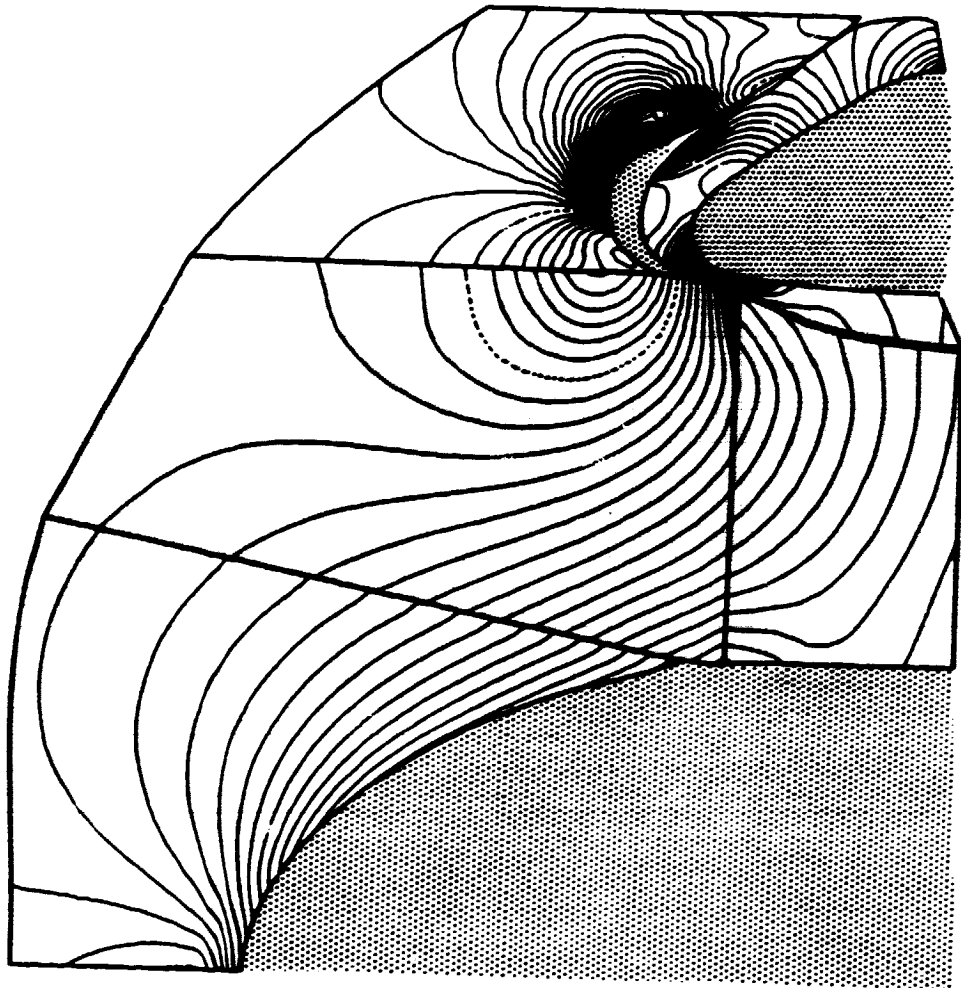
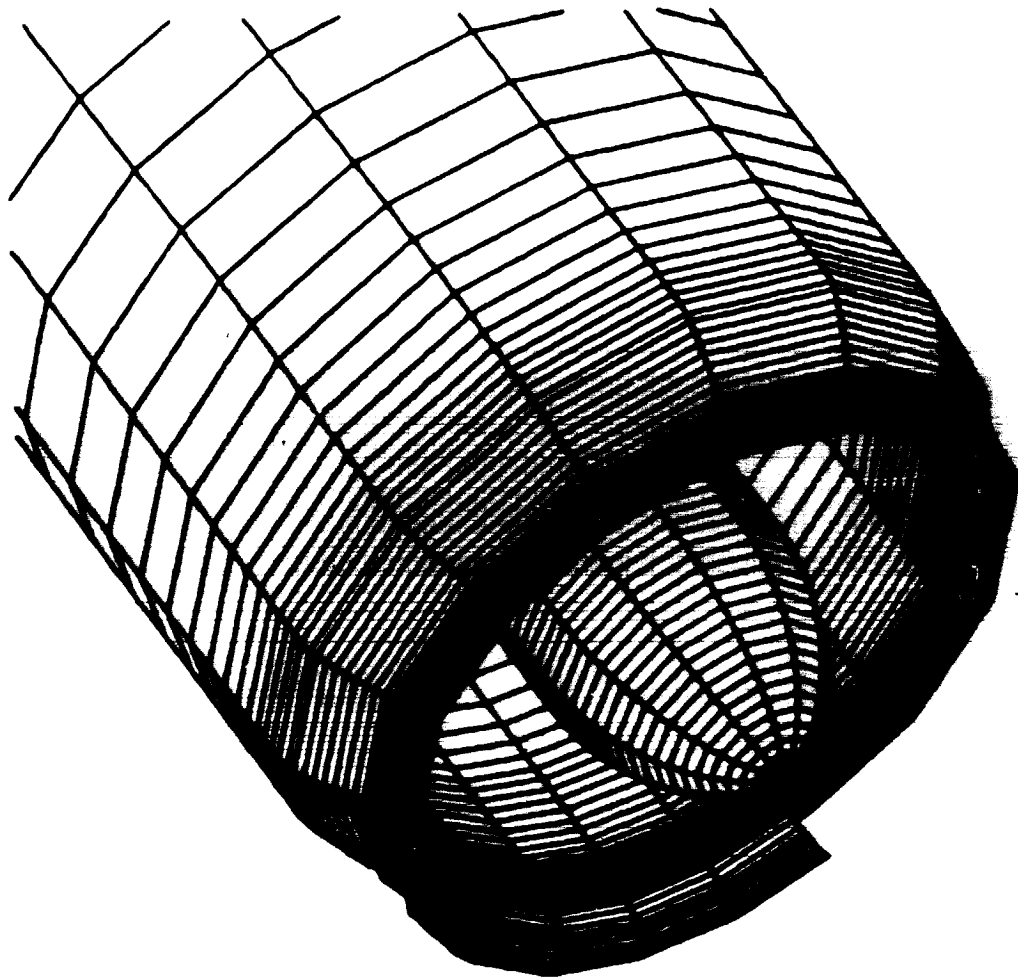


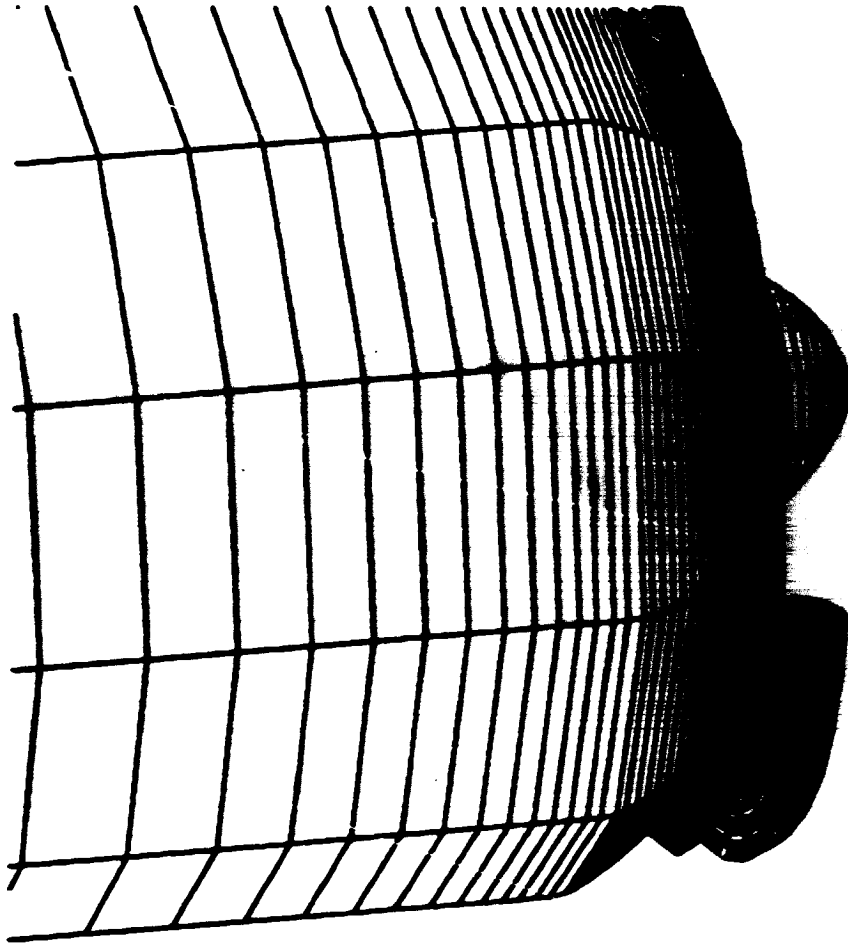
Figure 16. Off-Body Isobars for Inlet with Single Slat. Combined Solution, 40° Angle of Attack, Zero Yaw, Fan Face Velocity Twice Freestream.



(a)

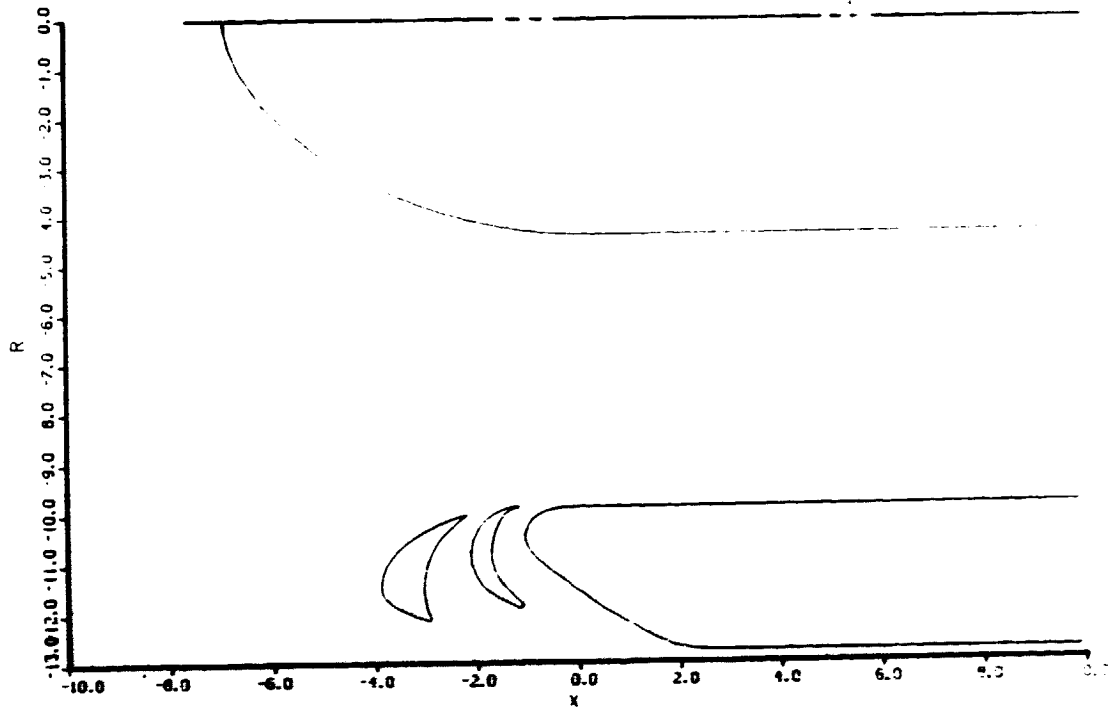
Figure 17. Three-Dimensional Double Slat Inlet Configuration. (a) Front View.

ORIGINAL PAGE IS
OF POOR QUALITY



(b)

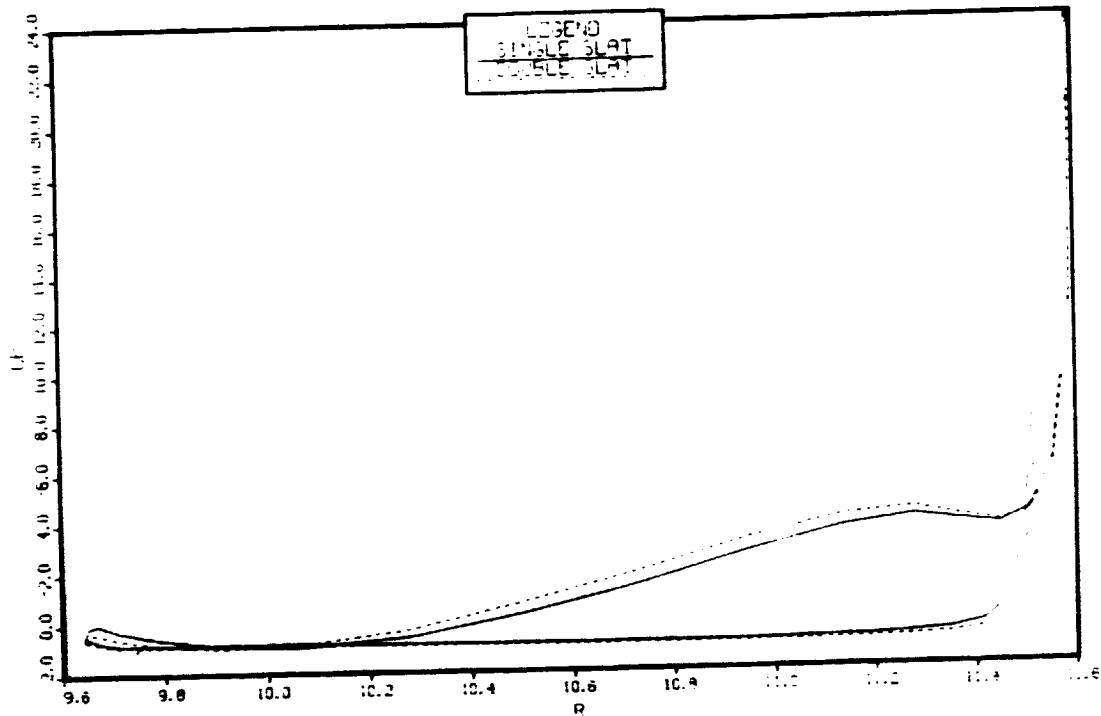
Figure 17. (b) Rear View of Double Slats.



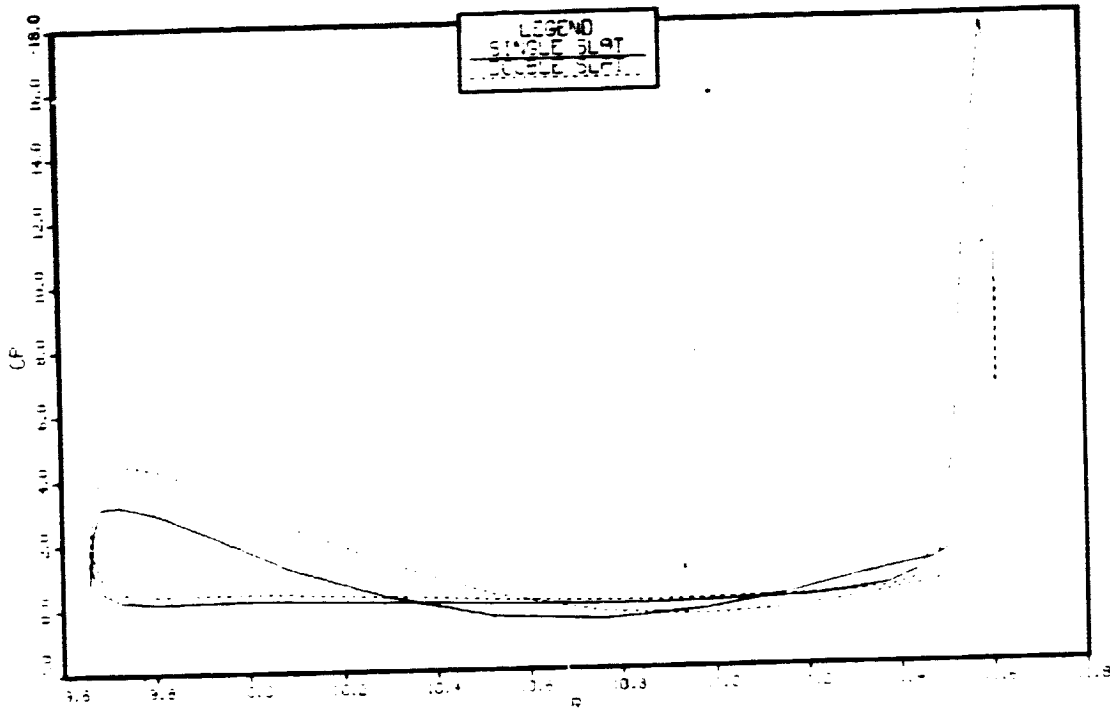
(c)

Figure 17. (c) Cross-Section Through Lower Half of Inlet.

ORIGINAL PAGE IS
OF POOR QUALITY

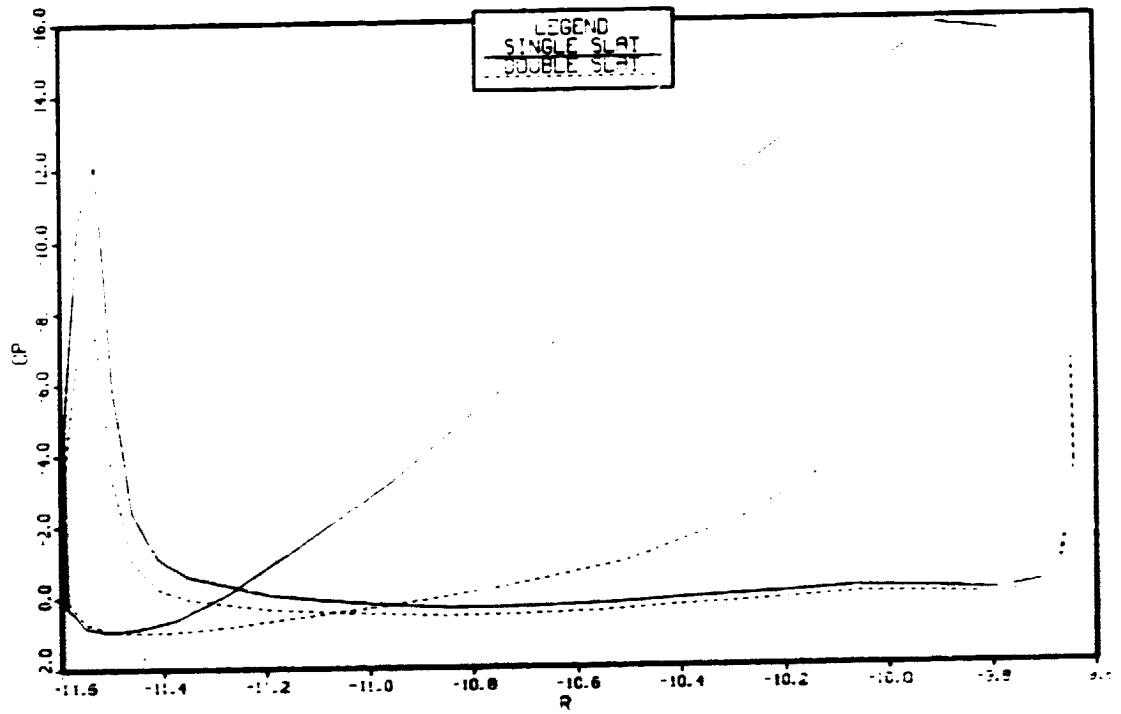


(a)



(b)

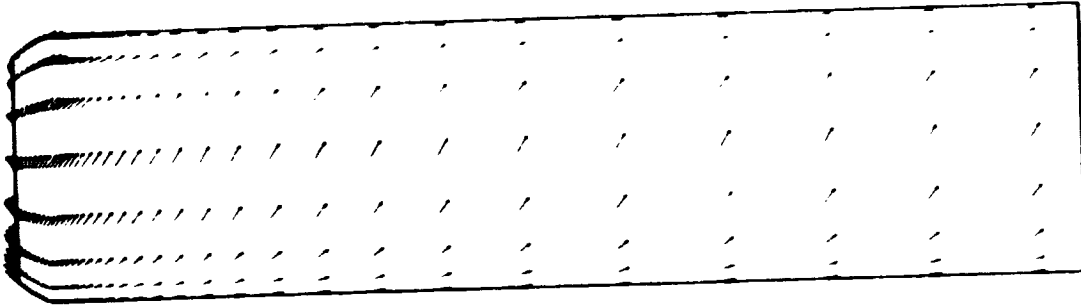
Figure 18. Comparison of Main Slat Pressure Distributions on Single and Double Slat Configurations. 40° Angle of Attack, Zero Yaw, Fan Face Velocity Twice Freestream. (a) 13° from Top Center. (b) 90° From Top Center.



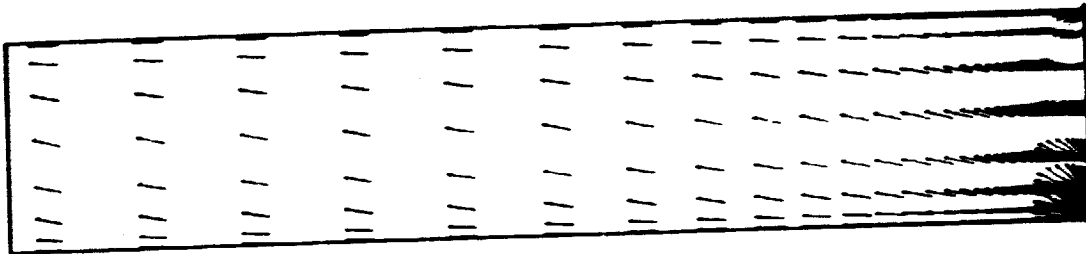
(c)

Figure 18. (c) 171° from Top Center.

ORIGINAL PAGE IS
OF POOR QUALITY

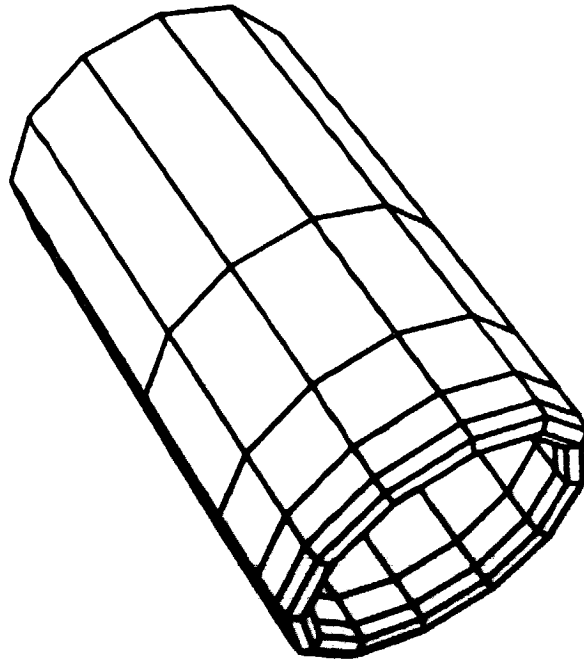


(a)

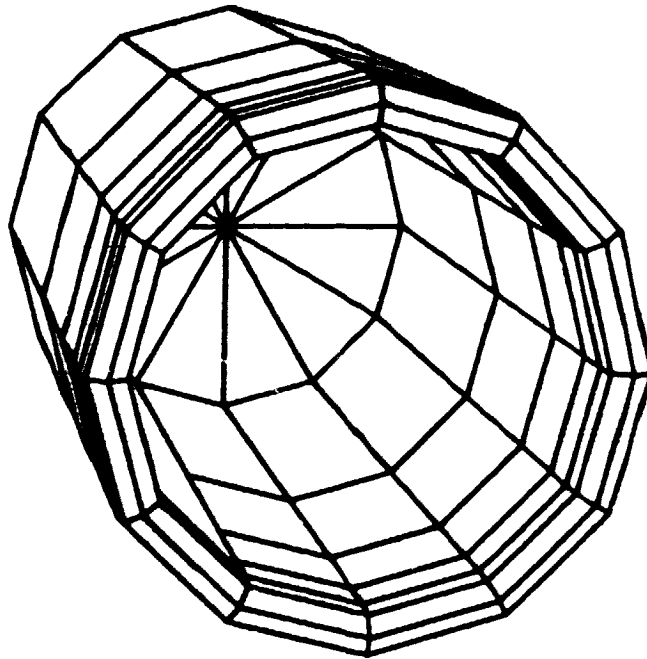


(b)

Figure 19. Velocity Vectors for Double Slat Configuration. 40° Angle of Attack. Zero Yaw, Fan Face Velocity Twice Freestream. (a) On Outer Cowl Surface. (b) On Inner Cowl Surface.



(a)



(b)

Figure 20. Wire-Frame Pictures of the 72-Panel (on the "Half-Body") Round Inlet. Note the "Doublet Surface" Visible Inside At the Rear of (b).

ORIGINAL PAGE IS
OF POOR QUALITY

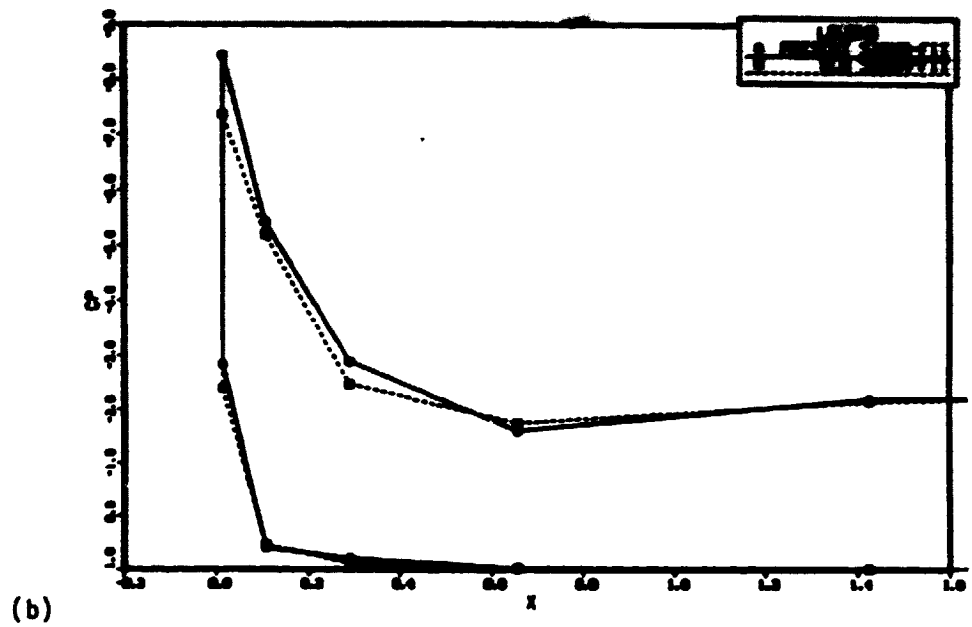
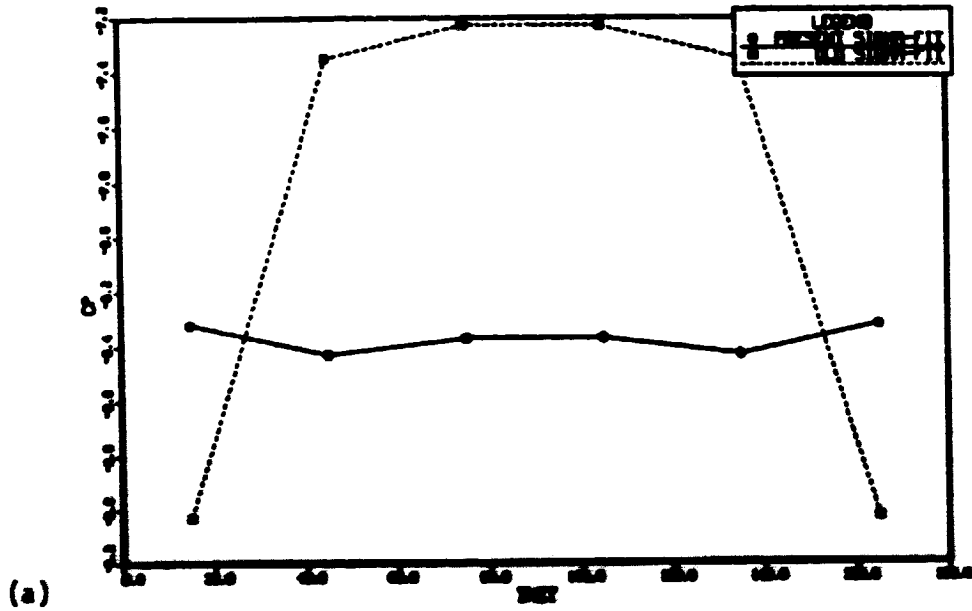


Figure 21. (a) Variation of Peak C_p with Theta (Circumferential Angle) (for the 72-Panel Round Inlet) for the Old and New Sigma-Fitting Procedure. (b) Sample Comparison of Chordwise Variations for a Fixed Theta ($\theta = 75$ Degrees).

ORIGINAL PAGE IS
OF POOR QUALITY

4.0790472-0.0000020	1.1999998241	0.1683279	0.9999989	0.000002000
1.9385128-0.0000020	1.199999800	0.4084057	0.9999989	0.000002000
0.9062307-0.0000020	1.199999800	0.9062307	0.9999989	0.000002000
0.4084057-0.0000020	1.199999800	1.9385128	0.9999989	0.000002000
0.1683279-0.0000020	1.199999800	4.0790472	0.9999989	0.000002000
0.0500000-0.0000020	1.186600700	4.0790472	1.0392303-0.599998010	
0.0	0.099997500	1.9385138	1.0392303-0.599998000	
0.0500000-0.0000020	1.013394400	0.9062312	1.0392303-0.599998000	
0.1683279-0.0000020	0.999998900	0.4084061	1.0392303-0.599998000	
0.4084057-0.0000020	0.999998900	0.1683283	1.0392303-0.599998000	
0.9062307-0.0000020	0.999998900	0.0500004	1.0276270-0.593299900	
1.9385128-0.0000020	0.999998900	0.0	0.9526286-0.549997300	
4.0790472-0.0000020	0.999998900	0.0500004	0.8776278-0.506695700	
4.0790472	0.5999980	1.039231310	0.1683283	0.8660259-0.499997000
1.9385118	0.5999980	1.039231300	0.4084057	0.8660259-0.499997000
0.9062304	0.5999980	1.039231300	0.9062309	0.8660259-0.499997000
0.4084049	0.5999980	1.039231300	1.9385138	0.8660259-0.499997000
0.1683289	0.5999978	1.039230300	4.0790472	0.8660259-0.499997000
0.0499990	0.5932995	1.027627000	4.0790472	0.6000010-1.039229410
0.0	0.5499979	0.952628000	1.9385128	0.6000010-1.039229400
0.0499990	0.5066960	0.877627100	0.9062316	0.6000010-1.039229400
0.1683289	0.4999970	0.866024000	0.4084059	0.6000010-1.039229400
0.4084049	0.4999978	0.866024000	0.1683283	0.6000007-1.039229400
0.9062302	0.4999970	0.866024000	0.0499990	0.5932995-1.027627000
1.9385118	0.4999970	0.866024000	0.0	0.5499979-0.952628000
4.0790472	0.4999970	0.866024000	0.0500000	0.8776278-0.506695700
4.0790472	1.0392284	0.600002010	0.1683284	0.4999989-0.866024000
1.9385128	1.0392284	0.600002000	0.4084059	0.4999989-0.866024000
0.9062304	1.0392284	0.600002000	0.9062314	0.4999989-0.866024000
0.4084051	1.0392284	0.600002000	1.9385128	0.4999989-0.866024000
0.1683279	1.0392275	0.600001600	4.0790472	0.4999989-0.866024000
0.0499995	1.0276251	0.593302800	4.0790472	0.0
0.0	0.9526258	0.550001000		-1.199999810
0.0500004	0.8776255	0.506698800		
0.1683288	0.8660239	0.499999800		
0.4084064	0.8660240	0.499999800		
0.9062319	0.8660240	0.499999800		
1.9385128	0.8660240	0.499999800		
4.0790472	0.8660240	0.499999800		
4.0790472	1.1999998	0.000002010		
1.9385128	1.1999998	0.000002000		
0.9062307	1.1999998	0.000002000		
0.4084057	1.1999998	0.000002000		
0.1683279	1.1999998	0.000002000		
0.0500000	1.1866007	0.000002000		
0.0	0.9999975	0.000002000		
0.0500000	1.0133944	0.000002000		
			1.9385128	0.0
			0.9062307	0.0
			0.4084057	0.0
			0.1683279	0.0
			0.0500000	0.0
			0.0	0.0
			0.0500000	0.0
			0.1683279	0.0
			0.4084057	0.0
			0.9062307	0.0
			1.9385128	0.0
			4.0790472	0.0
				-1.199999800
				-1.199999800
				-1.199999800
				-1.199999800
				-1.186600700
				-1.099997500
				-1.013394400
				-0.999998900
				-0.999998900
				-0.999998900
				-0.999998900
				-0.999998900
				-0.999998900
				-0.999998900

Figure 22. Coordinates used for the 72-panel simple inlet check case.

ORIGINAL PAGE IS
OF POOR QUALITY

02 0018

*** 3-D HIGHER-ORDER LIFTING HELMHOLTZ PROGRAM ***
(WITH OR WITHOUT INLETS)
LAST REVISION: 18 JUL 1968 ..

MODE OPTIONS:

- 1 - DELETE MOD-BASED MATRIX.
- 0 - RE-START FROM MOD-BASED MATRIX.
- 1 - GENERATE (FUNDAMENTAL) SOLUTIONS.
- 2 - COMBINE FUNDAMENTAL SOLUTIONS.

ENTER SELECTION (-1,0,1, OR 2) .. 1

ENTER A (NEW) 'CASE-ID' (UP TO 8 CHARACTERS, BEGINNING WITH AN ALPHABETIC CHARACTER) ...

CASEID = TEST1

ENTER THE GEOMETRY DATASET (3-D HELMHOLTZ FORMAT OR 'PCU') NAME ...
(PARALLELETT OR FULLY QUALIFIED, CATALOGED NAME (NO QUOTES))

DSN = H31H0871
 NAME LUL USER TYPE STAT PRINT ACCESS BLKS STATSTS ACT ANG S
 H31H0871 4 DAT TEA 081408 071705 2 01 42 08.4
 2 6X12-78 PANEL ROUND INLET FLAGGED AS A 'SDFV' SECT
 DONE
 DONE 01 STAT(S) LEVEL 004
 A TEMPORARY COPY HAS BEEN CREATED: DSN = TEST1F.TEMP080R.081705.T171054

FLAG DATASET 'TEST1F.0807F.MODE1.FLAGS' NOT FOUND. OPTIONS ARE ...

C/R ... CREATE IT NEW, OR

ENTER NEW FLAG DATASET (FULLY QUALIFIED, NO QUOTES)

ENTER OPTION (C/R OR DATASET NAME) ...

MODE 1 SECTION CURRENT: SDFV= 0, SDFP= 0, SDFE= 0, SDFL= 0, SDFU= 1, SDFW= 0
REFERENCE GEOMETRY:

TIME-----

MODE = 1-3D HIGHER ORDER HELMHOLTZ WITH OR WITHOUT INLETS.
 SDFV = 1-3D HIGHER ORDER HELMHOLTZ WITH OR WITHOUT INLETS.
 SDFP = 1-3D HIGHER ORDER HELMHOLTZ WITH OR WITHOUT INLETS.
 SDFE = 0.0
 SDFL = 0.0
 SDFU = 0.0
 SDFW = 0.0

FLAG NAME	PARENT VALUE	DEFAULT VALUE	FLAG DEFINITION
INPUTS	1	1	0-INPUT MODEL, 1-T.E. STRUCTURE, 2-PARALLEL TO T.E.
BOUND	0	0	0-DO NOT SAVE PANG.SOLA. FOR COMB.POR., 1-SAVE.
INFLDS	0	0	0-STORED FLAG LIST, 1-GENS FLAG LIST.
SPWOP	2	2	0-NO PANG.SOLA. PRINT, 1-RENDER, 2-FULL.
IPCW	0	0	0-COMPACT CIRCULAR VELOCITY, 1-PARALLEL CIRCULAR VELOCITY DISTRIBUTION.
IPWIZ	0	0	0-SMALL PRINTSIZE (104-COLUMNS), 1-LARGE PRINTSIZE (128-COLUMNS).
IPV	0	0	0-DO NOT SAVE P/V DATASET, 1-SAVE P/V DATASET (FOR 'ISOPLOT', ETC.).
ISMK	0	0	0-DO NOT SAVE 'SMAPLOT'-TYPE DATASET, 1-SAVE.
LO	0	0	0-HIGHER-ORDER SOLUTION, 1-LOWER-ORDER SOLUTION.
NOVW	1	1	0-NO SYMMETRY, 1-SYMMETRIC ABOUT V-O PLANE.

ALPHA(DES.) BETA(DES.)

*** NONE YET DEFINED ***

IXTRA - STRIP NUMBERS OF THE 'EXTRA' STRIPS (ENTER 'IXTRA=0' TO DELETE):
*** NONE YET DEFINED ***

ENTER UPDATES, OR 'LIST', OR 'RESTART', OR 'HELP' (FOR PRINT FLAG), OR C/R WHEN DONE

TIME=081408.071705 (4 PANEL ROUND INLET FLAGGED AS 'SDFV' SECTION.)
TIME=H31H0871 (2 PANEL ROUND INLET FLAGGED AS 'SDFV' SECTION.)

ENTER UPDATES, OR 'LIST', OR 'RESTART', OR 'HELP' (FOR PRINT FLAG), OR C/R WHEN DONE

MODE=1, SDFV=1, SDFP=0, SDFE=0, SDFL=0, SDFU=0, SDFW=0

ENTER UPDATES, OR 'LIST', OR 'RESTART', OR 'HELP' (FOR PRINT FLAG), OR C/R WHEN DONE

Figure 23. TSO submittal of DF12, Mode 1, for the 72-panel inlet check case.

ORIGINAL PAGE IS
OF POOR QUALITY

```
NOW COPYING 'TEST2P.0027P.RJZL1.FLASH'  
TO A TEMPORARY DATASET FOR USE IN THE BATCH SUBMITTA ...  
FUNDAMENTAL SOLUTIONS WILL BE STORED IN: TEST2P.0027P.FUNDSOLN  
(THE EXISTING DATASET WILL BE OVERRITTEN.)  
CPU TIME ESTIMATE: CPU =   
I/O TIME ESTIMATE: I/O =   
JOB CLASS OPTIONS:  
C/R FOR NON-DEFERRED  
B FOR DEFERRED (CHEAPER)  
B FOR BACKLOG-DEFERRED (CHEAPEST)  
SELECT JOB CLASS ..   
C/R FOR: SV%OUT =   
SV%OUT =   
C/R FOR: BEST = T3L  
BEST =   
DEFAULT: JOHNNIE = KMF1ET3  
JOHNNIE =   
C/R FOR DEFAULT: CCR =  
ENTER INPUT JOB STREAM:  
JOB PARAMETERS ARE ...  
//KMF1ET3 JOB 2 CPU(0.5) IO(0.2) LINES(40) RECLASS(0)  
//SWIN CLASS-BACKLOG  
JOB KMF1ET3(J000001) SUBMITTED  
READY
```

Figure 23. Concluded.

ORIGINAL PAGE IS
OF POOR QUALITY

H31HG027F: 72-PANEL SIMPLE INLET FLAGGED AS "SRFV" SECTION.
&Z ICOMBO=1, IPR132=1, ALPHA=0,10 &END

1

Figure 24(a). Alternative input dataset for DF12, Mode 1, for the 72-panel simple inlet check case.

```
/**
/** PC-PATCH FITTING FOR: H31HG027F
/**
/**PCPATCH EXEC PGM=H31K,PARM='1,0,0',REGION=1000K
/**STEPLIB DD DSN=TSOT3DF.DIF.LOAD,DISP=SHR
/**FT01F001 DD DSN=TSOT3DF.TEMPGEOM.D080985.T092117,
// DISP=(OLD,DELETE)
/**FT06F001 DD SYSOUT=A
/**FT11F001 DD UNIT=SYSDA,SPACE=(TRK,(30,10)),
// DCB=(RECFM=VBS,BLKSIZE=19069)
/**FT12F001 DD UNIT=SYSDA,SPACE=(TRK,(30,10)),DISP=(NEW,PASS),
// DCB=(RECFM=VBS,BLKSIZE=19069)
/**
/**
/**
/** 3-D HIGHER-ORDER LIFTING NEUMANN SOLUTION.
/** (WITH INLET CAPABILITY)
/**
/** MODE 1, CASEID: G027F
/**
/**NEUMANN EXEC PGM=MAIN,REGION=4000K
/**STEPLIB DD DSN=TSOT3DF.DF12.LOAD,DISP=SHR
/**FT01F001 DD DSN=*.PCPATCH.FT12F001,
// DISP=(OLD,DELETE)
/**FT02F001 DD DSN=TSOT3DF.G027F.FUNDSOLN,
// DISP=SHR
/**FT04F001 DD UNIT=SYSDA,DCB=(RECFM=VBS,BLKSIZE=19069),
// SPACE=(TRK,(1,10))
/**FT05F001 DD DSN=TSOT3DF.DF12.D080985.T092117,DISP=(OLD,DELETE)
/**FT06F001 DD SYSOUT=A,DCB=(RECFM=FBA,LRECL=169,BLKSIZE=16900)
/**FT08F001 DD UNIT=SYSDA,DCB=(RECFM=VBS,BLKSIZE=19069),
// SPACE=(TRK,(1,10))
/**FT09F001 DD UNIT=SYSDA,DCB=(RECFM=VBS,BLKSIZE=19069),
// SPACE=(TRK,(1,10))
/**FT10F001 DD UNIT=SYSDA,DCB=(RECFM=VBS,BLKSIZE=19069),
// SPACE=(TRK,(1,10))
/**FT11F001 DD UNIT=SYSDA,DCB=(RECFM=VBS,BLKSIZE=19069),
// SPACE=(TRK,(1,10))
/**FT12F001 DD UNIT=SYSDA,DCB=(RECFM=VBS,BLKSIZE=19069),
// SPACE=(TRK,(1,10))
/**FT13F001 DD UNIT=SYSDA,DCB=(RECFM=VBS,BLKSIZE=19069),
// SPACE=(TRK,(1,10))
/**FT14F001 DD UNIT=SYSDA,DCB=(RECFM=VBS,BLKSIZE=19069),
// SPACE=(TRK,(1,10))
/**FT15F001 DD UNIT=SYSDA,DCB=(RECFM=VBS,BLKSIZE=19069),
// SPACE=(TRK,(1,10))
/**FT16F001 DD UNIT=SYSDA,DCB=(RECFM=VBS,BLKSIZE=19069),
// SPACE=(TRK,(1,10))
/**FT17F001 DD UNIT=SYSDA,DCB=(RECFM=VBS,BLKSIZE=19069),
// SPACE=(TRK,(1,10))
/**FT18F001 DD UNIT=SYSDA,DCB=(RECFM=VBS,BLKSIZE=19069),
// SPACE=(TRK,(1,10))
/**FT20F001 DD DUPLIC
```

Figure 24(b). Mode 1 JCL stream for the 72-panel simple inlet check case.

```

-----
SECT# 0 PATCHES  NU  NV  MCURV  M-LINES  M-LINES  TYPE  TITLE
-----
1 72 12 6 1 1  CURVED  CURVED  SMPV  NEUMANN SECTION 1
-----
UNFORMATTED DATASET CREATION IN PROGRESS
UNFORMATTED PATCH DATA HAS BEEN CREATED. NPAT = 72
TIME USAGE ... CPU= 0.15 SECONDS, I/O = 0.18 SECONDS.

```

Figure 25. Sample output from the DF12 Mode 1 solution for the 72-panel simple inlet check case.

PAGE 1 DOUGLAS AIRCRAFT COMPANY HIGHER ORDER POTENTIAL FLOW: FUNDAMENTAL SOLUTIONS
CASE TITLE: H31H0827F: 72-PANEL SIMPLE INLET FLAGGED AS "SRFV" SECTION.
PAGE TITLE: INPUT FLAGS

REFERENCE QUANTITIES

TITLE=H31H0827F: 72-PANEL SIMPLE INLET FLAGGED AS "SRFV" SECTION.

AREF = 1.0000 REFERENCE AREA (USE SEMI-AREA IFF NSYMN1).
BOV2 = 1.0000 REFERENCE SEMI-SPAN.
CREF = 1.0000 REFERENCE CHORD LENGTH.
ORIGIN = 0.0 0.0 MOM. REF. CENTER.

FLAG NAME	PRESENT VALUE	DEFAULT VALUE	FLAG DEFINITION
IAUTOM	1	1	0=INPUT MAKES, 1=1. E. BISECTORS, 2=PARALLEL TO T.E.
ICOMBO	0	0	0=DO NOT SAVE FUND.SOLN. FOR COMBO. PLAN., 1=SAVE.
IDEBUG	0	0	0=STANDARD FLAG LIST, 1=DEBUG FLAG LIST.
IFUNDP	2	2	0=NO FUND.SOLN. PRINT, 1=MINIMUM, 2=FULL.
IPV	1	0	0=CONSTANT CHORDWISE VORTICITY, 1=PARABOLIC CHORDWISE VORTICITY DISTRIBUTION.
IPR132	0	0	0=SMALL PRINTSIZE (164-COLUMN), 1=LARGE PRINTSIZE (132-COLUMN).
IPV	0	0	0=DO NOT SAVE P/V DATASET, 1=SAVE P/V DATASET (FOR "ISOPLOT", ETC.).
IQWIK	0	0	0=DO NOT SAVE "QUICKPLOT"-TYPE DATASET, 1=SAVE.
LO	0	0	0=HIGHER-ORDER SOLUTION, 1=LOWER-ORDER SIMULATION.
NSYM	1	1	0=NO SYMMETRY, 1=SYMMETRIC ABOUT Y=0 PLANE.

ALPHA(DEG.)	BETA(DEG.)
1 0.0	0.0
2 10.00	0.0

IEXTRA = STRIP NUMBERS OF THE "EXTRA" STRIPS (ENTER "IEXTRA=0" TO DELETE);
*** NONE YET DEFINED ***

ORIGINAL PAGE IS
OF POOR QUALITY

Figure 25. Continued.

AGE 2 DOUGLAS AIRCRAFT COMPANY HIGHER ORDER POTENTIAL FLOW - FUNDAMENTAL SOLUTIONS

AGE TITLE: HJH0027F: 72-PANEL SIMPLE INLET FLAGGED AS "SRPV" SECTION.
 AGE TITLE: INPUT PANEL CORNER POINTS AND COMPUTED PANEL QUANTITIES

WEDNESDAY, JUL 17, 1985

NO.	IV	IU	X0	EA	DEFI	MINO	M	L	INES	ZB	NX	NORMALS	NZ	AVERAGE PR.	MAXIMUM	PROJECTD	P	CURVATURES	R
1	2	3	4	5	6	7	8	9	10	11	12	13	14	15	16	17	18	19	20
EC	1	1	1	1	1	1	1	1	1	1	1	1	1	1	1	1	1	1	1
1	1	1	1	1	1	1	1	1	1	1	1	1	1	1	1	1	1	1	1
2	2	2	2	2	2	2	2	2	2	2	2	2	2	2	2	2	2	2	2
3	3	3	3	3	3	3	3	3	3	3	3	3	3	3	3	3	3	3	3
4	4	4	4	4	4	4	4	4	4	4	4	4	4	4	4	4	4	4	4
5	5	5	5	5	5	5	5	5	5	5	5	5	5	5	5	5	5	5	5
6	6	6	6	6	6	6	6	6	6	6	6	6	6	6	6	6	6	6	6
7	7	7	7	7	7	7	7	7	7	7	7	7	7	7	7	7	7	7	7
8	8	8	8	8	8	8	8	8	8	8	8	8	8	8	8	8	8	8	8
9	9	9	9	9	9	9	9	9	9	9	9	9	9	9	9	9	9	9	9
10	10	10	10	10	10	10	10	10	10	10	10	10	10	10	10	10	10	10	10
11	11	11	11	11	11	11	11	11	11	11	11	11	11	11	11	11	11	11	11
12	12	12	12	12	12	12	12	12	12	12	12	12	12	12	12	12	12	12	12
13	13	13	13	13	13	13	13	13	13	13	13	13	13	13	13	13	13	13	13
14	14	14	14	14	14	14	14	14	14	14	14	14	14	14	14	14	14	14	14
15	15	15	15	15	15	15	15	15	15	15	15	15	15	15	15	15	15	15	15
16	16	16	16	16	16	16	16	16	16	16	16	16	16	16	16	16	16	16	16
17	17	17	17	17	17	17	17	17	17	17	17	17	17	17	17	17	17	17	17
18	18	18	18	18	18	18	18	18	18	18	18	18	18	18	18	18	18	18	18
19	19	19	19	19	19	19	19	19	19	19	19	19	19	19	19	19	19	19	19
20	20	20	20	20	20	20	20	20	20	20	20	20	20	20	20	20	20	20	20
21	21	21	21	21	21	21	21	21	21	21	21	21	21	21	21	21	21	21	21
22	22	22	22	22	22	22	22	22	22	22	22	22	22	22	22	22	22	22	22
23	23	23	23	23	23	23	23	23	23	23	23	23	23	23	23	23	23	23	23
24	24	24	24	24	24	24	24	24	24	24	24	24	24	24	24	24	24	24	24
25	25	25	25	25	25	25	25	25	25	25	25	25	25	25	25	25	25	25	25
26	26	26	26	26	26	26	26	26	26	26	26	26	26	26	26	26	26	26	26
27	27	27	27	27	27	27	27	27	27	27	27	27	27	27	27	27	27	27	27
28	28	28	28	28	28	28	28	28	28	28	28	28	28	28	28	28	28	28	28
29	29	29	29	29	29	29	29	29	29	29	29	29	29	29	29	29	29	29	29
30	30	30	30	30	30	30	30	30	30	30	30	30	30	30	30	30	30	30	30
31	31	31	31	31	31	31	31	31	31	31	31	31	31	31	31	31	31	31	31
32	32	32	32	32	32	32	32	32	32	32	32	32	32	32	32	32	32	32	32
33	33	33	33	33	33	33	33	33	33	33	33	33	33	33	33	33	33	33	33
34	34	34	34	34	34	34	34	34	34	34	34	34	34	34	34	34	34	34	34
35	35	35	35	35	35	35	35	35	35	35	35	35	35	35	35	35	35	35	35
36	36	36	36	36	36	36	36	36	36	36	36	36	36	36	36	36	36	36	36
37	37	37	37	37	37	37	37	37	37	37	37	37	37	37	37	37	37	37	37
38	38	38	38	38	38	38	38	38	38	38	38	38	38	38	38	38	38	38	38
39	39	39	39	39	39	39	39	39	39	39	39	39	39	39	39	39	39	39	39
40	40	40	40	40	40	40	40	40	40	40	40	40	40	40	40	40	40	40	40
41	41	41	41	41	41	41	41	41	41	41	41	41	41	41	41	41	41	41	41
42	42	42	42	42	42	42	42	42	42	42	42	42	42	42	42	42	42	42	42
43	43	43	43	43	43	43	43	43	43	43	43	43	43	43	43	43	43	43	43

Figure 25. Continued.

WEDNESDAY, JUL 17, 1985

PAGE 4 DOUGLAS AIRCRAFT COMPANY HIGHER ORDER POTENTIAL FLOW : FUNDAMENTAL SOLUTIONS
CASE TITLE: H31H027F: 72-PANEL SIMPLE INLET FLAGGED AS "SRFV" SECTION.
PAGE TITLE: VAFORM. INTERMEDIATE MATRIX FORMATION DATA.

"ORDERED SECTIONS" ("MAKE" SECTIONS POSITIONED AFTER "LIFT" SECTIONS):

	SOURCE(PERCENT)	SMALL LOSS	EDGE VORTEX(PERCENT)	SNEAR EXTENDED LINE
NEAR	5952 (57.4)	0	0 (0.0)	0
INTERMEDIATE	3180 (30.7)		0 (0.0)	
FAR	1236 (11.9)			
SUPER FAR	0 (0.0)			
TOTAL	10368			

VAFORM TIME USAGE: CPU = 6.730 SEC. I/O = 0.120 SEC.
TOTAL NUMBER OF RIGHT-HAND SIDES: NRHS = 3.

Figure 25. Continued.

PAGE 5 DOUGLAS AIRCRAFT COMPANY HIGHER ORDER POTENTIAL FLOW : FUNDAMENTAL SOLUTIONS
WEDNESDAY, JUL 17, 1985

CASE TITLE: H3ING027F: 72-PANEL SIMPLE INLET FLAGGED AS "SRPV" SECTION.

PAGE TITLE: ITERATIVE MATRIX SOLUTION

MATRIX BLOCK STRUCTURE ...

IB (IBLK) 48 72

C O N V E R G E N C E H I S T O R Y

IT	ERR(1)	RMAX(1)	ERR(2)	RMAX(2)	ERR(3)	RMAX(3)
0	4.2813501	7.9216003	4.1123705	7.0593090	4.1163664	7.1346331
1	0.4527583	1.8214226	0.4557284	1.8157825	0.4513286	1.4783493
2	0.0222049	0.4231811	0.0807289	0.4174115	0.0868359	0.4396946
3	0.0122458	0.0556487	0.0123880	0.0571038	0.0121345	0.0569237
4	0.0006059	0.0031748	0.0005989	0.0031547	0.0006005	0.0032152
5	0.0000279	0.0001449	0.0000037	0.0000085	0.0000226	0.0001204

TIME TO SOLVE EQUATIONS = 0.9600 1.0800

ORIGINAL PAGE IS
OF POOR QUALITY

Figure 25. Continued.

PAGE 6 DOUGLAS AIRCRAFT COMPANY HIGHER ORDER POTENTIAL FLOW : FUNDAMENTAL SOLUTIONS WEDNESDAY, JUL 17, 1985

CASE TITLE: H31H022F: 72-PANEL SIMPLE INLET FLAGGED AS "SRFV" SECTION.
PAGE TITLE: SUBROUTINE ITSOLV: COMPUTED RESIDUALS (MPRINT(20).0E.1)

CONVERGENCE SUMMARY

NORMAL VELOCITY R.M.S. ERROR	...	0.542327E-04	0.483089E-04	0.478188E-04
NORMAL VELOCITY MAXIMUM RESIDUAL	...	0.215538E-03	0.224113E-03	0.120103E-03
MAX. VN OCCURS ON PANEL	...	1	1	41

ORIGINAL PAGE IS
OF POOR QUALITY

Figure 25. Continued.

PNL. SEC. SEC. NO. NO. TYPE IV IU	X	Z	SIGMA	VN	VX	VY	VZ	VT	CP
1	4.076115	0.317580	1.169948	0.000000	1.326783	-0.427373	0.113247	1.398508	-0.955825
2	3.007472	0.317022	1.158098	0.000000	1.282424	-0.236591	0.063795	1.305988	-0.705606
3	0.455895	0.317061	1.159045	0.000000	1.214672	0.041232	0.009504	1.217407	0.482880
4	0.290277	0.315913	1.158075	0.000000	1.498856	0.133200	-0.047171	1.703606	1.989089
5	0.162219	0.317011	1.158925	0.000000	0.419805	0.281814	-0.804890	4.496859	-19.22174
6	0.014386	0.303308	1.188113	0.000000	11.63284	5.28424	19.11497	22.98599	527.3568
7	0.014386	0.277872	1.042784	0.000000	-10.10808	0.853764	29.78345	35.77814	-1278.932
8	0.162219	0.263369	0.962772	0.000000	-10.72835	0.478879	1.682104	30.77815	-946.2944
9	0.290277	0.264466	0.964792	0.000000	-10.10316	0.03732	0.220206	22.10468	-687.6077
10	0.455895	0.263319	0.963554	0.000000	-10.10316	0.03732	0.055765	19.30553	-371.7031
11	1.423468	0.264186	0.963759	0.000000	-10.72835	-0.02961	0.024623	19.26538	-370.1548
12	3.007472	0.263358	0.962781	0.000000	-10.75635	0.035588	-0.014804	18.75662	-350.8103
EXTRAP:	4.076114	0.262800	0.960636	0.000000	-10.41325	0.039887	-0.041537	18.41354	-338.0586
13	4.076115	0.849481	0.651526	0.000000	1.304065	0.028725	-0.030280	1.304732	-0.702326
14	3.007472	0.849771	0.651926	0.000000	1.259310	0.016069	-0.014168	1.259310	-0.586430
15	1.423469	0.845733	0.847774	0.000000	1.130010	-0.026889	0.004750	1.130010	-0.423323
16	0.655895	0.848879	0.850122	0.000000	1.088439	-0.037410	0.009054	1.088439	-1.851211
17	0.290277	0.844976	0.847016	0.000000	0.832228	0.013950	0.050088	0.832228	-19.54376
18	0.162219	0.847992	0.850030	0.000000	0.694108	0.358814	0.371293	0.694108	-74.83215
19	0.455895	0.811325	0.832726	0.000000	11.71442	14.07410	14.13579	14.13579	-534.1282
20	0.162219	0.741058	0.742850	0.000000	-10.10619	21.87047	21.92445	21.92445	-128.8723
21	0.290277	0.704390	0.704095	0.000000	-10.70541	1.29825	1.222727	30.84500	-950.4141
22	0.455895	0.707400	0.707109	0.000000	-10.70541	0.086641	0.260235	22.15143	-489.6680
23	1.423469	0.704350	0.708352	0.000000	-10.13623	-0.017032	0.079155	19.33640	-372.8960
24	3.007472	0.704412	0.704111	0.000000	-10.70541	0.031912	0.008704	19.29913	-371.4533
EXTRAP:	4.076116	0.702901	0.704599	0.000000	-10.43871	-0.039351	0.045734	18.78545	-351.8928
25	4.076117	1.162912	0.311370	0.000000	1.306536	0.017448	-0.070021	1.306527	-0.712242
26	3.007473	1.168849	0.310617	0.000000	1.261291	0.010243	-0.038879	1.261901	-0.592394
27	1.423469	1.157788	0.309997	0.000000	1.194151	-0.004336	0.007282	1.194173	-0.426048
28	0.655896	1.160995	0.310856	0.000000	1.085132	-0.012356	0.023588	1.085331	-1.840333
29	0.290277	1.156754	0.307280	0.000000	0.499773	0.036253	0.038617	0.499052	-19.25067
30	0.162220	1.160871	0.310824	0.000000	0.637649	0.469814	0.145332	0.631636	-73.85080
31	0.455897	1.110676	0.297384	0.000000	12.45048	19.14301	5.143970	23.02568	-529.1909
32	0.162220	0.964301	0.251630	0.000000	-10.12220	29.84003	7.991534	35.81483	-1281.702
33	0.290278	0.968419	0.259293	0.000000	-10.73574	1.084628	0.469864	30.80542	-947.9739
34	0.455897	0.964177	0.258157	0.000000	-10.12220	0.287345	0.079745	22.12552	-688.5364
35	1.423469	0.967385	0.259016	0.000000	-10.73574	0.014335	0.003589	19.32376	-372.4077
36	3.007473	0.964324	0.258197	0.000000	-10.28548	0.020857	0.112594	19.28548	-370.9297
EXTRAP:	4.076116	0.962257	0.257643	0.000000	-10.42663	0.008659	-0.032558	18.77286	-351.4199
37	4.076117	1.162913	-0.311366	0.000000	1.306591	0.017397	0.070117	1.306586	-0.712399
38	3.007473	1.168850	-0.310813	0.000000	1.261291	0.010256	-0.038910	1.261928	-0.592461
39	1.423469	1.157790	-0.310993	0.000000	1.194151	-0.004329	0.007289	1.194149	-0.425991
40	0.655896	1.160996	-0.310852	0.000000	1.085137	-0.012359	0.023630	1.085348	-1.840337
EXTRAP:	4.076116	1.156755	-0.309716	0.000000	0.499666	0.036180	-0.038619	0.499993	-19.24994

Figure 25. Continued.

ORIGINAL PAGE IS OF POOR QUALITY

DOUGLAS AIRCRAFT COMPANY HIGHER ORDER POTENTIAL FLOW - FUNDAMENTAL SOLUTIONS

PAGE 8
CASE TITLE: H31NG027F: 7Z-PANEL SIMPLE INLET FLAGGED AS "SRFV" SECTION.
PAGE TITLE: FUNDAMENTAL FLOW SOLUTION

PHL NO.	SEC NO.	TYPE	IV	IU	X	Z	SIGMA	VN	VX	VY	VZ	VT	CP
41	1	SRFV	4	5	0.18628	0.31852	-1.65881	0.00078	0.637742	0.46954	-0.145320	0.651730	-73.85243
42	6				0.014387	0.297388	-1.315763	0.00049	11.65104	19.18304	-5.143842	23.02396	-529.1946
43	7				0.014387	0.271626	-0.174262	0.00013	10.12818	20.84816	-7.991377	35.81691	-1281.708
44	8				0.18628	0.258186	2.159145	-0.00034	-38.73811	1.684536	0.669830	30.80550	-947.9783
45	9				0.298277	0.259228	2.527437	0.00016	-22.18448	-0.87717	0.079717	22.12558	-488.5415
46	10				0.655896	0.258154	0.854178	0.00018	-19.82333	-0.871475	0.003588	19.32367	-372.6043
47	11				1.423449	0.259013	0.927969	-0.00014	-17.82843	0.828948	0.011313	19.28542	-370.9275
48	12				3.087473	0.258193	-2.946560	0.00034	-18.72883	0.888653	0.02548	18.77286	-351.4199
		EXTRAP:			4.076116	0.257648	-0.962259	0.000078	-18.42697	0.888654	0.062139	18.42786	-338.5569
		EXTRAP:			4.076116	0.851523	0.849483	-0.00061	1.30867	0.028719	0.030158	1.304730	-0.782322
49	1				3.087473	0.850012	2.489988	0.00022	1.259317	0.816849	0.01085	1.259522	-0.586396
50	2				1.423470	0.847771	-0.451115	0.00022	1.190987	-0.802738	-0.004762	1.192999	-0.42347
51	3				0.655897	0.850119	-2.184867	0.00051	4.82828	-0.017488	0.009023	1.688534	-1.851146
52	4				0.298277	0.847813	-1.184373	0.00048	0.674181	-0.813939	0.05826	4.532422	-19.54285
53	5				0.18628	0.858827	-1.678884	0.00074	0.674181	14.07484	-14.13365	8.708158	-74.83200
54	6				0.014387	0.813274	-0.170789	0.00041	11.71816	21.87861	-21.92489	35.91284	-534.1282
55	7				0.014387	0.782847	2.164932	-0.00044	-18.73858	1.249784	-1.222746	30.84508	-950.4192
56	8				0.18628	0.789188	2.688698	-0.00044	-22.18448	1.186548	-0.126112	22.15115	-489.6733
57	9				0.298277	0.789188	2.009672	-0.00032	-19.32367	-0.879173	0.079173	19.33633	-372.8948
58	10				0.655896	0.786358	0.829843	-0.00008	-19.32367	-0.879173	0.008624	19.29916	-371.4575
59	11				1.423470	0.786358	0.529843	-0.00008	-18.72883	-0.879173	-0.008624	18.78546	-351.8933
60	12				3.087473	0.786189	-2.955488	0.00014	-18.42697	-0.879173	-0.008624	18.43906	-338.9983
		EXTRAP:			4.076116	0.784597	-2.955488	0.00014	-18.42697	-0.879173	-0.008624	18.43906	-338.9983
		EXTRAP:			4.076116	1.16959	2.448738	-0.00057	1.30867	0.427475	-0.113418	1.308476	-0.955733
61	1				3.087473	1.158897	-2.448738	0.00057	1.30867	-0.218659	0.063898	1.305978	-0.785557
62	2				1.423470	1.158897	-0.443672	0.00019	1.259317	0.816849	0.009525	1.217438	-0.482154
63	3				0.655896	1.15984	-1.669469	0.00034	1.097982	-0.81214	0.047199	1.70533	-1.908842
64	4				0.298277	1.158897	-2.161633	0.0004	4.482789	0.191887	0.004904	4.498819	-19.22139
65	5				0.18628	1.158897	-1.653244	0.00074	0.674181	0.285798	-0.430543	8.650465	-73.48492
66	6				0.014387	1.10812	-1.314043	0.00058	11.61482	23.8479	-19.11490	22.98599	-527.3560
67	7				0.014387	1.012783	-0.174443	0.00034	-18.73858	0.665799	-1.681938	35.77828	-1278.937
68	8				0.18628	0.962672	2.156568	-0.00074	-22.18448	0.478838	-0.228142	30.77812	-946.2930
69	9				0.298277	0.966792	2.156568	-0.00074	-19.32367	0.38887	-0.228142	22.10454	-487.6104
70	10				0.655896	0.962353	1.996604	-0.00031	-19.32367	-0.879173	0.035777	19.30557	-371.7051
71	11				1.423470	0.965758	0.527889	-0.00008	-18.72883	-0.879173	-0.008624	19.26547	-370.1582
72	12				3.087473	0.962788	-2.938298	-0.00008	-18.42697	-0.879173	-0.008624	18.75661	-358.8183
		EXTRAP:			4.076116	0.968635	-2.938298	-0.00008	-18.42697	-0.879173	-0.008624	18.41335	-338.5552

Figure 25. Continued.

 BASED UPON INPUT VALUES OF AREF,BOVS,CREF "---->|
 TYPE SEC NV CL CD CSF CPITCH CROLL CYAM ETA SECTCL SECTCD ASTRIP CIRCULTM

TYPE SEC	NV	CL	CD	CSF	CPITCH	CROLL	CYAM	ETA	SECTCL	SECTCD	ASTRIP	CIRCULTM	
SRFV	1	1-783.39127	-91.41360	-209.88411	11385	18579	378.62902	378.62482	0.51762	MMMMMMMMMM-223.61407	2.4462	0.0	
		2-576.35815	-92.22218	-574.32148	1018	83301	1015.52247	1015.52247	0.84797	MMMMMMMMMM-165.40813	1.7936	0.0	
		3-209.58334	-91.65488	-785.12500	378.52661	1388.32544	1388.32544	1.16085	136.89160	-59.86536	0.6532	0.0	
		4-209.57979	-91.65535	-785.12524	-378.52691	1388.32642	1388.32642	1.16085	114.25903	-49.96883	0.5452	0.0	
		5-576.35815	-92.22273	-574.32588	1015.52251	1015.52251	1015.52251	0.84797	862.87988	-138.06892	1.4971	0.0	
		6-783.39542	-91.41378	-209.88643	11385	18579	378.62728	378.62728	0.51762	1599.38698	-186.85245	2.0418	0.0
SECT. TOTAL		0.00073	-550.58203	MMMMMMMMMM	0.00293	5548.96875	5548.96875						
CONFIG. TOTAL		0.00073	-550.58203	MMMMMMMMMM	0.00293	5548.96875	5548.96875						

ORIGINAL PAGE IS
 OF POOR QUALITY

Figure 25. Continued.

PNL NO.	SEC NO.	SEC TYPE	IV	IU	X	Z	SIGMA	VN	VX	VY	VZ	VT	CP
1	1	SRFV	1	1	0.076115	0.317550	1.160960	0.000171	2.326490	-0.026071	0.112203	2.367988	-4.607364
2	1	SRFV	1	2	0.007472	0.317022	1.158890	0.000171	2.326490	-0.026071	0.063309	2.362112	-4.299719
3	1	SRFV	1	3	0.007472	0.316193	1.158890	0.000171	2.326490	-0.026071	0.008966	2.33824	-3.989966
4	1	SRFV	1	4	0.007472	0.317061	1.159045	0.000171	2.326490	-0.026071	0.051324	2.766751	-6.544641
5	1	SRFV	1	5	0.007472	0.315913	1.158890	0.000171	2.326490	-0.026071	0.008966	2.33824	-3.989966
6	1	SRFV	1	6	0.007472	0.317011	1.158925	0.000171	2.326490	-0.026071	0.051324	2.766751	-6.544641
7	1	SRFV	1	7	0.007472	0.303308	1.108813	0.000171	2.326490	-0.026071	0.008966	2.33824	-3.989966
8	1	SRFV	1	8	0.007472	0.277472	1.012784	0.000171	2.326490	-0.026071	0.008966	2.33824	-3.989966
9	1	SRFV	1	9	0.007472	0.263369	0.962672	0.000171	2.326490	-0.026071	0.008966	2.33824	-3.989966
10	1	SRFV	1	10	0.007472	0.264466	0.966792	0.000171	2.326490	-0.026071	0.008966	2.33824	-3.989966
11	1	SRFV	1	11	0.007472	0.263319	0.962554	0.000171	2.326490	-0.026071	0.008966	2.33824	-3.989966
12	1	SRFV	1	12	0.007472	0.264186	0.962759	0.000171	2.326490	-0.026071	0.008966	2.33824	-3.989966
13	1	SRFV	1	13	0.007472	0.263358	0.962761	0.000171	2.326490	-0.026071	0.008966	2.33824	-3.989966
14	1	SRFV	1	14	0.007472	0.262800	0.960636	0.000171	2.326490	-0.026071	0.008966	2.33824	-3.989966
15	1	SRFV	1	15	0.007472	0.049481	0.851326	0.000171	2.326490	-0.026071	0.008966	2.33824	-3.989966
16	1	SRFV	1	16	0.007472	0.047971	0.850019	0.000171	2.326490	-0.026071	0.008966	2.33824	-3.989966
17	1	SRFV	1	17	0.007472	0.045733	0.847774	0.000171	2.326490	-0.026071	0.008966	2.33824	-3.989966
18	1	SRFV	1	18	0.007472	0.048079	0.850182	0.000171	2.326490	-0.026071	0.008966	2.33824	-3.989966
19	1	SRFV	1	19	0.007472	0.049922	0.847016	0.000171	2.326490	-0.026071	0.008966	2.33824	-3.989966
20	1	SRFV	1	20	0.007472	0.047992	0.849030	0.000171	2.326490	-0.026071	0.008966	2.33824	-3.989966
21	1	SRFV	1	21	0.007472	0.041325	0.813274	0.000171	2.326490	-0.026071	0.008966	2.33824	-3.989966
22	1	SRFV	1	22	0.007472	0.041058	0.812550	0.000171	2.326490	-0.026071	0.008966	2.33824	-3.989966
23	1	SRFV	1	23	0.007472	0.043366	0.814306	0.000171	2.326490	-0.026071	0.008966	2.33824	-3.989966
24	1	SRFV	1	24	0.007472	0.043020	0.812878	0.000171	2.326490	-0.026071	0.008966	2.33824	-3.989966
25	1	SRFV	1	25	0.007472	0.043006	0.812878	0.000171	2.326490	-0.026071	0.008966	2.33824	-3.989966
26	1	SRFV	1	26	0.007472	0.043006	0.812878	0.000171	2.326490	-0.026071	0.008966	2.33824	-3.989966
27	1	SRFV	1	27	0.007472	0.043006	0.812878	0.000171	2.326490	-0.026071	0.008966	2.33824	-3.989966
28	1	SRFV	1	28	0.007472	0.043006	0.812878	0.000171	2.326490	-0.026071	0.008966	2.33824	-3.989966
29	1	SRFV	1	29	0.007472	0.043006	0.812878	0.000171	2.326490	-0.026071	0.008966	2.33824	-3.989966
30	1	SRFV	1	30	0.007472	0.043006	0.812878	0.000171	2.326490	-0.026071	0.008966	2.33824	-3.989966
31	1	SRFV	1	31	0.007472	0.043006	0.812878	0.000171	2.326490	-0.026071	0.008966	2.33824	-3.989966
32	1	SRFV	1	32	0.007472	0.043006	0.812878	0.000171	2.326490	-0.026071	0.008966	2.33824	-3.989966
33	1	SRFV	1	33	0.007472	0.043006	0.812878	0.000171	2.326490	-0.026071	0.008966	2.33824	-3.989966
34	1	SRFV	1	34	0.007472	0.043006	0.812878	0.000171	2.326490	-0.026071	0.008966	2.33824	-3.989966
35	1	SRFV	1	35	0.007472	0.043006	0.812878	0.000171	2.326490	-0.026071	0.008966	2.33824	-3.989966
36	1	SRFV	1	36	0.007472	0.043006	0.812878	0.000171	2.326490	-0.026071	0.008966	2.33824	-3.989966
37	1	SRFV	1	37	0.007472	0.043006	0.812878	0.000171	2.326490	-0.026071	0.008966	2.33824	-3.989966
38	1	SRFV	1	38	0.007472	0.043006	0.812878	0.000171	2.326490	-0.026071	0.008966	2.33824	-3.989966
39	1	SRFV	1	39	0.007472	0.043006	0.812878	0.000171	2.326490	-0.026071	0.008966	2.33824	-3.989966
40	1	SRFV	1	40	0.007472	0.043006	0.812878	0.000171	2.326490	-0.026071	0.008966	2.33824	-3.989966

Figure 25. Continued.

PML HO.	SEC NO.	TYPE	IV	IU	X	Z	SIGMA	VN	VX	VY	VZ	VT	CP
41	1	SRFV	4	5	0.106220	0.310628	-1.688385	0.000116	10.13588	0.552034	-0.167907	10.15169	-102.0568
42	6				0.814387	0.297380	-1.211681	0.000004	12.15778	20.01738	-5.367349	24.02737	-576.3145
43	7				0.014496	0.271424	-0.056082	0.000004	17.77684	29.27150	-7.639843	35.13266	-1233.3004
44	8				0.106220	0.258186	2.160288	0.000007	-29.38810	1.609096	-0.449880	29.42955	-865.0986
45	9				0.290277	0.259290	2.616405	-0.000037	-21.00017	0.19259	-0.077355	21.08922	-643.7554
46	10				0.655896	0.258154	2.031041	-0.000025	-18.28777	-0.080014	-0.004844	18.28787	-333.4465
47	11				1.423469	0.259013	0.557352	0.000003	-10.28408	0.819561	-0.011281	18.26402	-332.5747
48	12				3.007473	0.258193	-2.929623	0.000004	-17.74782	0.008633	0.032355	17.74783	-313.9858
	EXTRAP:				4.076116	0.257640			-17.38994	0.001260	0.061795	17.38964	-301.7473
49	1	SRFV	4	5	0.076116	0.851523	2.466592	0.000000	2.303364	0.028075	0.030663	2.303939	-4.308134
50	2				3.007473	0.850012	-0.475714	0.000000	2.265744	0.015962	0.015995	2.265857	-4.134107
51	3				0.655896	0.850119	-1.709796	0.000023	2.208008	-0.001994	-0.005743	2.209693	-3.882745
52	4				0.290277	0.849779	0.847014	0.000034	2.732600	-0.020179	-0.006593	2.732690	-6.467594
53	5				0.106220	0.850023	-1.709097	0.000078	9.616071	0.021837	-0.057331	5.637307	-30.77924
54	6				0.814387	0.813328	1.218387	0.000001	18.28782	0.387681	-0.430707	10.20917	-103.2272
55	7				0.014387	0.743061	0.852349	0.000009	18.28782	14.68561	-14.74646	24.13524	-161.5093
56	8				0.106220	0.706393	2.166104	0.000007	-20.49148	2.145546	-21.50592	35.22966	-1240.129
57	9				0.290277	0.707409	2.624191	-0.000043	-21.13066	1.195421	-1.16741	29.46839	-867.4214
58	10				0.655896	0.706002	2.837343	-0.000003	-18.30040	-0.179776	-0.118255	21.11475	-444.8328
59	11				1.423470	0.706350	0.559269	0.000006	-10.27774	-0.014057	0.077007	18.30055	-333.9104
60	12				3.007473	0.706415	-2.933685	0.000006	-17.74783	-0.045559	-0.043393	17.76044	-314.4331
	EXTRAP:				4.076115	0.704597			-17.41182	-0.092154	-0.071047	17.41161	-302.1638
61	1	SRFV	4	5	0.076117	0.317583	2.470450	0.000002	2.326414	0.026932	-0.112433	2.367934	-4.607113
62	6				3.007473	0.315897	-0.470007	0.000002	2.208008	-0.237271	0.003522	2.302083	-4.299584
63	7				0.655896	0.316196	-1.689119	0.000013	2.270397	0.043855	0.008976	2.233845	-3.990063
64	8				0.290277	0.315944	2.183752	0.000043	2.740893	0.154482	0.033356	2.746681	-6.544257
65	9				0.106220	0.315916	-1.483499	0.000079	9.59884	0.195809	-0.034442	5.599978	-30.35976
66	10				0.814387	0.317014	1.483499	0.000077	18.28782	0.307161	-0.512921	10.12953	-101.6073
67	11				0.014387	0.303310	0.851195	0.000061	17.74782	3.07807	-19.94948	23.98706	-574.3789
68	12				0.106220	0.27075	-0.012783	0.000061	-17.38994	7.910388	-29.21568	35.09380	-1230.575
69	EXTRAP:				0.204469	0.966792	2.137788	-0.000001	-29.38493	0.448025	-1.607214	29.40231	-863.4958
70	10				0.655896	0.962253	2.027144	-0.000007	-18.28408	-0.027069	-0.210477	21.06830	-442.8730
71	11				1.423469	0.962553	2.027144	-0.000008	-18.28408	-0.054274	-0.052118	18.26978	-332.7847
72	12				3.007472	0.962708	-2.923332	0.000003	-18.28408	-0.003766	-0.023557	18.24402	-331.8445
	EXTRAP:				4.076114	0.962802	-2.923397	-0.000001	-17.38994	0.055458	0.014816	17.73163	-313.6106
													-301.2759

ORIGINAL PAGE IS OF POOR QUALITY

Figure 25. Continued.

PAGE 12 DOUGLAS AIRCRAFT COMPANY HIGHER ORDER POTENTIAL FLOW : FUNDAMENTAL SOLUTIONS WEDNESDAY, JUL 17, 1985
CASE TITLE: N31M0027P: 72-PANEL SIMPLE INLET FLAGGED AS "SRFV" SECTION. ALPHA= 0.0 , BETA= 0.0 +SUCTION
PAGE TITLE: INTEGRATED PRESSURES

TYPE	SEC	NV	CL	CD	CSF	CPITCH	CROLL	CYAN	ETA	SECTCL	SECTCD	ASTRIP	CIRCULTM
<----- BASED UPON INPUT VALUES OF AREF,BOV2,CREF ----->													
SRFV	1	1-689.06958	-91.32813	-184.63493	1289.43726	323.53174	323.53174	323.53174	0.31702	MMMMMMMMMM-223.40497		2.4462	0.0
		2-507.19458	-92.14409	-505.57812	849.93335	887.04346	887.04346	887.04346	0.84797	989.69531-165.26805		1.7936	0.0
		3-184.48299	-91.57231	-690.87134	323.61923	1212.59106	1212.59106	1212.59106	1.14089	-120.45746 -59.61143		0.6532	0.0
		4 184.41979	-91.57251	-690.87158	323.60986	1212.59106	1212.59106	1212.59106	1.14089	180.54228 -49.92366		0.5452	0.0
		5 507.19331	-92.14461	-505.58331	-889.93457	887.04351	887.04351	887.04351	0.84797	789.33447-337.95197		1.4971	0.0
		6 689.07397	-91.32808	-184.63712	MMMMMMMM 323.53491	323.53491	323.53491	323.53491	0.31702	1406.98096-186.47763		2.0418	0.0
SECT. TOTAL		0.00220	-550.08936	MMMMMMMM -0.00090	8446.33084	8446.33084	8446.33084	8446.33084					
CONFIO.TOTAL		0.00220	-550.08936	MMMMMMMM -0.00090	8446.33084	8446.33084	8446.33084	8446.33084					

Figure 25. Continued.

PNL. SEC. NO.	SEC. NO.	TYPE	IV	IU	X	Y	Z	SIGMA	VN	VX	VY	VZ	VT	CP
41	1	SRPV	4	5	0.106220	1.160872	-0.310020	-1.672168	0.000151	10.04400	0.606414	0.055797	10.06245	-100.2528
42	6			0.014387	1.110677	-0.297380	-1.207443	0.000074	12.07177	19.92712	-5.137415	23.85814	-568.2104	
43	7			0.014387	1.014496	-0.271626	-0.063337	0.000014	-17.09777	29.18155	-7.054247	34.97658	-1222.361	
44	8			0.106220	0.964302	-0.258186	2.142104	-0.000147	-29.31630	1.633934	-0.342551	29.33378	-661.2322	
45	9			0.202277	0.968421	-0.259290	2.587125	-0.000110	-21.05264	0.214719	-0.010857	21.05373	-442.2595	
46	10			0.655896	0.964178	-0.258154	1.996007	-0.000052	-10.20822	-0.053117	0.027641	18.28833	-331.4631	
47	11			1.423469	0.967386	-0.259013	0.513437	0.000114	-10.27293	0.021454	-0.003767	18.27295	-332.9009	
48	12			3.007473	0.964325	-0.258193	-2.970220	-0.000038	-17.76360	0.010172	0.037959	17.76363	-314.5464	
		EXTRAP:		4.076114	0.962259	-0.257640			-17.41994	0.003560	0.066110	17.42006	-302.4583	
49	EXTRAP:			4.076114	0.649483	-0.851523			2.312192	0.180093	0.182120	2.326334	-4.411831	
50	1			1.423470	0.847973	-0.650012	2.561179	-0.000045	2.257559	0.160700	0.168229	2.270095	-4.153331	
51	2			0.655896	0.845736	-0.847771	-0.378035	0.000018	2.176379	0.158013	0.147639	2.168856	-3.782341	
52	3			0.202277	0.844081	-0.850119	-1.628651	0.000058	2.682965	0.123406	0.136286	2.689258	-6.232104	
53	4			0.106220	0.844979	-0.847013	-2.142204	0.000037	5.910922	0.153258	0.153562	5.939937	-29.39937	
54	5			0.014387	0.847994	-0.850027	-1.657057	0.000067	11.901208	0.470240	0.370535	9.998243	-98.96486	
55	6			0.014387	0.811328	-0.813274	-1.202065	0.000031	11.94914	14.34996	-14.37506	23.69495	-360.4507	
56	7			0.106220	0.741061	-0.742847	-0.669569	0.000040	-17.61109	21.26360	-21.15230	34.78261	-1208.830	
57	8			0.202277	0.704393	-0.706093	2.114278	-0.000033	-20.20474	1.245843	1.102048	20.23194	-854.6755	
58	9			0.655896	0.707409	-0.705108	2.544718	-0.000033	-20.98851	0.213113	-0.083246	20.98975	-439.5696	
59	10			1.423470	0.704307	-0.706002	1.942187	-0.000029	-10.27393	0.003942	0.092431	18.27415	-332.9446	
60	11			3.007473	0.706652	-0.708350	0.444877	-0.000009	-10.27499	0.023263	-0.005616	18.27501	-332.9758	
		EXTRAP:		4.076114	0.704415	-0.706109	-3.049373	0.000016	-17.77470	-0.048782	-0.044617	17.77681	-315.0149	
		EXTRAP:		4.076115	0.702984	-0.704597			-17.44081	-0.092837	-0.070928	17.44009	-303.1843	
61	EXTRAP:			4.076117	0.317583	-1.150959			2.343433	-0.335481	0.088564	2.369293	-4.613550	
62	1			1.423469	0.317024	-1.158897	2.562765	-0.000047	2.203271	-0.147560	-0.039490	2.288375	-4.236658	
63	2			0.655896	0.316196	-1.159044	-0.337536	0.000018	2.194095	0.134248	0.033251	2.198449	-3.833178	
64	3			0.202277	0.317064	-1.159044	-1.579137	0.000047	2.680440	0.237804	0.073476	2.691978	-6.246744	
65	4			0.106220	0.315914	-1.154806	-2.093032	0.000070	5.432119	0.273240	0.016474	5.438905	-28.58168	
66	5			0.014387	0.317014	-1.158924	-1.624094	0.000070	9.933629	0.308732	-0.480040	9.952236	-96.06654	
67	6			0.014387	0.303310	-1.108012	-1.189901	0.000050	11.03913	7.400238	-17.44069	23.39375	-546.2676	
68	7			0.106220	0.277875	-1.012783	-0.070667	0.000032	17.48007	0.000000	0.000000	34.48001	-1187.871	
69	8			0.202277	0.263371	-0.982672	2.089669	-0.000033	-20.05054	0.408099	-28.69463	34.48001	-845.6492	
70	9			0.655896	0.264469	-0.966792	2.503851	-0.000031	-20.05054	0.000000	-1.585888	29.09723	-845.6492	
71	10			1.423469	0.263321	-0.942553	1.897352	-0.000031	-20.05054	0.048136	0.208916	20.89136	-635.4404	
72	11			3.007472	0.264189	-0.945758	0.400337	0.000004	-10.23463	-0.023662	-0.030397	18.23466	-331.5032	
		EXTRAP:		4.076114	0.263361	-0.962700	-3.072695	-0.000071	-17.74023	0.029896	0.007937	17.74826	-314.0007	
		EXTRAP:		4.076114	0.262802	-0.960635			-17.42007	0.066074	-0.033799	17.42024	-302.4646	

Figure 25. Continued.

PAGE 15 DOUGLAS AIRCRAFT COMPANY HIGHER ORDER POTENTIAL FLOW : FUNDAMENTAL SOLUTIONS ALPHA= 10.00, BETA= 0.0 +SUCTION
 CASE TITLE: H31H027F: 72-PANEL SIMPLE INLET FLAGGED AS "SRFV" SECTION.
 PAGE TITLE: INTEGRATED PRESSURES

WEDNESDAY, JUL 17, 1985

TYPE	SEC	NV	CL	CD	CSF	CPITCH	CROLL	GYAM	ETA	SECTCL	SECTCD	ASTRIP	CIRCUITM
SRFV	1	1-666	19531	-213.88036	-185.74594	1209.33301	319.21411	317.92139	0.31702	XXXXXXXXXXXX	-523.18970	2.4462	0.0
		2-485	44334	-181.86781	-508.02612	890.35016	874.02895	873.92683	0.84797	-870.68457	-326.19482	1.7936	0.0
		3-166	03339	-123.24911	-692.86182	324.05078	195.68579	1195.87158	1.16085	-108.47392	-80.50148	0.6532	0.0
		4	197.48022	-57.19611	-691.35229	-324.36792	1197.08542	1196.86963	1.16085	107.66261	-31.18227	0.5452	0.0
		5	514.54248	-0.17699	-505.08423	-893.07422	876.61108	876.70728	0.84797	770.33423	-0.26497	1.4971	0.0
		6	692.58934	32.98204	-184.28914	XXXXXXXXXXXX	319.30819	328.68164	0.31702	1414.11792	67.34416	2.0418	0.0
SECT. TOTAL													
CONFIG. TOTAL													

Figure 25. Concluded.

ORIGINAL PAGE IS
OF POOR QUALITY

US DF12

DES 3-D HIGHER-ORDER LIFTING METHOD PROGRAM DES
(WITH OR WITHOUT INLETS)
LAST REVISION: 15 JUL 1985

MODE OPTIONS:
-1 = DELETE NSS-SAVED MATRIX.
0 = RE-START FROM NSS-SAVE MATRIX.
1 = GENERATE (FUNDAMENTAL) SOLUTIONS.
2 = COMBINE FUNDAMENTAL SOLUTIONS.
ENTER SELECTION (-1,0,1, OR 2) . . . 2

ENTER THE OLD "CASE-ID" (UPTO 8 CHARACTERS, BEGINNING WITH AN ALPHABETIC CHARACTER) ...
CASEID: 0077
FUNDAMENTAL SOLUTION DATASET 'TSOT3DF.0077F.FUNDSOLN' FOUND.

ENTER A FLAG-SECTION BSN OR C/R FOR NONE ...
(PARALLEL OR FULLY QUALIFIED, CATALOGED NAME (NO QUOTES))
BSN = 0077f.Fluzsect.0077f.data
(SECURITY DATASET FOUND; COPY IN PROGRESS ...)
TEMPORARY COPY CREATED: BSN = TSOT3DF.TEMPGEN.D071005.T102000

FLAG DATASET 'TSOT3DF.0077F.MODE2.FLAGS' NOT FOUND. OPTIONS ARE ...
C/R ... CREATE IT NEW, OR
ENTER NEW FLAG DATASET (FULLY QUALIFIED, NO QUOTES)
ENTER OPTION (C/R OR DATASET NAME) ...

MODE 1: OPTION CURRENT: SCLP= 0, SCLT= 0, SCLM= 0, SCLY= 0, SCLZ= 1, SCLN= 0
MODE 2: OPTION CURRENT: SCLP= 0, SCLT= 0, SCLM= 0, SCLY= 0, SCLZ= 0, SCLN= 1
TITLE: FLAGS

FLAG NAME	PARENT VALUE	DEFAULT VALUE	FLAG DEFINITION
COMP	0	0	0-INCOMPRESSIBLE, 1-COMPRESSIBLE.
SP	0	0	0-NO SP-SAVE PANELS, 1-SP-SAVE PANELS INPUT ON A SEPARATE DATASET (I.E. 8000-SPAN PANELS).
SPRZ	0	0	0-SMALL PANELS (124-COLUMNS), 1-LARGE PANELS (128-COLUMNS)
IPU	0	0	0-DO NOT SAVE ON-BOARD P/U DATASET, 1-SAVE ON-BOARD P/U DATASET UPON "ENDPLT", ETC.).
IPU	0	0	0-DO NOT SAVE FLAG-SECTION P/U DATASET, 1-SAVE FLAG-SECTION P/U DATASET UPON "ENDPLT", ETC.).
ISCL	0	0	0-DO NOT SAVE "ENDPLT" DATASET, 1-SAVE "ENDPLT" DATASET.
MODE	1	1	0 OF COMBINATION CASES (I.E. 00) TO BE CALCULATED.

1(----- PRESTREAM CONDITIONS -----)1 1(--- FLAG SPEC. ---)1
(IND.) (IND.) (COND.1)
ALPHAC BETAC VINF VINF UC OR CC

ICONS: 1: -90.00 0.0 1.000 1.000 NONE YET DEFINED.

ALPHAC(),BETAC() = REQUESTED ANGLES OF ATTACK AND YAW (IN DEGREES).
VINF() = PRESTREAM SPEED.
VINF() = REFERENCE SPEED (FOR CP CALCULATION).
UC(ICON,I) = REQUESTED FLAM VELOCITY AT THE ITH FLAM SECTION.
CC(ICON,I) = COMBINATION CONSTANT FOR THE ITH GENERATING FUNDAMENTAL SOLUTION.

ENTER UPDATES, OR "LIST", OR "RESTART", OR "HELP" (FOR NPRINT FLAG), OR C/R WHEN DONE

1(--- INCOMPRESSIBLE COMBINATION RESULTS FOR THE 72-PANEL INLET. ---)
TITLE: INCOMPRESSIBLE COMBINATION RESULTS FOR THE 72-PANEL INLET.

ENTER UPDATES, OR "LIST", OR "RESTART", OR "HELP" (FOR NPRINT FLAG), OR C/R WHEN DONE

1(--- 1.1v=1.2comb=2.alpha=0.5.vc=1.3.1.5 ---)
1(--- 1.1v=1.2comb=2.alpha=0.5.vc=1.3.1.5 ---)

ENTER UPDATES, OR "LIST", OR "RESTART", OR "HELP" (FOR NPRINT FLAG), OR C/R WHEN DONE

Figure 26. TSD submittal for DF12, Mode 2, for the 72-panel simple inlet check case.

ORIGINAL PAGE IS
OF POOR QUALITY

NON COPYING 'TSOT3DF.G887F.NODES.FLAGS'
TO A TEMPORARY DATASET FOR USE IN THE BATCH SUBMITTAL ...

ON-BODY 'P/U' (PRESSURE/VELOCITY) DATASET WILL BE CREATED ...
ENTER DATASET NAME
(C/R FOR NON-TSOT3DF.PU.G887F.NODES.ON)

NON
'TSOT3DF.PU.G887F.NODES.ON' IS A NEW DATASET

CPU TIME ESTIMATE: CPU .5
I/O TIME ESTIMATE: I/O 2.

JOB CLASS OPTIONS:
C/R FOR NON-DEFERRED
D FOR DEFERRED (CHEAPER)
B FOR BACKLOG-DEFERRED (CHEAPEST)
SELECT JOB CLASS .D

C/R FOR: SYBOUT .A
SYBOUT .

C/R FOR: BEST .TLL
BEST .

DEFAULT: JOHNE = M0F1E7J
JOHNE .

C/R FOR DEFAULT: CEN .

DO YOU WISH TO EXECUTE A CUSTOMIZED 'VECPLOT' OF THE ON-BODY P/U DATASET? (Y OR C/R) .-Y

***** VECPLOT *****
S
S DATA ENTRY PROMPTS FOR SURFACE VELOCITY VECTOR S
S PLOTTING OF ARBITRARY 3-D GEOMETRIES S
S

OPTIONS: YES ONLINE PAGES(60) SERIES TEST
LAST UPDATE: 7/00/88(RUC)

'VECPLOT TWO' TO DIRECT PLOTS TO ON-LINE DATASET FOR DISPLAY
'VECPLOT ONLINE' FOR INTERACTIVE EXECUTION

SELECT VIEW:

- (1) SIDE
 - (2) TOP
 - (3) BOTTOM
 - (4) INSIDE
 - (5) FRONT
 - (6) REAR
 - (7) LOWER OUTSIDE FRONT 45 DEGREE
 - (8) UPPER OUTSIDE FRONT 45 DEGREE
 - (9) LOWER OUTSIDE REAR 45 DEGREE
 - (10) UPPER OUTSIDE REAR 45 DEGREE
 - (11) SPECIFY YOUR OWN
- C/R ALL 10 STANDARD VIEWS

ENTER THE DESIRED VIEW, SEPARATED BY SPACES (OR C/R)

Figure 26. Continued.

YOU MAY SELECT UP TO 40 GEOMETRY SECTIONS TO BE PLOTTED FROM YOUR DATASET.
ENTER THE DESIRED SECTIONS, SEPARATED BY SPACES (C/R FOR ALL)

ENTER WREF (TO BE USED TO NORMALISE VELOCITIES)
(NOTE: WREF = 0.0 WILL PLOT ALL VECTORS AS UNIT VECTORS)
(C/R FOR DEFAULT = 1.0)
WREF 0

ENTER LENGTH OF UNIT VECTOR IN RASTERS (NOTE: PAGE WIDTH = 4K RASTERS) ...
(C/R FOR DEFAULT = 100.0)
LENGTH 100

CLASS IS "DEFER", NETWORKED TO: K30P12T3
ENTER INPUT JOB STREAM:

THE FOLLOWING JOB WILL SEND THE PLOTS TO THE SAC COMPO:

JOB K30P12T3(J000000) SUBMITTED

DO YOU WISH TO SUBMIT A (NETWORKED) "ISOPLOT" OF THE ON-BODY P/U DATASET? (Y OR C/R) ...Y

```
##### ISOPLOT #####  
S  
S BATCH SUBMIT PROCEDURE FOR SURFACE ISOPLOT PLOTTING S  
S OF ARBITRARY 3-D GEOMETRIES S  
S  
#####
```

LAST UPDATED: 7/12/85

OPTIONS: TSS PAGES(00) BEING

'ISOPLOT TSS' TO DIRECT PLOTS TO ON-LINE DATASET FOR ISOPW
'ISOPLOT ONLINE' FOR INTERACTIVE EXECUTION

SELECT VIEW:

- (1) SIDE
- (2) TOP
- (3) BOTTOM
- (4) INSIDE
- (5) FRONT
- (6) REAR
- (7) LOWER OUTSIDE FRONT 45 DEGREE
- (8) UPPER OUTSIDE FRONT 45 DEGREE
- (9) LOWER OUTSIDE REAR 45 DEGREE
- (10) UPPER OUTSIDE REAR 45 DEGREE
- (11) SPECIFY YOUR OWN
- C/R ALL 10 STANDARD VIEWS

ENTER THE DESIRED VIEW, SEPARATED BY SPACES (OR C/R)

0

SELECT PLOT TYPES:

- (1) CP'S ONLY
- (2) DELTA-STEP'S ONLY
- (3) CP'S (SEP.) ONLY
- C/R ALL

ENTER OPTION (NO. OR C/R) 1

SELECT CP CONTOUR RANGE AND INCREMENT:

	MINIMUM CP PLOTTED	CP INCREMENT
(1)	-1.0	0.02
(2)	-3.0	0.05
(3)	-7.0	0.10
(4)	-10.0	0.20
C/R	NO LIMIT	AUTOMATIC

ENTER OPTION (NO. OR C/R) 0
CLASS IS "DEFER", NETWORKED TO:
ENTER INPUT JOB STREAM:

THE FOLLOWING JOB WILL SEND THE PLOTS TO THE SAC COMPO:

JOB K30P12T3(J000001) SUBMITTED

```
ENTER INPUT JOB STREAM:  
JOB PARAMETERS ARE ...  
//K30P12T3 JOB 2 CPU(1.5) IO(2.) LINES(40) RSOCLASS(A)  
//SMIT NETID=V102000, HOLD=0  
//S RELEASE=(K30P12T3, K30P12T3)  
//MAIN CLASS=BACKGROUND  
JOB K30P12T3(J000001) SUBMITTED  
READY
```

Figure 26. Concluded.

INCOMPRESSIBLE COMBINATION RESULTS FOR THE 72-PANEL INLET.
&Y IPR132=1, IPV=1, NCOMB=2, ALPHAC=0,5, VC=1.3,1.5 &END

2

Figure 27(a). Alternative input dataset for DF12, Mode 2, for the 72-panel simple inlet check case.

```

/**
/**
/** PC-PATCH FITTING FOR: TSOT3DF.H31H.G027E.DATA
/**
//PCPATCH EXEC PGM=H31K,PARM='1,0,0',REGION=1000K
//STEPLIB DD DSN=TSOT3DF.CMF.LOAD,DISP=SHR
//FT01F001 DD DSN=TSOT3DF.TEMPGEOM.D080985.T154000,
// DISP=(OLD,DELETE)
//FT06F001 DD SYSOUT=A
//FT11F001 DD UNIT=SYSDA,SPACE=(TRK,(30,10)),
// DCB=(RECFM=VBS,BLKSIZE=19069)
//FT12F001 DD UNIT=SYSDA,SPACE=(TRK,(30,10)),DISP=(NEW,PASS),
// DCB=(RECFM=VBS,BLKSIZE=19069)
/**
/**
/** 3-D HIGHER-ORDER LIFTING NEUMANN SOLUTION.
/** (WITH INLET CAPABILITY)
/**
/** MODE 2, CASEID: G027F
/**
//NEUMANN EXEC PGM=MAIN,REGION=4000K
//STEPLIB DD DSN=TSOT3DF.DF12.LOAD,DISP=SHR
//FT02F001 DD DSN=TSOT3DF.G027F.FUNDSOLN,
// DISP=SHR
/**
/** PV DATASET:
//FT03F001 DD DSN=TSOT3DF.PV.G027F.MODE2.ON,
// DISP=(NEW,CATLG),UNIT=TSODA,SPACE=(TRK,(10,10),MSE)
/**
//FT04F001 DD UNIT=SYSDA,DCB=(RECFM=VBS,BLKSIZE=19069),
// SPACE=(TRK,(1,10))
//FT05F001 DD DSN=TSOT3DF.DF12.D080985.T154000,DISP=(OLD,DELETE)
//FT06F001 DD SYSOUT=A,DCB=(RECFM=FBA,LRECL=169,BLKSIZE=16900)
//FT08F001 DD UNIT=SYSDA,DCB=(RECFM=VBS,BLKSIZE=19069),
// SPACE=(TRK,(1,10))
//FT09F001 DD UNIT=SYSDA,DCB=(RECFM=VBS,BLKSIZE=19069),
// SPACE=(TRK,(1,10))
//FT10F001 DD UNIT=SYSDA,DCB=(RECFM=VBS,BLKSIZE=19069),
// SPACE=(TRK,(1,10))
//FT11F001 DD UNIT=SYSDA,DCB=(RECFM=VBS,BLKSIZE=19069),
// SPACE=(TRK,(1,10))
//FT12F001 DD UNIT=SYSDA,DCB=(RECFM=VBS,BLKSIZE=19069),
// SPACE=(TRK,(1,10))
//FT13F001 DD UNIT=SYSDA,DCB=(RECFM=VBS,BLKSIZE=19069),
// SPACE=(TRK,(1,10))
//FT14F001 DD UNIT=SYSDA,DCB=(RECFM=VBS,BLKSIZE=19069),
// SPACE=(TRK,(1,10))
//FT15F001 DD UNIT=SYSDA,DCB=(RECFM=VBS,BLKSIZE=19069),
// SPACE=(TRK,(1,10))
//FT16F001 DD UNIT=SYSDA,DCB=(RECFM=VBS,BLKSIZE=19069),
// SPACE=(TRK,(1,10))
//FT17F001 DD UNIT=SYSDA,DCB=(RECFM=VBS,BLKSIZE=19069),
// SPACE=(TRK,(1,10))
//FT18F001 DD UNIT=SYSDA,DCB=(RECFM=VBS,BLKSIZE=19069),
// SPACE=(TRK,(1,10))
//FT20F001 DD DSN=*PCPATCH.FT12F001,
// DISP=(OLD,DELETE)

```

Figure 27(b). Mode 2 JCL stream for the 72-panel inlet check case.


```

/**
/**          JCL TO VECPLOT A 3-D PRESSURE/VELOCITY FILE
/**
//VECPLOT EXEC PGM=UVECLT,REGION=950K
//STEPLIB      DD DSN=TSOT3CP.H17.LOAD,DISP=SHR
//FT05F001     DD *
/**
//FT06F001     DD SYSOUT=A,DCB=(RECFM=VA,BLKSIZE=141)
//FT13F001     DD DSN=TSOT3DF.PV.G027F.MODE2.ON,
//              DISP=SHR
//SD4060       DD DSN=ROUTE.DAC.GCMIF.BON.FL0060.VECLT,
//              DISP=(NEW,KEEP),
//              UNIT=TAPE16,LABEL=RETPD=10,DCB=DEN=3

```

Figure 27(c). JCL stream to execute the VECPLT program.

```

.....
/**
/**          JCL TO ISOPLT A 3-D PRESSURE/VELOCITY FILE
/**
//ISOPLT EXEC PGM=UIOPLT,REGION=750K
//STEPLIB      DD DSN=TSOT3CP.H17.LOAD,DISP=SHR
//FT05F001     DD *
/**
//FT06F001     DD SYSOUT=A,DCB=(RECFM=VA,BLKSIZE=141)
//FT18F001     DD DSN=TSOT3DF.PV.G027F.MODE2.ON,
//              DISP=SHR
//SD4060       DD DSN=ROUTE.DAC.GCMIF.BON.FL0060.ISOPLT,
//              DISP=(NEW,KEEP),
//              UNIT=TAPE16,LABEL=RETPD=10,DCB=DEN=3

```

Figure 27(d). JCL stream to execute the ISOPLT program.

SECT#	# PATCHES	NU	NV	MCURV	N-LINES	M-LINES	TYPE	TITLE
1	6	6	1	0	CURVED	CURVED	FLUX	NEUMANN SECTION 1

UNFORMATTED DATASET CREATION IN PROGRESS
 UNFORMATTED PATCH DATA HAS BEEN CREATED. NPAT = 6
 TIME USAGE ... CPU= 0.07 SECONDS, I/O = 0.08 SECONDS.

Figure 28. Sample output from the 72-panel simple inlet check case.

CASE TITLE: INCOMPRESSIBLE COMBINATION RESULTS FOR THE 72-PANEL INLET.
 PAGE TITLE: INPUT FLAGS

TITLE=INCOMPRESSIBLE COMBINATION RESULTS FOR THE 72-PANEL INLET.

FLAG NAME	PRESENT VALUE	DEFAULT VALUE	FLAG DEFINITION
COMPRS	0	0	0=INCOMPRESSIBLE, 1=COMPRESSIBLE.
IOFF	0	0	0=NO OFF-BODY POINTS, 1=OFF-BODY POINTS INPUT ON A SEPARATE DATASET (.E. 2000=8FLUX PANELS).
IPR132	1	M	0=SMALL PRINTSIZE (164-COLUMN), 1=LARGE PRINTSIZE (132-COLUMN).
IPV	0	0	0=DO NOT SAVE ON-BODY P/V DATASET, 1=SAVE ON-BODY P/V DATASET (FOR "ISOPLOT", ETC.).
JPV	0	0	0=DO NOT SAVE FLUX-SECTION P/V DATASET, 1=SAVE FLUX-SECTION P/V DATASET (FOR "ISOPLOT", ETC.).
IQWIK	0	0	0=DO NOT SAVE "QMIKPLOTT" DATASET, 1=SAVE "QMIKPLOTT" DATASET.
ICOMB	2	M	0 OF COMBINATION CASES (.E. 20) TO BE CALCULATED.

ICOMB = 1:	ALPHAC	BETAC	VINF	VREF	VC(1,1) =
	0.0	0.0	1.0000	1.0000	1.5000
ICOMB = 2:	ALPHAC	BETAC	VINF	VREF	VC(2,1) =
	5.00	0.0	1.0000	1.0000	1.5000

ALPHAC(1), BETAC(1) = REQUESTED ANGLES OF ATTACK AND YAW (IN DEGREES).
 VINF(1) = FREESTREAM SPEED.
 VREF(1) = REFERENCE SPEED (FOR CP CALCULATION).
 VC(1,1) = REQUESTED FLUX VELOCITY AT THE 1TH FLUX SECTION.
 CC(1,1) = COMBINATION CONSTANT FOR THE 1TH FLUX-GENERATING FUNDAMENTAL SOLUTION.

SECTION SUMMARY: 0NLIF= 0, 0LIFT= 0, 0SHAKE= 0, 0DBLT= 0, 0SRFV= 1, 0FLUX= 0

Figure 28. Continued.

THURSDAY, JUL 18, 1985

PAGE 2 DOUGLAS AIRCRAFT COMPANY HIGHER ORDER POTENTIAL FLOW : COMBINATION SOLUTIONS

CASE TITLE: INCOMPRESSIBLE COMBINATION RESULTS FOR THE 72-PANEL INLET.

PAGE TITLE: FLUX SECTION PANEL FORMATION.

PNL.	IV	IU	X	Y	Z	AREA	UX	UY	UZ
1	1		0.4080	0.1319	0.4822	0.2617	1.0000	0.0	0.0
2	2		0.4080	0.3528	0.3537	0.2615	1.0000	0.0	0.0
3	3		0.4080	0.4830	0.1293	0.2618	1.0000	0.0	0.0
4	4		0.4080	0.4830	-0.1293	0.2618	1.0000	0.0	0.0
5	5		0.4080	0.3528	-0.3537	0.2615	1.0000	0.0	0.0
6	6		0.4080	0.1319	-0.4822	0.2617	1.0000	0.0	0.0

Figure 28. Continued.

CASE TITLE: INCOMPRESSIBLE COMBINATION RESULTS FOR THE 72-PANEL INLET.
 PAGE TITLE: VAPORM. INTERMEDIATE MATRIX FORMATION DATA.

"ORDERED SECTIONS" ("MAKER" SECTIONS POSITIONED AFTER "LIFT" SECTIONS):

	SOURCE(PERCENT)	SMALL LOGS	EDGE VORTEX(PERCENT)	ONEAR EXTENDED LINE
NEAR	708 (81.9)	0	0 (0.0)	0
INTERMEDIATE	136 (16.1)			
FAR	0 (0.0)			
SUPER FAR	0 (0.0)			
TOTAL	844			

VAPORM TIME USAGE: CPU = 0.677 SEC. I/O = 0.040 SEC.

TOTAL NUMBER OF RIGHT-HAND SIDES: HRHS = 3.

Figure 28. Continued.

PAGE 4 DOUGLAS AIRCRAFT COMPANY HIGHER ORDER POTENTIAL FLOW : COMBINATION SOLUTIONS

CASE TITLE: INCOMPRESSIBLE COMBINATION RESULTS FOR THE 72-PANEL INLET.
 PAGE TITLE: FLOCHB. FLOW COMBINATION MATRIX DATA.

N (= 4) EQUATIONS TO BE SOLVED FOR M (= 3) COMBINATION CONSTANTS

ROW RMS INPUT COEFFICIENT MATRIX ...

1	1.0000	1.00000	0.98481	0.0
2	0.0	0.0	0.0	0.0
3	0.0	0.0	0.17365	0.0
4	1.30000	-17.12364	-17.13911	-18.13988

IFLAG (J) = 0
 CALCULATED FLOW COMBINATION CONSTANTS FOR ICOMB = 1 (IRET = 0):
 CC (J) = 1.00000 0.0 -1.03564

N (= 4) EQUATIONS TO BE SOLVED FOR M (= 3) COMBINATION CONSTANTS

ROW RMS INPUT COEFFICIENT MATRIX ...

1	0.99619	1.00000	0.98481	0.0
2	0.0	0.0	0.0	0.0
3	0.08716	0.0	0.17365	0.0
4	1.50000	-17.12364	-17.13911	-18.13988

IFLAG (J) = 0
 CALCULATED FLOW COMBINATION CONSTANTS FOR ICOMB = 2 (IRET = 0):
 CC (J) = 0.50191 0.50191 -1.03070

Figure 28. Continued.

PAGE 6 DOUGLAS A1-CRAFT COMPANY HIGHER ORDER POTENTIAL FLOW : COMBINATION SOLUTIONS THURSDAY, JUL 18, 1985
CASE TITLE: INCOMPRESSIBLE COMBINATION RESULT FOR THE 72-PANEL INLET. ALPHA= 0.0 , BETAC= 0.0 DEGREES
PAGE TITLE: COMBINED ON-BODY FLOW SOLUTION NUMBER 1 OF 2

PNL NO.	SEC NO.	TYPE	IV	IU	X	Y	Z	SIGMA	VN	VX	VY	VZ	VT	CP
41	1	SRFV	4	5	0.106220	1.160872	-0.310820	-0.004369	0.000036	1.362427	0.078031	-0.020314	1.364631	-0.862217
42				6	0.014387	1.110677	-0.293200	0.124663	-0.000007	0.324472	-0.536271	-0.143046	0.641241	0.588810
43				7	0.014387	1.014496	-0.271626	0.120989	-0.000021	0.620783	-1.035416	0.276536	1.242517	-0.543849
44				8	0.106220	0.964302	-0.250186	-0.032631	0.000053	1.054797	-0.101810	0.027299	1.857789	-2.451382
45				9	0.290277	0.968421	-0.250297	-0.014891	-0.000032	1.302385	0.013264	0.003608	1.382453	-0.911177
46				10	0.655896	0.964178	-0.258154	-0.003734	-0.000019	1.338043	0.004579	-0.001200	1.338051	-0.790380
47				11	1.423469	0.967388	-0.259013	0.021125	0.000151	1.323044	-0.001735	0.000209	1.323045	-0.750447
48				12	3.007473	0.964325	-0.258193	0.063027	-0.000151	1.318049	-0.000155	-0.000702	1.318649	-0.738835
		EXTRAP:			4.076116	0.962259	-0.257640			1.315082	0.000910	-0.000136	1.315682	-0.7331021
49		EXTRAP:			4.076116	0.849483	-0.851523			0.979099	-0.001093	0.000091	0.979099	0.041364
50				1	3.007473	0.847973	-0.850012	-0.053073	0.000003	0.986729	-0.000339	-0.000241	0.986729	0.026366
51				2	1.423470	0.845736	-0.847771	-0.017603	0.000003	0.990037	-0.000780	-0.000908	0.990038	0.003920
52				3	0.655897	0.848081	-0.850119	0.009462	0.000000	1.017777	0.002498	0.002571	1.017783	-0.035882
53				4	0.290277	0.844979	-0.847013	0.009462	0.000000	1.033955	0.007680	-0.006922	1.034005	-0.065167
54				5	0.106220	0.847994	-0.850027	0.044844	-0.000002	1.362620	0.055797	-0.053605	1.364615	-0.862720
55				6	0.014387	0.81328	-0.813274	0.124715	-0.000012	0.638447	-0.391421	-0.389703	0.640554	-0.589691
56				7	0.014387	0.741061	-0.742847	0.120310	-0.000015	0.638447	-0.757050	0.761093	1.244930	0.549850
57				8	0.106220	0.704393	-0.706093	-0.032253	0.000006	0.855991	-0.073831	0.075130	1.858578	-2.454311
58				9	0.290277	0.707409	-0.709108	-0.016904	0.000000	1.055991	-0.009481	0.009370	1.382881	-0.912360
59				10	0.655896	0.704307	-0.706002	-0.003762	-0.000000	1.302013	0.003266	-0.003504	1.382881	-0.790912
60				11	1.423470	0.706652	-0.708350	0.003762	0.000000	1.302013	-0.000838	0.001392	1.323274	-0.751032
		EXTRAP:			3.007473	0.704415	-0.706109	0.021334	0.000001	1.323273	-0.000994	0.000392	1.318864	-0.739491
		EXTRAP:			4.076115	0.702904	-0.704597	0.063224	0.000001	1.318086	0.002229	0.000722	1.315887	-0.731559
61		EXTRAP:			4.076117	0.317583	-1.160950			0.989961	0.007229	0.002759	0.978991	0.041576
62				1	3.007473	0.317024	-1.158897	-0.052582	0.000005	0.986463	-0.005121	0.001366	0.986509	0.026800
63				2	1.423469	0.316196	-1.158440	-0.017364	0.000000	0.987463	-0.001995	-0.000698	0.997665	0.004665
64				3	0.655896	0.317064	-1.159044	0.003385	-0.000010	1.037312	0.001136	0.003419	1.017318	-0.034936
65				4	0.290277	0.315916	-1.154806	0.009693	0.000000	1.033955	0.001002	-0.010422	1.033604	-0.068336
66				5	0.106220	0.317014	-1.158926	-0.004395	0.000003	1.302013	0.016901	-0.075644	1.364332	-0.864902
67				6	0.014387	0.303310	-1.108812	0.124893	0.000000	0.844669	-0.139074	0.053583	0.641562	-0.588399
68				7	0.014387	0.272075	-1.012783	0.189978	-0.000002	1.055991	-0.030170	1.033539	1.242007	-0.542583
69				8	0.106220	0.263371	-0.962672	-0.033593	0.000000	1.055991	-0.042119	0.101033	1.857284	-2.449352
70				9	0.290277	0.264469	-0.966792	-0.016859	0.000001	1.055991	-0.004219	0.031350	1.381996	-0.909913
71				10	0.655896	0.263321	-0.962553	-0.003737	0.000004	1.302013	0.001301	-0.004531	1.337776	-0.785645
72				11	1.423469	0.264189	-0.965728	0.028998	0.000001	1.302013	-0.000801	0.001419	1.322784	-0.749760
		EXTRAP:			3.007472	0.263361	-0.962700	0.003855	0.000000	1.318086	-0.001166	-0.000278	1.318359	-0.730072
		EXTRAP:			4.076114	0.262802	-0.960635			1.315372	-0.001446	-0.001423	1.315372	-0.730206

ORIGINAL PAGE IS
OF POOR QUALITY

Figure 2a. Continued.

CASE TITLE: INCOMPRESSIBLE COMBINATION RESULTS FOR THE 72-PANEL INLET.
 PAGE TITLE: INTEGRATED PRESSURES

TYPE	SEC	NV	CL	CD	CSF	CPITCH	CRULL	CYAN	ETA	SECTCL	SECTCD	ASTRIP	CIRCULTM
<----- BASED UPON INPUT VALUES OF AREP,BOVZ,CREF ----->													
SRFV	1	1	-1.61661	-0.00872	-0.43317	3.18872	0.85438	0.85438	0.31702	-3.95451	-0.02133	2.4462	0.0
	2	1	-1.18663	-0.00908	-1.10285	2.34006	2.33240	2.33240	0.8797	-2.12832	-0.21615	1.7936	0.0
	3	0	-0.43172	-0.00877	-1.61727	0.85151	3.18986	3.18986	1.16885	-0.28198	-0.00573	0.6532	0.0
	4	0	0.43171	-0.00877	-1.61728	-0.85153	3.19001	3.19001	1.16885	0.23536	-0.00478	0.5452	0.0
	5	1	1.28559	-0.00901	-1.18281	-2.33993	2.33249	2.33249	0.84797	1.77647	-0.01348	1.4971	0.0
	6	1	1.61660	-0.00872	-0.43317	-3.18862	0.85435	0.85435	0.31702	3.30084	-0.01780	2.0418	0.0
SECT.	TOTAL		-0.00006	-0.05299	-6.46655	0.00021	12.75369	12.75369					
CONFIG.	TOTAL		-0.00006	-0.05299	-6.46655	0.00021	12.75369	12.75369					

Figure 28. Continued.

PNL. SEC. SEC. NO. TYPE IV IU	<--- CONTROL POINTS --->			<--- SIGMA --->			<--- INCOMPRESSIBLE POTENTIAL FLOW SOLUTION --->							
	X	Y	Z	VM	VX	VY	VZ	VT	CP					
41	1	SRFV	4	5	0.106220	1.100872	-0.310850	0.022292	0.000053	1.252247	0.097157	0.093512	1.232645	-0.519414
42				6	0.014367	1.110677	-0.297350	0.141957	0.000012	0.152297	0.276550	0.029322	0.317071	0.899466
43				7	0.014387	1.014496	-0.271656	0.119714	-0.000012	0.123413	-1.418152	0.460089	0.727914	-1.985685
44				8	0.106220	0.964302	-0.258186	-0.060822	-0.000003	2.238754	-0.108585	0.065525	2.243054	4.031292
45				9	0.290277	0.968421	-0.259290	-0.000009	-0.000009	1.652847	-0.008869	0.37890	1.653296	-1.733386
46				10	0.655896	0.944178	-0.258154	-0.000006	-0.000006	1.558960	0.009761	0.051140	1.559064	-1.430679
47				11	1.423469	0.967386	-0.259013	-0.000002	-0.000002	1.558246	-0.001026	0.051108	1.539251	-1.368294
48				12	3.007473	0.964325	-0.258193	0.075834	-0.000052	1.523665	0.000520	0.001744	1.525666	-1.327657
				EXTRAP:	4.076116	0.962259	-0.257640			1.516502	0.001563	0.000150	1.516502	-1.299781
49				EXTRAP:	4.076116	0.849483	-0.051523			0.92589	0.074881	0.075722	0.978402	0.042729
50				5	3.007473	0.847973	-0.050012	-0.035809	0.000011	0.973310	0.076141	0.075885	0.978235	0.043057
51				6	1.423470	0.845736	-0.047771	0.036429	-0.000001	0.971895	0.078010	0.076126	0.977988	0.043539
52				7	0.655897	0.848081	-0.050119	0.000995	0.000004	0.978872	0.069754	0.075394	0.983175	0.033567
53				8	0.290277	0.849979	-0.047013	0.008682	0.000006	0.973969	0.073515	0.060255	0.928846	0.137246
54				9	0.106220	0.847994	-0.050027	0.036389	-0.000004	1.165467	0.107848	0.04170	1.169536	-0.367814
55				10	0.655896	0.811328	-0.043274	0.17143	-0.000016	0.948661	0.152428	-0.046745	0.179589	0.967248
56				11	1.423470	0.741061	-0.0742847	0.14458	-0.000009	0.948660	-1.100861	1.186356	1.876584	-2.521366
57				12	3.007473	0.704309	-0.0706093	-0.00891	-0.000001	2.315826	-0.064283	0.121548	2.319904	-4.381957
58				EXTRAP:	4.076116	0.704309	-0.0706093	-0.00891	-0.000001	1.698563	0.004928	0.028849	1.698814	-1.885970
59				EXTRAP:	4.076116	0.704309	-0.0706093	-0.00891	-0.000001	1.578813	0.011299	0.003539	1.572859	-1.473885
60				EXTRAP:	4.076116	0.704309	-0.0706093	-0.00891	-0.000001	1.549486	-0.000228	0.002372	1.545487	-1.388533
61				EXTRAP:	4.076116	0.704309	-0.0706093	-0.00891	-0.000001	1.529711	0.001900	0.001896	1.525713	-1.327800
62				EXTRAP:	4.076116	0.702904	-0.0704597			1.513368	0.003335	0.001574	1.512372	-1.287270
63				EXTRAP:	4.076117	0.317583	-1.160959			0.976410	0.056832	0.016018	0.978194	0.043137
64				1	3.007473	0.317024	-1.158897	-0.015657	0.000009	0.975080	0.052835	0.014148	0.974616	0.050124
65				2	1.423469	0.316196	-1.159840	0.058040	-0.000003	0.968143	0.046911	0.011377	0.969346	0.060368
66				3	0.655896	0.317064	-1.159044	0.073201	-0.000006	0.971390	0.039007	0.014006	0.972273	0.054684
67				4	0.290277	0.315916	-1.154806	0.050433	-0.000007	0.968737	0.036721	0.003483	0.905482	0.180103
68				5	0.106220	0.317014	-1.158924	0.043088	-0.000002	1.131363	0.044673	-0.054616	1.133560	-0.284959
69				6	0.655896	0.303310	-1.108812	0.149950	-0.000009	0.843056	0.040879	-0.068358	0.891659	0.991599
70				7	1.423470	0.277075	-1.012783	0.112112	-0.000000	0.989334	-0.423565	1.631989	1.954885	-2.821575
71				8	3.007473	0.263371	-0.962672	-0.000078	-0.000000	2.323788	-0.029188	0.130927	2.361570	-4.577013
72				EXTRAP:	4.076114	0.263371	-0.962672	-0.000078	-0.000000	1.723236	-0.005194	0.016423	1.723322	-1.969838
				EXTRAP:	4.076114	0.263371	-0.962672	-0.000078	-0.000000	1.567943	-0.005247	-0.007171	1.579873	-1.496000
				EXTRAP:	4.076114	0.263371	-0.962672	-0.000078	-0.000000	1.524734	-0.013619	0.001734	1.548004	-1.396316
				EXTRAP:	4.076114	0.262602	-0.960635	0.020008	0.000025	1.524734	-0.014643	-0.003098	1.524809	-1.325033
				EXTRAP:	4.076114	0.262602	-0.960635	0.020008	0.000025	1.509076	-0.015333	-0.005558	1.509163	-1.277574

Figure 28. Continued.

PAGE 10 DOUGLAS AIRCRAFT COMPANY HIGHER ORDER POTENTIAL FLOW : COMBINATION SOLUTIONS THURSDAY, JUL 18, 1985
CASE TITLE: INCOMPRESSIBLE COMBINATION RESULTS FOR THE 72-PANEL INLET. ALPHAC= 5.00, BETAC= 0.0 DEGREES
PAGE TITLE: INTEGRATED PRESSURES

TYPE	SEC	MV	CL	CD	CSF	CPITCH	CROLL	CYAN	ETA	SECICL	SECTCD	ASTRIP	CIRCULTM
SRFV	1	-2.80804	-0.27009	-0.75585	5.77050	1.54154	1.53887	0.31702	-6.86890	-0.66070	2.4662	0.0	
	2	-2.08501	-0.21380	-2.08903	4.20373	4.17448	4.17428	0.84797	-3.73363	-0.38347	1.7936	0.0	
	3	-0.77571	-0.11313	-2.93179	1.51905	5.66883	5.66922	1.16085	-0.50667	-0.07389	0.6532	0.0	
	4	0.81619	0.00342	-3.04773	-1.52242	5.68195	5.68153	1.16085	0.44497	0.00296	0.5652	0.0	
	5	2.32628	0.11503	-2.32006	-4.22325	4.19345	4.19308	0.84797	3.48273	0.17222	1.4971	0.0	
	6	3.24565	0.18207	-0.87061	-5.80010	1.54613	1.54922	0.31702	6.62710	0.37176	2.0418	0.0	
SECT.	TOTAL	0.71935	-0.29450	-12.01507	-0.05240	22.80655	22.80698						
CONFIG.	TOTAL	0.71935	-0.29450	-12.01507	-0.05240	22.80655	22.80698						

ORIGINAL PAGE IS
OF POOR QUALITY

Figure 28. Continued.

PAGE 11 DOUGLAS AIRCRAFT COMPANY HIGHER ORDER POTENTIAL FLOW : COMBINATION SOLUTIONS THURSDAY, JUL 18, 1985
 ALPHA= 0.0 , BETAC= 0.0 DEGREES

CASE TITLE: INCOMPRESSIBLE COMBINATION RESULTS FOR THE 72-PANEL INLET.
 PAGE TITLE: COMBINED OFF-BODY FLOW SOLUTION NUMBER 1 OF 2

INL. NO.	SEC. NO.	SEC. TYPE	IV	IU	X	Y	Z	SIGMA	VN	VX	VY	VZ	VT	CP
1	1	FLUX	1	1	0.408000	0.131906	0.482175	0.0	1.299850	1.299850	-0.008468	-0.030882	1.300244	-0.690636
2	2			2	0.408000	0.352806	0.353656	0.0	1.300034	1.300034	-0.022647	-0.022673	1.300427	-0.691113
3	3			3	0.408000	0.482990	0.129321	0.0	1.300016	1.300016	-0.030981	-0.083302	1.300413	-0.691075
4	4			4	0.408000	0.482990	-0.129321	0.0	1.300034	1.300034	-0.030981	0.082293	1.300428	-0.691114
5	5			5	0.408000	0.352806	-0.353656	0.0	1.300049	1.300049	-0.022653	0.022658	1.300444	-0.691133
6	6			6	0.408000	0.131906	-0.482174	0.0	1.299850	1.299850	-0.008467	0.030878	1.300244	-0.690635

Figure 28. Continued.

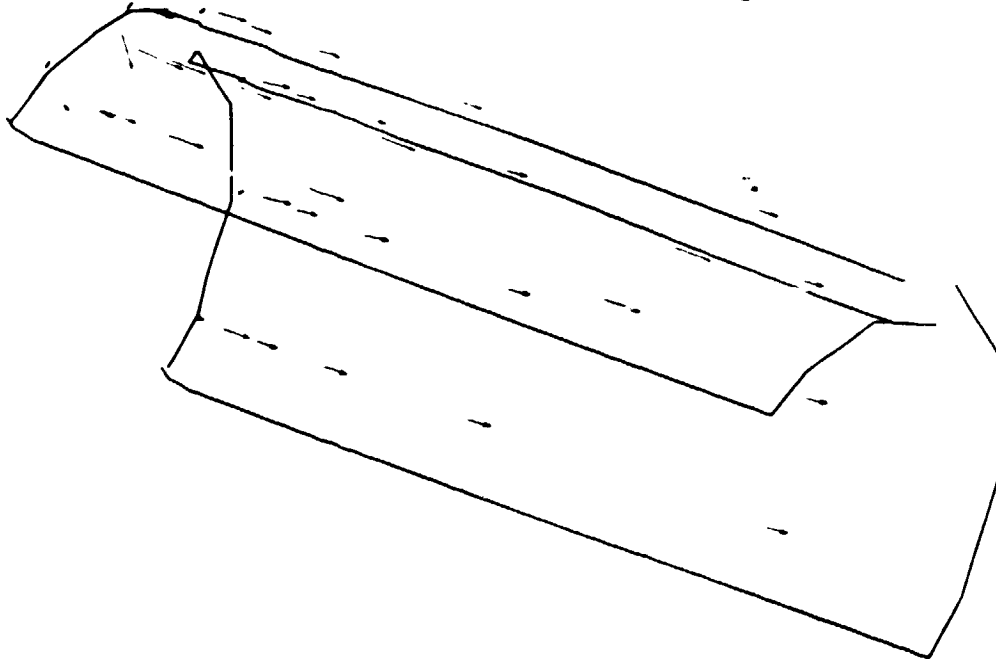
PAGE 12 DOUGLAS AIRCRAFT COMPANY HIGHER ORDER POTENTIAL FLOW : COMBINATION SOLUTIONS THURSDAY, JUL 18, 1985
 ALPHA= 5.00, BETAC= 0.0 DEGREES

CASE TITLE: INCOMPRESSIBLE COMBINATION RESULTS FOR THE 72-PANEL INLET.
 PAGE TITLE: COMBINED OFF-BODY FLOW SOLUTION NUMBER 2 OF 2

PML NO.	SEC NO.	TYPE	IV	IU	CONTROL POINTS			INCOMPRESSIBLE POTENTIAL FLOW SOLUTION			CP		
					X	Y	Z	VN	VX	VY		VZ	VT
1	1	FLUX	1	1	0.408000	0.131906	0.482175	0.0	1.470413	-0.012643	-0.010707	1.470506	-1.162388
2	0	408000	0	352806	0.352806	0.353656	0.0	1.478607	1.478607	-0.033560	0.002886	1.478990	-1.187411
3	0	408000	0	482990	0.482990	0.129321	0.0	1.492203	1.492203	-0.044413	0.024875	1.493071	-1.229259
4	0	408000	0	482990	0.482990	-0.129321	0.0	1.507904	1.507904	-0.042601	0.048147	1.509274	-1.277905
5	0	408000	0	352806	0.352806	-0.353656	0.0	1.521591	1.521591	-0.029955	0.066385	1.523333	-1.320541
6	0	408000	0	131906	0.131906	-0.482174	0.0	1.529144	1.529144	-0.010916	0.076146	1.531077	-1.344197

Figure 28. Concluded.

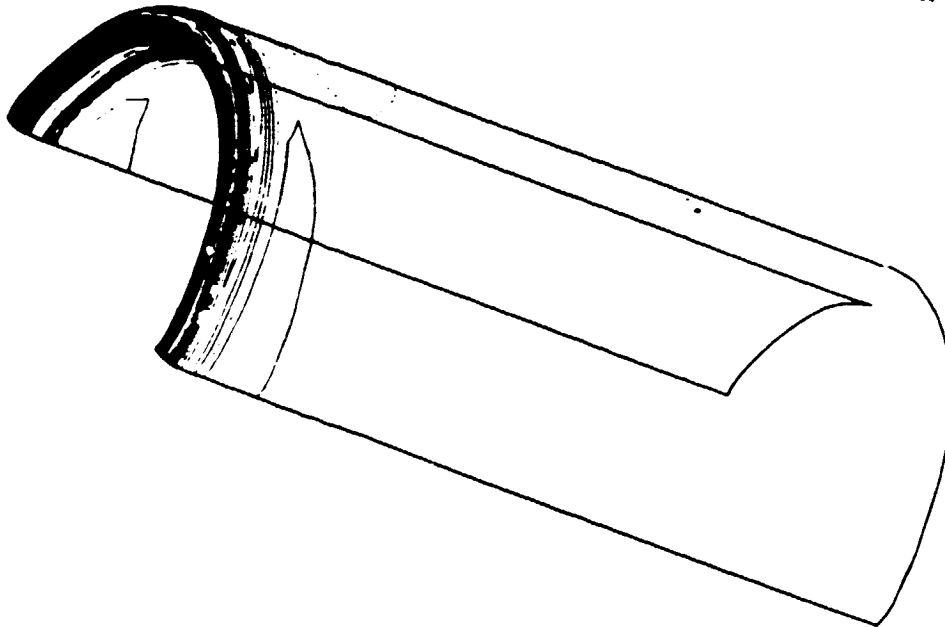
(a)



SURFACE VELOCITY VECTORS IN LOWER FRONT 45 DEGREE VIEW
INCOMPRESSIBLE COMBINATION RESULTS FOR THE 72-PANEL INLET.

MACH NO. = 0.0 ALPHA = 5.000 DEG. REF: DF12: MO NEUMANN
REYNOLDS = 0.0 MIL. CL = 0.719 07/18/85

(b)



SURFACE ISOBARS IN LOWER FRONT 45 DEGREE VIEW
INCOMPRESSIBLE COMBINATION RESULTS FOR THE 72-PANEL INLET.

MACH NO. = 0.0 ALPHA = 5.000 DEG CPMIN = -4.68 REF: DF12: MO NEUMANN
REYNOLDS = 0.0 MIL. CL = 0.719 CPMAX = 0.99 07/18/85

HEAVY LINE INDICATES ISOVALUE = -2.4000
DASHED LINE INDICATES ISOVALUE = 0.0000
INCREMENTS IN ISOVALUE = 0.1000

Figure 29. (a) Sample VECPLOT output from DF12 Mode 2 for a combined ALPHA=5 degrees. (b) Sample ISOPLOT output for same case.

**ORIGINAL PAGE IS
OF POOR QUALITY**

```
*****
|                                     |
|          3-D SOLUTION FORMAT         |
|      Pressures and Velocities       |
|                                     |
*****
```

<pre>NFLAGS, (IFLAG(I), I=1, NFLAGS) NTITLE : (TITLE(I), I=1, 20) N T I T L E : SREF, CREF, BREF, XREF, YREF, ZREF NSECT : NLINE1, N1max, ISTYPE, ID, (DESCRP(I), I=1, ID) : M1, (X(I), Y(I), Z(I), I=1, M1) : N L I N E : S E 1 : NLINE2, N2max, ISTYPE, ID, (DESCRP(I), I=1, ID) : M2, (X(I), Y(I), Z(I), I=1, M2) : N L I N E : 2 : NSOLNS, NREC ALPHA, BETA, MACH, RE, MFR : N (Vx(I), Vy(I), Vz(I), Cp(I), I=1, M1) : R (distr(I), cf(I), I=1, M1) : E C : N L I N E : 1 : C1, Cm, Cdv I N M (Vx(I), Vy(I), Vz(I), Cp(I), I=1, M2) R (distr(I), cf(I), I=1, M1) : E C : N S N : C1, Cm, Cdv : S O L E : CL, CD, CSF, CM, CROL, CYAW, CDv : N (Vx(I), Vy(I), Vz(I), Cp(I), I=1, M1) : R E C : N L I N E : 1 : C1, Cm, Cdv I N M (Vx(I), Vy(I), Vz(I), Cp(I), I=1, M2) R (distr(I), cf(I), I=1, M1) : E C : 2 : C1, Cm, Cdv : : CL, CD, CSF, CM, CROL, CYAW, CDv : : CL, CDt, CSF, CM, CROL, CYAW, CDv, N, (DUM(I), I=1, N) ALPHA, BETA, MACH, RE, MFR : : CL, CDt, CSF, CM, CROL, CYAW, CDv, N, (DUM(I), I=1, N)</pre>	<pre>Must have one flag. Must have one title. Multiple titles. Reference quantities. Number of sections. Nline info per section, ie. geometry definition. Next Nline, etc. Number of solutions, records. Flow conditions. Nline Velos, Pressures. Nline B.L. Quantities. T.B.D. T.B.D. T.B.D. Nline characteristics. Next Nline, etc. Section characteristics. Next Section, etc. Total Configuration char. Next Solution, etc End of File.</pre>
--	---

Figure 30. P/V (Pressure/Velocity) dataset format.

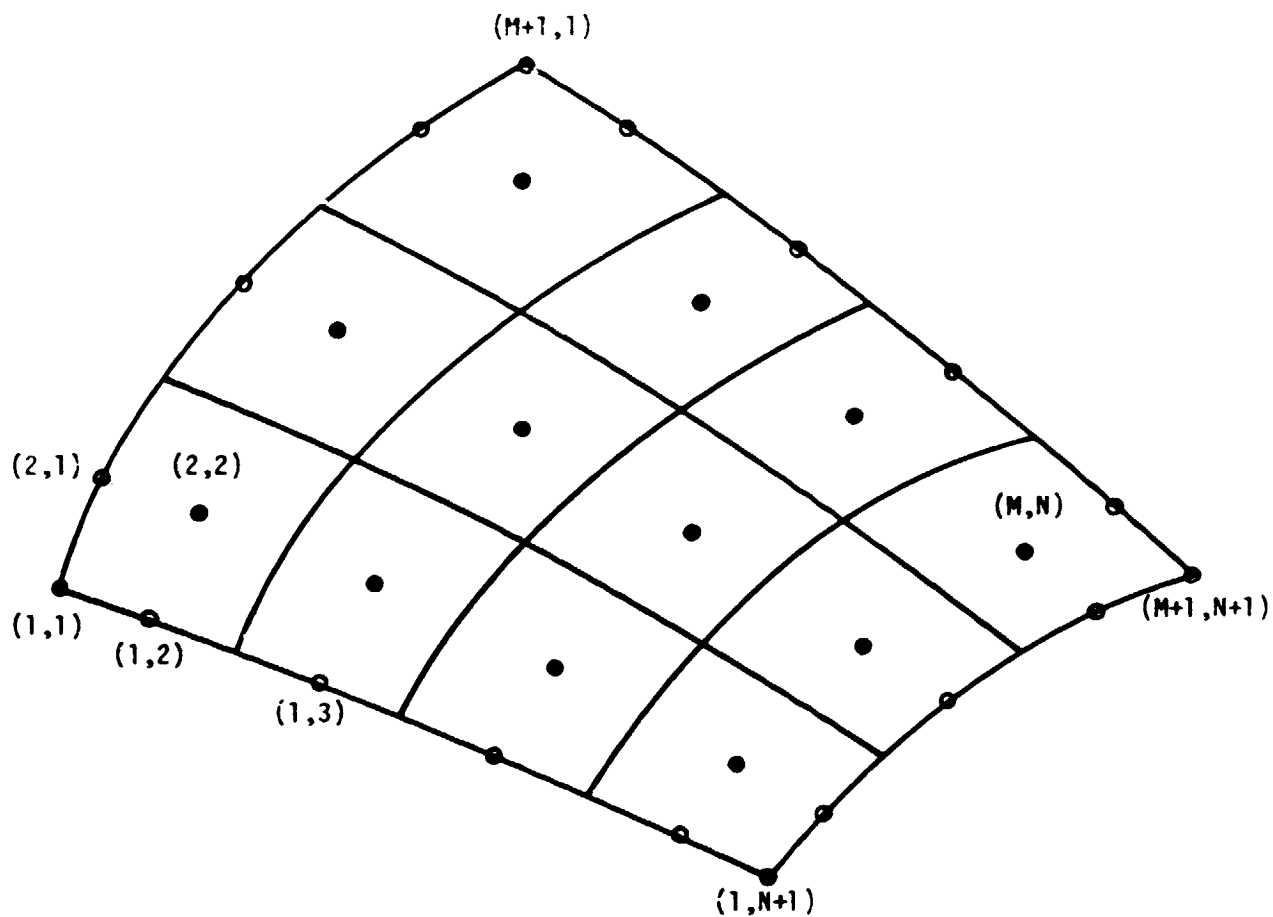


Figure 31. Extended set of velocity points stored in the P/V dataset: solid symbols are standard panel control points, hollow symbols are interpolated/extrapolated points. For $M \times N$ input panel defining points, $(M-1) \times (N-1)$ panels are produced, and $(M+1) \times (N+1)$ velocity points are calculated and saved.

ORIGINAL PAGE IS
OF POOR QUALITY

*Traces

*** INTERACTIVE 3-D SURFACE STREAMLINE TRACING ***
*** FROM A '3-D PRESSURE'-TYPE DATASET ***

LAST UPDATE: 7/18/85 (BWF)

DO YOU WANT CEBCI BOUNDARY LAYER CALCULATIONS? (Y OR C/R)

ENTER THE DATASET NAME OF THE 3-D P/V DATASET
(FULLY QUALIFIED, WITHOUT QUOTES)
DSN = Lee42df.pv.g027f.m0208.ca
(FOUND)

TO PERMIT SAVING OF THE STREAMLINES IN A 'QUIKLOT'-TYPE DATASET
COMPLETE THE FOL' WING DATASET NAME, OR C/R FOR NONE:
DSN = TS0730F.AIKPLOT.

TO PERMIT SAVING OF THE STREAMLINES IN A 'NEURGEN'-TYPE
(CARD IMAGE) DATASET, COMPLETE THE FOLLOWING
DATASET NAME, OR C/R FOR NONE:
DSN = TS0730F.NEURGEN.g027f

SUMMARY OF INPUT GEOMETRY SECTION N & N VALUES:

<u>ISCT</u>	<u>N</u>	<u>N</u>
1	8	14

STREAMLINE TRACING CONTROL PARAMETERS:

DELTA = 0.0000 MAXIMUM 'DELTA-PANEL' ALLOWED BETWEEN SUCCESSIVE STREAMLINE POINTS (IN 'FRACTIONS-OF-A-PANEL')
JUMP = 0.0000 ALLOWABLE 'JUMP' DISTANCE BETWEEN SECTION EDGES
IDIRC = 1 +1-DOWNSTREAM TRACING.
0-UPSTREAM AND DOWNSTREAM TRACING.
-1-UPSTREAM TRACING.
IPRINT = 0 0-MINIMUM PRINT.
1-STANDARD PRINT.
2-DEBUG PRINT.
ISCT = 1 SECTION NUMBER
ISOLN = 1 SOLUTION NUMBER
ITSELF = 0 0-SECTION JUMPING-TO-ITSELF INHIBITED
1-SECTION JUMPING-TO-ITSELF ALLOWED
NPTS = 100 MAXIMUM NUMBER OF POINTS ON A STREAMLINE (.LE. 200)
USTART = 1.0000 'U'-VALUE FOR START OF STREAMLINE (1 .LE. USTART .LE. N)
VSTART = 1.0000 'V'-VALUE FOR START OF STREAMLINE (1 .LE. VSTART .LE. N)
XMAX = 100.0000 X-CUTOFF VALUE

ENTER ANY CHANGES, 'LIST' OR C/R TO EXIT

ipoin=2,ustart=8,vstart=4
isolv=8,ustart=0,vstart=4

ENTER ANY CHANGES, 'LIST', OR C/R TO TRACE

FROM = 0.0 EN = 0.0 ALPHA = 8.00 14.0000 3.95320
SECTION 1 EDGE REACHED.
STREAMLINE RUNNING OFF THE EDGE OF SECTION NUMBER 1. NO CONTIGUOUS SECTION FOUND.
COMPUTATIONS TERMINATING FOR THIS STREAMLINE.

ENTER C/R TO PROCEED TO NEXT STREAMLINE
OR 1 TO EXIT

1

Figure 32. Sample interactive TRACE-ON execution for a streamline on the 72-panel simple inlet check case.

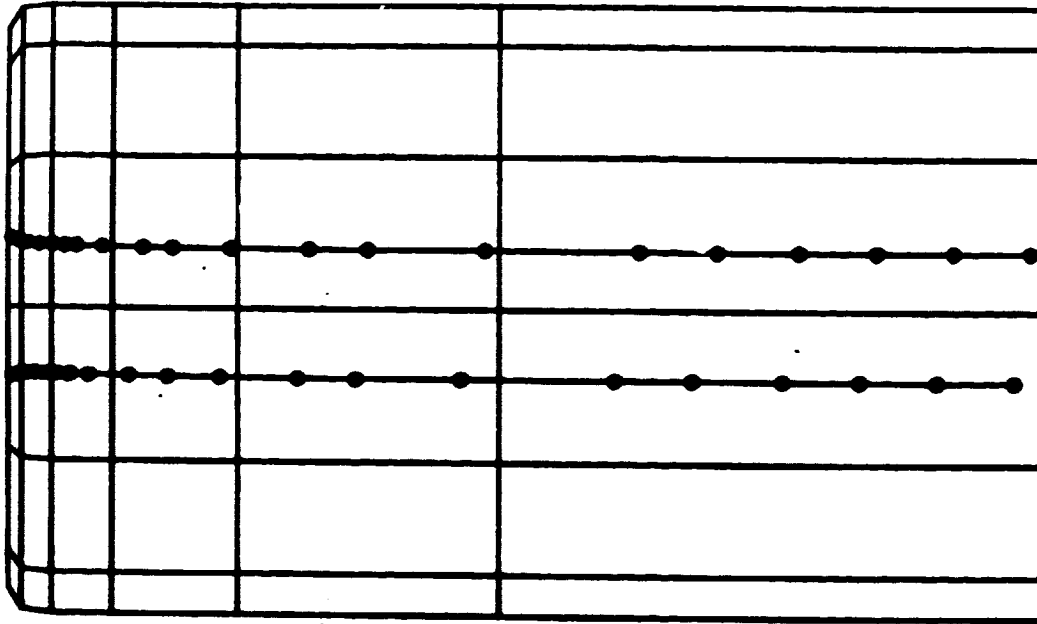
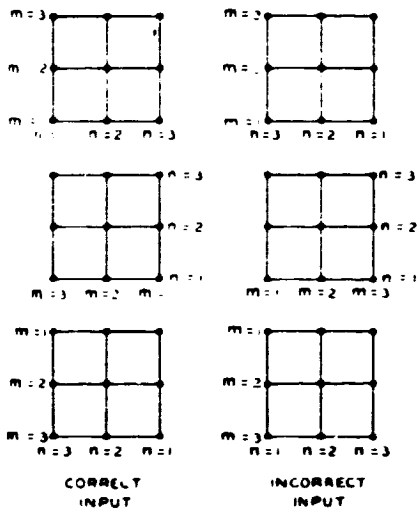


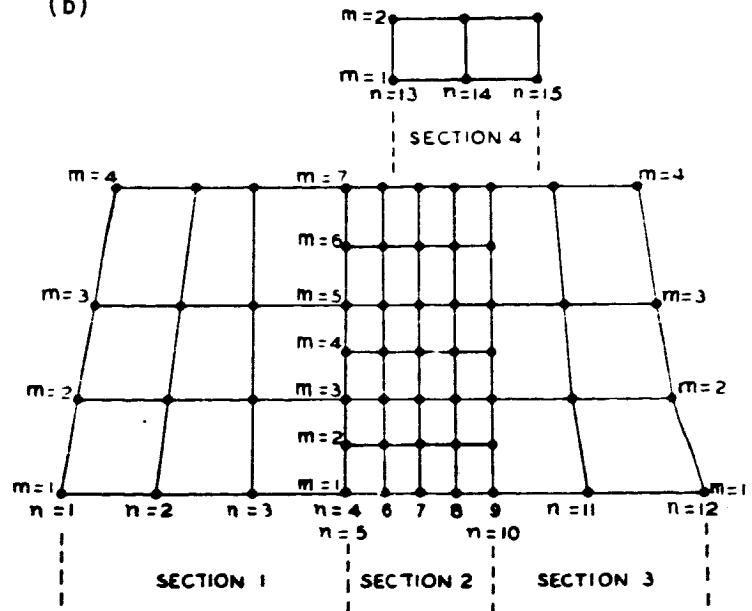
Figure 33. Two streamlines calculated by TRACE-ON for the 72-panel simple inlet check case.

ORIGINAL PAGE IS
OF POOR QUALITY

(a)



(b)



(c)

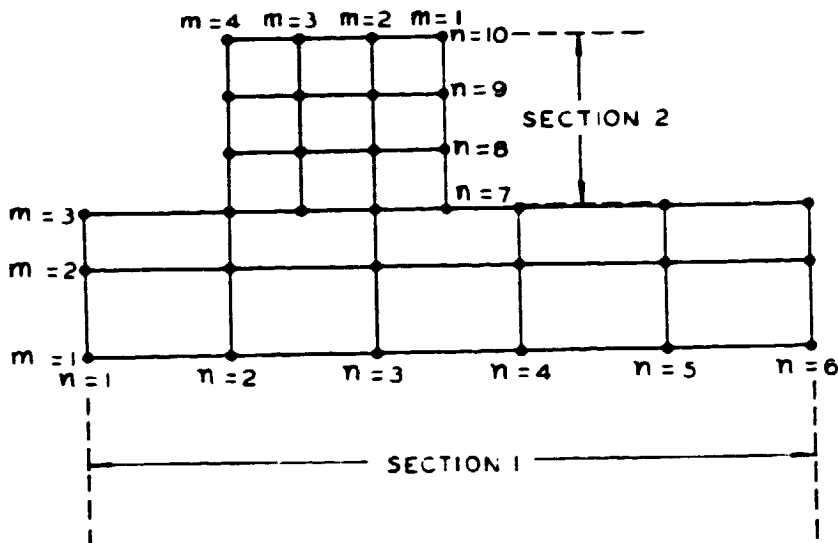


Figure 34. (a) Examples of correct and incorrect input; (b) Plan view of the input points on a body divided into sections; (c) Another possible division into sections.

APPENDIX A
 CONSISTENT EXPANSIONS FOR THE POTENTIAL AND VELOCITY INDUCED BY
 A CURVED PANEL AT A POINT IN SPACE

A "true" panel on a body surface is the curved four-sided region of the surface whose corners are input points lying exactly on the surface (Fig. 8). The boundary curves of the true panel that connect the corner points will be defined shortly. Consider a plane tangent to the surface at some central point of the true panel. A panel coordinate system is constructed whose origin is the tangency point and whose z or ζ axis is normal to the tangent plane. The x or ξ and y or η axes lie in this section. The corner points of the true panel are projected into the tangent plane along the normal direction. By joining adjacent projected corner points with straight lines, a flat panel is produced, which is assumed to be the projection of the true panel in the tangent plane. This construction now defines the boundary curves of the true panel. They are the curves joining the true corner points that have straight-line projections in the tangent plane.

It is a fundamental assumption of the present method that the dimensions of the panel are small in certain senses. Certainly variations over the panel of the normal direction are assumed small. Moreover, if a physical quantity is expanded in a Maclaurin series, successive terms become small, i.e., if

$$f(\xi, \eta) = \sum_{n=0}^{\infty} \frac{1}{n!} \left(\xi \frac{\partial}{\partial \xi} + \eta \frac{\partial}{\partial \eta} \right)_0^n f(\xi, \eta) \equiv \sum_{n=0}^{\infty} Q_n(\xi, \eta) \quad (A.1)$$

then

$$|Q_n| \ll |Q_m| \quad \text{if} \quad m < n \quad (A.2)$$

Also, the vertical distance ζ of a point on the true panel is of the order of the square of the horizontal distance, i.e.,

$$\zeta = O(\xi^2 + \eta^2) \ll \sqrt{\xi^2 + \eta^2} \quad (A.3)$$

The potential at a point (x, y, z) in space due to a source distribution on the true panel is

$$\phi = \iint_S \frac{q}{r} dS \quad (\text{A.4})$$

where

$$r^2 = (x - \xi)^2 + (y - \eta)^2 + (z - \zeta)^2 \quad (\text{A.5})$$

and where S is the surface area of the true panel. It is desired to express ϕ in terms of a series of integrals over the projected flat panel. Thus it may be stated that the potential of the true panel is "expanded about" that of the flat panel. To illustrate the process more completely, a three-term expansion is derived, although only the first two terms are ultimately retained in the present method.

In panel coordinates the equation $\zeta = f(\xi, \eta)$ of the surface of the true panel may be expanded in a Maclaurin series in the form

$$\begin{aligned} \zeta &= [P\xi^2 + 2Q\xi\eta + R\eta^2] + [T_{30}\xi^3 + T_{21}\xi^2\eta + T_{12}\xi\eta^2 + T_{03}\eta^3] + \dots \quad (\text{A.6}) \\ &= \zeta_2 + \zeta_3 + \dots \end{aligned}$$

There are no constant or linear terms in (A.6) because the origin is at the tangency point. All coefficients in (A.6) are constants proportional to derivatives of ζ at the origin. The coefficients P , Q and R , which are the only ones actually used in the present method, are the second derivatives. They are referred to below as the surface curvatures to which they are closely related. The quantity ζ_2 is second order in ξ and η and thus in panel dimension t , and ζ_3 is third order.

The equation of the true panel may be written

$$F(\xi, \eta, \zeta) = \zeta - \zeta_2(\xi, \eta) - \zeta_3(\xi, \eta) - \dots = 0 \quad (\text{A.7})$$

Then, taking the gradient gives

$$\text{grad } F = \vec{k} - (\zeta_{2\xi} + \zeta_{3\xi} + \dots)\vec{i} - (\zeta_{2\eta} + \zeta_{3\eta} + \dots)\vec{j} \quad (\text{A.8})$$

where subscripts ξ and η denote partial derivatives and \vec{i} , \vec{j} , \vec{k} are the unit vectors of the panel coordinate system. The vector $\text{grad } F$ is normal to the panel at any point. The unit normal at any point is

$$\vec{n} = \frac{\text{grad } F}{|\text{grad } F|} \quad (\text{A.9})$$

so the ζ -component of the unit normal is

$$n_\zeta = \frac{1}{|\text{grad } F|} = \frac{1}{\sqrt{1 + (\zeta_{2\xi} + \zeta_{3\xi} + \dots)^2 + (\zeta_{2\eta} + \zeta_{3\eta} + \dots)^2}} \quad (\text{A.10})$$

This can be expanded in the form

$$\begin{aligned} n_\zeta = 1 - \frac{1}{2} [(\zeta_{2\xi} + \zeta_{3\xi} + \dots)^2 + (\zeta_{2\eta} + \zeta_{3\eta} + \dots)^2] \\ + \frac{3}{8} [(\zeta_{2\xi} + \zeta_{3\xi} + \dots)^2 + (\zeta_{2\eta} + \zeta_{3\eta} + \dots)^2]^2 + \dots \end{aligned} \quad (\text{A.11})$$

From (A.6) it is clear that $\zeta_{2\xi}$ and $\zeta_{2\eta}$ are first order, $\zeta_{3\xi}$ and $\zeta_{3\eta}$ are second order, etc., so the leading terms from the first square bracket of (A.11) are second order, and the leading terms in the second square bracket are fourth order. Thus,

$$n_\zeta = 1 - \frac{1}{2} (\zeta_{2\xi}^2 + \zeta_{2\eta}^2) \quad (\text{A.12})$$

is a valid three-term expansion with second (linear) term zero. More precisely,

$$\begin{aligned} n_\zeta = 1 - \frac{1}{2} [(2P\xi + 2Q\eta)^2 + (2Q\xi + 2R\eta)^2] \\ = 1 - 2[(P^2 + Q^2)\xi^2 + 2(PQ + QR)\xi\eta + (Q^2 + R^2)\eta^2] \end{aligned} \quad (\text{A.13})$$

$$n_\zeta = 1 - 2\psi_2$$

where ψ_2 is second order. The elementary surface area dS on the true panel is related to the elementary area $dA = d\xi d\eta$ in the tangent plane by

$$n_\zeta dS = dA \quad (\text{A.14})$$

$$dS = (1 + 2\psi_2) d\xi d\eta \quad (\text{A.15})$$

The source density is strictly a function of surface distances along the panel. However, it can be shown that there is no difference between surface distances and ξ and η through second order. Thus it suffices to define σ in terms of ξ and η in the form

$$\begin{aligned}\sigma &= \sigma_0 + (\sigma_x \xi + \sigma_y \eta) + (\sigma_{xx} \xi^2 + 2\sigma_{xy} \xi \eta + \sigma_{yy} \eta^2) + \dots \\ &= \sigma_0 + \sigma_1 + \sigma_2\end{aligned}\tag{A.16}$$

where σ_n is n-th order in ξ and η and thus in panel dimension t . The coefficients in (A.16) are constants proportional to derivatives of σ at the origin.

Thus, to three terms

$$\begin{aligned}\sigma dS &= (\sigma_0 + \sigma_1 + \sigma_2)(1 + 2\psi_2) d\xi d\eta \\ &= (\sigma_0 + \sigma_1 + \sigma'_2) d\xi d\eta\end{aligned}\tag{A.17}$$

where

$$\sigma'_2 = \sigma_2 + 2\psi_2 \sigma_0\tag{A.18}$$

All of the above expansions are independent of the location of the point (x, y, z) .

It remains to expand $1/r$, which of course, does depend on x, y, z . It is necessary to differentiate three ranges of value of r :

$$\begin{aligned}(a) \quad r &\gg t && \text{for all } \xi, \eta \\ (b) \quad r &= O(t) && \text{for all } \xi, \eta \\ (c) \quad r &\ll t && \text{for some } \xi, \eta \\ &r = O(t) && \text{for other } \xi, \eta\end{aligned}\tag{A.19}$$

In other words, the ranges amount to the situations where the distance of the point (x, y, z) from the origin of panel coordinates is, respectively large, of the order of, and small compared to the dimensions of the panel. It turns out that the range (b) where r is of the order of the panel dimensions is the essential one. In the far-field, range (a), $1/r$ is expanded in negative powers of $r_0 = (x^2 + y^2 + z^2)^{1/2}$. The resulting expansion differs in no important way

from the usual far-field multipole expansion and thus is relatively easy to derive. An order-of-magnitude comparison of the expansions of ranges (a) and (b) shows that while certain terms become small faster than others as the distance r increases, the expansion derived for range (b) is valid for range (a), although it is conservative in that some retained terms could be eliminated. For points close to the panel, range (c), it is necessary to assume that they lie on a line through the origin having a finite slope with respect to the tangent plane. Under this condition the order-of-magnitude analysis of range (b) remains valid. This is just what the physics of a panel method requires in any event. Eventually, the control point of the panel is identified with the origin of panel coordinates and the above condition states that if a point approaches the surface, it does so at a control point. Since it is only at the control points that the normal velocity boundary condition is applied, approaching any other surface point would give physically meaningless results. Thus the derivation below concentrates on range (b), which may be thought of as the effect of a panel on control points of nearby panels.

The distance r can be written

$$\begin{aligned} r^2 &= (x - \xi)^2 + (y - \eta)^2 + z^2 - 2z\zeta + \zeta^2 \\ &= r_f^2 - 2z\zeta + \zeta^2 \end{aligned} \quad (\text{A.20})$$

where r_f is the distance between (x, y, z) and the point $(\xi, \eta, 0)$ on the flat panel (Fig. 3). Thus

$$\begin{aligned} \frac{1}{r} &= \frac{1}{r_f} \frac{1}{\sqrt{1 + (-2z\zeta + \zeta^2)/r_f^2}} = \frac{1}{r_f} \left[1 - \frac{1}{2} \frac{-2z\zeta + \zeta^2}{r_f^2} + \frac{3}{8} \frac{4z^2\zeta^2}{r_f^4} + \dots \right] \\ &= \frac{1}{r_f} \left[1 + \frac{z}{r_f} \frac{\zeta}{r_f} + \left(\frac{3}{2} \frac{z^2}{r_f^2} - \frac{1}{2} \right) \frac{\zeta^2}{r_f^2} + \dots \right] \end{aligned} \quad (\text{A.21})$$

Note that (z/r_f) is of order unity, and, since r_f is $O(t)$, the quantity ζ/r_f is also $O(t)$, i.e., $O(\xi)$. If use is made of (A.6), the above becomes

$$\frac{1}{r} = \frac{1}{r_f} \left[1 + \frac{z}{r_f} \frac{\zeta_2 + \zeta_3 + \dots}{r_f} + \left(\frac{3}{2} \frac{z^2}{r_f^2} - \frac{1}{2} \right) \left(\frac{\zeta_2 + \zeta_3 + \dots}{r_f} \right)^2 \right] \quad (\text{A.22})$$

from which the desired three-term expansion is obtained in the form

$$\frac{1}{r} = \frac{1}{r_f} \left\{ 1 + \frac{z}{r_f} \frac{\zeta_2}{r_f} + \left[\frac{z}{r_f} \frac{\zeta_3}{r_f} + \left(\frac{3}{2} \frac{z^2}{r_f^2} - \frac{1}{2} \right) \frac{\zeta_2^2}{r_f^2} \right] \right\} \quad (\text{A.23})$$

or, for abbreviation,

$$\frac{1}{r} = \frac{1}{r_f} (1 + c_1 + c_2) \quad (\text{A.24})$$

where c_n is of order n in ξ or n and thus in t . Now this is multiplied by (A.17) to obtain the expansion

$$\begin{aligned} \frac{\sigma}{r} dS &= \frac{1}{r_f} (\sigma_0 + \sigma_1 + \sigma_2') (1 + c_1 + c_2) dA \\ &= \frac{dA}{r} [\sigma_0 + \sigma_1 + \sigma_2' \\ &\quad + c_1 \sigma_0 + c_1 \sigma_1 + c_1 \sigma_2' \\ &\quad + c_2 \sigma_0 + c_2 \sigma_1 + c_2 \sigma_2'] \end{aligned} \quad (\text{A.25})$$

The square bracket in (A.25) must be reduced to a three-term expansion using the facts that

$$\sigma_0 \gg \sigma_1 \gg \sigma_2 \quad (\text{A.26})$$

and

$$1 \gg c_1 \gg c_2 \quad (\text{A.27})$$

The leading (lowest order) term is clearly σ_0 because all terms are small compared to it. Possible members of the second term are σ_1 and $c_1 \sigma_0$ because all remaining terms are small compared to one or the other. Thus, both of these are retained in the second term, because neither can be guaranteed to be small compared to the other in all cases. The question then arises as to which of the remaining six terms of the square bracket of (A.24) need to be retained in

the third term of the expansion. Obviously, if any of these six is small compared to any other, it may be discarded. This eliminates all but σ_2 , $c_1\sigma_1$ and $c_2\sigma_0$. Thus, the three-term expansion of the integrand of (A.4) has the form

$$\frac{\sigma}{r} dS = \frac{dA}{r_f} [\sigma_0 + (c_1\sigma_0 + \sigma_1) + (c_2\sigma_0 + c_1\sigma_1 + \sigma_2')] \quad (A.28)$$

when the abbreviations of (A.16) and (A.24) are replaced by their actual expressions, the three-term expansion of (A.4) is

$$\begin{aligned} \phi = & \sigma_0 \iint_A \frac{dA}{r_f} + \left[\sigma_0 \iint_A z \frac{\zeta_2}{r_f^3} dA + \iint_A \frac{\sigma_x \zeta + \sigma_y \eta}{r_f} dA \right] \\ & + \left[\sigma_0 \iint_A \left(z \frac{\zeta_3}{r_f^3} + \frac{3}{2} z^2 \frac{\zeta_2^2}{r_f^5} - \frac{1}{2} \frac{\zeta_2^2}{r_f^3} \right) + \iint_A z \frac{\zeta_2}{r_f} (\sigma_x \xi + \sigma_y \eta) dA \right] \\ & + \iint_A \frac{1}{r_f} \left[\sigma_{xx} \zeta^2 + 2\sigma_{xy} \xi \eta + \sigma_{yy} \eta^2 + 2(P^2 + Q^2) \xi^2 + 4(PQ + QR) \xi \eta \right. \\ & \left. + 2(Q^2 + R^2) \eta^2 \right] dA \end{aligned} \quad (A.29)$$

where the integrals are over the projected flat panel. Defining the integrals,

$$I_{mnp} = \iint_A \frac{\xi^m \eta^n}{r_f^p} dA \quad (A.30)$$

the three-term expansion of the potential can be written

$$\begin{aligned} \phi = & \phi^{(0)} \sigma_0 + [\phi^{(c)} \sigma_0 + \phi^{(1x)} \sigma_x + \phi^{(1y)} \sigma_y] \\ & + [\phi^{(20)} \sigma_0 + \phi^{(2x)} \sigma_x + \phi^{(2y)} \sigma_y + \phi^{(2xx)} \sigma'_{xx} + 2\phi^{(2xy)} \sigma'_{xy} + \phi^{(2yy)} \sigma'_{yy}] \end{aligned} \quad (A.31)$$

where

$$\begin{aligned} \sigma'_{xx} &= \sigma_{xx} + 2(P^2 + Q^2) \\ \sigma'_{xy} &= \sigma_{xy} + 2(PQ + QR) \\ \sigma'_{yy} &= \sigma_{yy} + 2(Q^2 + R^2) \end{aligned} \quad (A.32)$$

The individual potentials in (A.30) are

$$\phi^{(0)} = I_{001} \quad (\text{A.33})$$

$$\phi^{(c)} = z[PI_{203} + 2QI_{113} + RI_{023}] \quad (\text{A.34})$$

$$\phi^{(1x)} = I_{101} \quad (\text{A.35})$$

$$\phi^{(1y)} = I_{011}$$

$$\begin{aligned} \phi^{(20)} = & z[T_{30}I_{303} + T_{21}I_{123} + T_{12}I_{123} + T_{03}I_{033}] \\ & + \frac{3}{2} z^2 [P_2 I_{405} + 4PQI_{315} + (2PR + 4Q^2)I_{225} + 4QRI_{135} + R^2 I_{045}] \\ & - \frac{1}{2} [P^2 I_{403} + 4PQI_{313} + (2PR + 4Q^2)I_{223} + 4QRI_{133} + R^2 I_{043}] \end{aligned} \quad (\text{A.36})$$

$$\phi^{(2x)} = z[PI_{303} + 2QI_{213} + RI_{123}] \quad (\text{A.37})$$

$$\phi^{(2x)} = z[PI_{213} + 2QI_{123} + RI_{033}]$$

$$\phi^{(2xx)} = I_{201}$$

$$\phi^{(2xy)} = I_{111} \quad (\text{A.38})$$

$$\phi^{(2yy)} = I_{021}$$

The first term of (A.31), $\phi^{(0)}_{\sigma_0}$, corresponds to a flat panel with a constant source density. This is, of course, the term used in the first-order method. The second term of (A.31) contains the second derivatives P, Q and R, of the surface shape but no higher derivatives and first derivatives of the source density but no higher derivatives. Thus the second term of (A.31) corresponds to a paraboloidal panel shape with a linearly varying source density. The third term of (A.31) contains all the preceding quantities and also the third

derivatives of the surface shape and the second derivatives of the source density: a cubic panel with a quadratic source density.

The equations above illustrate the fact that succeeding terms in the expansion for the potential of a panel increase rapidly in complexity. A single first term is followed by a second term containing five individual parts, each with its own integral of the form, Eq. (A.30). The third term contains 23 individual parts which together involve 17 different integrals of the form of Eq. (A.30). The great increase in complexity associated with retaining the third term of (A.31) appears to be unjustified at this time. Accordingly, the higher-order method accounts for the source density effect by considering the first two terms in Eq. (A.31). This is the approach that has previously been followed in the two-dimensional and axisymmetric higher-order methods (Refs. 17 and 18).

APPENDIX B

GENERATION OF PANEL GEOMETRIC QUANTITIES BY MEANS OF BICUBIC SPLINES

Very elaborate geometry fitting procedures based on parametric bicubic splines have been developed at Douglas Aircraft Company over many years. A description of this technique is beyond the scope of the present report. A survey is contained in Ref. 19. In the present application the method is considered a "black box," although several minor changes had to be made.

The points defining the body are input in the usual way. Each panel is fitted by a bicubic surface in terms of two parameters, u and v , that vary from 0 to 1 over the panel. (The panel is the unit square in parameter space.) This permits the well-known procedures of Ref. 20 to be used as follows.

Let a point, (x,y,z) , of the panel be represented as a vector

$$\vec{x} = \vec{x}i + \vec{y}j + \vec{z}k \quad (\text{B.1})$$

The parametric cubic fit then yields

$$\vec{x} = \vec{x}(u,v) \quad (\text{B.2})$$

These expressions may be differentiated analytically to give

$$\vec{x}_u, \quad \vec{x}_v, \quad \vec{x}_{uu}, \quad \vec{x}_{uv}, \quad \vec{x}_{vv} \quad (\text{B.3})$$

as functions of u and v . The vectors \vec{x}_u and \vec{x}_v are tangent to the curves, $v = \text{constant}$ and $u = \text{constant}$, respectively, and thus lie in the surface although they are not perpendicular.

The point corresponding to $u = v = 1/2$ is in the "center" of the panel in some sense. It is selected as the control point and origin of coordinates of the flat projected panel. The derivatives of Eq. (B.3) are evaluated there, and in all that follows \vec{x} and its derivatives are assumed to be those at $u = v = 1/2$.

The unit normal vector to the panel, which is also the unit vector along the z axis of panel coordinates is

$$\vec{n} = \vec{k}_e = \pm \frac{\vec{x}_u \times \vec{x}_v}{|\vec{x}_u \times \vec{x}_v|} \quad (\text{B.4})$$

where the sign is selected to give an outward normal. The unit vector along the ξ axis of panel coordinates is taken tangent to the $v = \text{constant}$ curve which nearly parallels the N-lines,

$$\vec{i}_e = \frac{\vec{x}_u}{|\vec{x}_u|} \quad (\text{B.5})$$

Thus the unit vector along the η axis of panel coordinates is

$$\vec{j}_e = \vec{k}_e \times \vec{i}_e \quad (\text{B.6})$$

The components of the three unit vectors thus obtained comprise the transformation matrix.

Now define

$$h = u - 1/2, \quad k = v - 1/2 \quad (\text{B.7})$$

and consider the Maclaurin series for ξ , η and ζ in terms of h and k . They have the form

$$\begin{aligned} \xi &= Ah + Bk + (\text{second order}) \\ \eta &= Ch + Dk + (\text{second order}) \\ \zeta &= 1/2(eh^2 + 2fhk + gk^2) + (\text{third order}) \end{aligned} \quad (\text{B.8})$$

There are not constant terms in (B.8), because the origin of panel coordinates corresponds to $h = k = 0$. Furthermore, since the $\xi\eta$ plane is tangent to the surface at the origin (\vec{k}_e is the normal vector), the series for ζ has no linear terms. Reference 20 gives the coefficients of Eqs. (B.8) as

$$A = \vec{x}_u \cdot \vec{i}_e \quad B = \vec{x}_v \cdot \vec{i}_e \quad (\text{B.9})$$

$$C = \vec{x}_u \cdot \vec{j}_e = 0 \quad D = \vec{x}_v \cdot \vec{j}_e$$

$$e = \vec{x}_{uu} \cdot \vec{n} \quad f = \vec{x}_{uv} \cdot \vec{n} \quad g = \vec{x}_{vv} \cdot \vec{n} \quad (B.10)$$

The first two of Eqs. (B.8) may be inverted to give

$$h = a\xi + b\eta + (\text{second order})$$

$$k = c\xi + d\eta + (\text{second order}) \quad (B.11)$$

where

$$a = \frac{D}{\Delta}, \quad b = -\frac{B}{\Delta}, \quad c = \frac{C}{\Delta}, \quad d = \frac{A}{\Delta} \quad (B.12)$$

$$\Delta = AD - BC$$

Equation (B.12) may be inserted into the third equation of (B.8) to give the desired form

$$\zeta = P\xi^2 + 2Q\xi\eta + R\eta^2 \quad (B.13)$$

The result is

$$P = 1/2[ea^2 + 2fac + gc^2]$$

$$Q = 1/2[eab + f(ad + bc) + gcd] \quad (B.14)$$

$$R = 1/2[eb + 2fbd + gd^2]$$

For generality c has been included in Eq. (B.14), but in the present application it is zero, which simplifies (B.14).

It remains to compute corner points in panel coordinates. The four input points bounding the panel are transformed into panel coordinates to obtain $(\xi_k^*, \eta_k^*, \zeta_k^*)$, $k = 1, 2, 3, 4$. They are projected into the plane by simply ignoring ζ_k^* . Next the side between points 1 and 2 is rotated to make $\eta_1 = \eta_2$. The midpoint and length of the side are, respectively,

$$\bar{\xi} = \frac{1}{2} (\xi_1^* + \xi_2^*), \quad \bar{\eta} = \frac{1}{2} (\eta_1^* + \eta_2^*) \quad (\text{B.15})$$

$$d = \sqrt{(\xi_1^* - \xi_2^*)^2 + (\eta_1^* - \eta_2^*)^2}$$

Then the final corner point coordinates are

$$\eta_1 = \eta_2 = \bar{\eta}$$

$$\xi_1 = \bar{\xi} - \frac{d}{2} \quad (\text{B.16})$$

$$\xi_2 = \bar{\xi} + \frac{d}{2}$$

A similar calculation is performed for the side between the points 3 and 4.

It should be noted that the underlying parametric cubic geometry routine uses the surrounding input points to generate the fit to a panel. The routine considers only points on the same section, and thus slightly different results can be obtained depending on how the body is sectioned. For fitting purposes, the wake is considered a separate section, so that the routine does not try to fit around the trailing edge. On the semi-infinite last-wake panel the derivatives P and Q are set equal to zero, so that the panel has straight generators in the stream direction, but R, the spanwise second derivative, may be nonzero.

APPENDIX C
AREA MOMENTS OF A PANEL

The normalized moments of the area of the tangent panel are required. These are defined by

$$I_{nm} = \frac{1}{t^{n+m+2}} \iint_A \xi^n \eta^m d\xi d\eta \quad (C.1)$$

where the region of integration is the area of the panel. For example, $t^2 I_{00}$ is the area $t^4 I_{20}$, $t^4 I_{11}$, $t^4 I_{02}$ are the moments of inertia or second moments. The order of a moment is the sum of its subscripts $n + m$. There are two first-order moments, three second-order, four third-order, and five fourth-order. The present method uses up through fourth order. The moments are calculated by a straightforward but rather lengthy set of formulas.

First, normalize the corner point coordinates by the maximum diagonal,

$$\xi_k = \xi_k/t, \quad \eta_k = \eta_k/t, \quad k = 1, 2, 3, 4 \quad (C.2)$$

Now the normalized moment may be defined in terms of certain auxiliary functions

$$I_{nm} = -I_{nm}^{(32)} + I_{nm}^{(41)} + \frac{1}{(m+1)(n+1)} [\eta_1^{m+1} (\xi_2^{n+1} - \xi_1^{n+1}) + \eta_3^{m+1} (\xi_4^{n+1} - \xi_3^{n+1})] \quad (C.3)$$

The auxiliary function $I_{nm}^{(32)}$ is as follows:

If $|m_{32}| > 1$:

$$I_{nm}^{(32)} = \frac{1}{(m+1)(n+1)} [\xi^{n+1} \eta^{m+1}]_3^2 - \frac{1}{(n+1)(n+2)} \frac{1}{m_{32}} [\xi^{n+2} \eta^m]_3^2 + \frac{n}{(n+1)(n+2)(n+3)} \frac{1}{m_{32}^2} [\xi^{n+3} \eta^{n-1}]_3^2 \quad (C.4)$$

$$\begin{aligned}
& - \frac{n(m-1)}{(n+1)(n+2)(n+3)(n+4)} \frac{1}{m_{32}^3} [\xi^{n+4} \eta^{m-2}]_3^2 \\
& + \frac{n(m-1)(m-2)}{(n+1)(n+2)(n+3)(n+4)(n+5)} \frac{1}{m_{32}^4} [\xi^{n+5} \eta^{m-3}]_3^2 \\
& - \frac{n(m-1)(m-2)(m-3)}{(n+1)(n+2)(n+3)(n+4)(n+5)(n+6)} \frac{1}{m_{32}^5} [\xi^{n+6} \eta^{m-4}]_3^2
\end{aligned}$$

If $|m_{32}| \leq 1$:

$$\begin{aligned}
I_{nm}^{(32)} &= \frac{1}{(m+1)(m+2)} m_{32} [\xi^{n+m+2} \eta^2]_3^2 \\
& - \frac{n}{(m+1)(m+2)(m+3)} m_{32}^2 [\xi^{n-1} \eta^{m+3}]_3^2 \\
& + \frac{n(n-1)}{(m+1)(m+2)(m+3)(m+4)} m_{32}^3 [\xi^{n-2} \eta^{m+4}]_3^2 \quad (C.5) \\
& - \frac{n(n-1)(n-2)}{(m+1)(m+2)(m+3)(m+4)(m+5)} m_{32}^4 [\xi^{n-3} \eta^{m+5}]_3^2 \\
& + \frac{n(n-1)(n-2)(n-3)}{(m+1)(m+2)(m+3)(m+4)(m+5)(m+6)} m_{32}^5 [\xi^{n-4} \eta^{m+6}]_3^2
\end{aligned}$$

where the bracketed symbols are defined by

$$[\xi^k \eta^p]_3^2 = \xi_2^k \eta_2^p - \xi_3^k \eta_3^p \quad (C.6)$$

(The superscripts in the above equations denote simple powers of the quantities except for the bracketed double superscript (32), which denotes the side of the quadrilateral.) It is clear from the above that the calculation of $I_{nm}^{(32)}$ requires $m+2$ terms of Eq. (C.4) or $n+1$ terms of Eq. (C.5). The calculation is simply terminated at this number of terms. The auxiliary function $I_{nm}^{(41)}$ is obtained from the above by an obvious substitution of subscripts.

APPENDIX D
NEAR-FIELD SOURCE FORMULAS

If $r_0/t < \rho_2$, the near field formulas are used to compute induced velocities. The calculation starts with the element coordinates x, y, z of the field point and the geometric quantities associated with the element that are discussed in Section 2.3.

Preliminary quantities to be calculated are:

$$r_k = \sqrt{(x - \xi_k)^2 + (y - \eta_k)^2 + z^2}, \quad k = 1, 2, 3, 4 \quad (D.1)$$

$$\alpha_k = \frac{x - \xi_k}{r_k}, \quad \beta_k = \frac{y - \eta_k}{r_k}, \quad \gamma_k = \frac{z}{r_k} \quad k = 1, 2, 3, 4$$

$$p_k^{(32)} = m_{32}[z^2 + (y - \eta_k)^2] - (x - \xi_k)(y - \eta_k), \quad k = 3 \text{ or } 2 \quad (D.2)$$

$$p_k^{(41)} = m_{41}[z^2 + (y - \eta_k)^2] - (x - \xi_k)(y - \eta_k), \quad k = 4 \text{ or } 1$$

The basic functions are

$$L^{(mn)} = \log \frac{r_m + r_n - d_{mn}}{r_m + r_n + d_{mn}} \quad m, n \text{ consecutive, i.e., } mn = 12, 32, 34 \text{ or } 41 \quad (D.3)$$

and

$$T_k^{(32)} = \tan^{-1} \left[\frac{p_k^{(32)}}{zr_k} \right], \quad k = 3 \text{ or } 2 \quad (D.4)$$

$$T_k^{(41)} = \tan^{-1} \left[\frac{p_k^{(41)}}{zr_k} \right], \quad k = 4 \text{ or } 1$$

Also needed are derivatives of the T's and L's. The derivatives of $T_k^{(32)}$ are

$$\frac{\partial T_k^{(32)}}{\partial x} = - \frac{z(r_k^2 \beta_k + p_k^{(32)} \alpha_k)}{D_k^{(32)}}$$

$$\frac{\partial T_k^{(32)}}{\partial y} = \frac{z[(2m_{32}\beta_k - \alpha_k)r_k^2 - p_k^{(32)}\beta_k]}{D_k^{(32)}} \quad k = 3 \text{ or } 2 \quad (D.5)$$

$$\frac{\partial T_k^{(32)}}{\partial z} = \frac{2m_{32}z^2r_k - p_k^{(32)}(r_k + z\gamma_k)}{D_k^{(32)}}$$

$$D_k^{(32)} = z^2r_k^2 + [p_k^{(32)}]^2$$

There is an analogous set of formulas for the derivatives of $T_k^{(41)}$.

The derivatives of $L^{(mn)}$ are

$$\frac{\partial L^{(mn)}}{\partial x} = D_{mn}(\alpha_m + \alpha_n), \quad \frac{\partial L^{(mn)}}{\partial y} = D_{mn}(\beta_m + \beta_n), \quad \frac{\partial L^{(mn)}}{\partial z} = D_{mn}(\gamma_m + \gamma_n),$$

$$D_{mn} = \frac{2d_{mn}}{(r_m + r_n)^2 - d_{mn}^2} \quad (D.6)$$

$$mn = 12, 32, 34, 41$$

The flat-panel constant-source velocities are

$$V_x^{(0)} = -\frac{1}{S_{32}} L^{(32)} + \frac{1}{S_{41}} L^{(41)}$$

$$V_y^{(0)} = -L^{(12)} + L^{(34)} + \frac{m_{32}}{S_{32}} L^{(32)} - \frac{m_{41}}{S_{41}} L^{(41)} \quad (D.7)$$

$$V_z^{(0)} = -T_2^{(32)} + T_3^{(32)} + T_1^{(41)} - T_4^{(41)}$$

Referring again to Appendix A, it can be seen that the integrals I_{mnp} of Eq. (A.30) are source potentials if $p = 1$ and, when multiplied by z , are dipole potentials if $p = 3$. Specifically if ϕ_{mn} represents the potential of a dipole distribution $\mu = \xi^m \eta^n$ on the panel, then

$$\phi_{mn} = zI_{mn3} \quad (D.8)$$

It turns out that the higher-order source terms for a panel are expressible in terms of derivatives of the dipole potentials, Eq. (D.8), and the derivatives of the source velocities, Eq. (D.7).

Only the derivatives of V_x and V_y are needed (since $V_z = \phi_{00}$, its derivatives are exactly a potential derivative). The derivatives of V_x and V_y are

$$\begin{aligned} \frac{\partial V_x^{(0)}}{\partial x} &= -\frac{1}{S_{32}} \frac{\partial L^{(32)}}{\partial x} + \frac{1}{S_{41}} \frac{\partial L^{(41)}}{\partial x} \\ \frac{\partial V_x^{(0)}}{\partial y} &= -\frac{1}{S_{32}} \frac{\partial L^{(32)}}{\partial y} + \frac{1}{S_{41}} \frac{\partial L^{(41)}}{\partial y} \\ \frac{\partial V_x^{(0)}}{\partial z} &= -\frac{1}{S_{32}} \frac{\partial L^{(32)}}{\partial z} + \frac{1}{S_{41}} \frac{\partial L^{(41)}}{\partial z} \\ \frac{\partial V_y^{(0)}}{\partial x} &= -\frac{\partial L^{(12)}}{\partial x} + \frac{\partial L^{(34)}}{\partial x} + \frac{m_{32}}{S_{32}} \frac{\partial L^{(32)}}{\partial x} - \frac{m_{41}}{S_{41}} \frac{\partial L^{(41)}}{\partial x} \\ \frac{\partial V_y^{(0)}}{\partial y} &= -\frac{\partial L^{(12)}}{\partial y} + \frac{\partial L^{(34)}}{\partial y} + \frac{m_{32}}{S_{32}} \frac{\partial L^{(32)}}{\partial y} - \frac{m_{41}}{S_{41}} \frac{\partial L^{(41)}}{\partial y} \\ \frac{\partial V_y^{(0)}}{\partial z} &= -\frac{\partial L^{(12)}}{\partial z} + \frac{\partial L^{(34)}}{\partial z} + \frac{m_{32}}{S_{32}} \frac{\partial L^{(32)}}{\partial z} - \frac{m_{41}}{S_{41}} \frac{\partial L^{(41)}}{\partial z} \end{aligned} \tag{D.9}$$

Now the potential derivatives are as follows.

$$\begin{aligned} \frac{\partial \phi_{00}}{\partial x} &= -\frac{\partial T_2^{(32)}}{\partial x} + \frac{\partial T_3^{(32)}}{\partial x} + \frac{\partial T_1^{(41)}}{\partial x} - \frac{\partial T_4^{(41)}}{\partial x} \\ \frac{\partial \phi_{00}}{\partial y} &= -\frac{\partial T_2^{(32)}}{\partial y} + \frac{\partial T_3^{(32)}}{\partial y} + \frac{\partial T_1^{(41)}}{\partial y} - \frac{\partial T_4^{(41)}}{\partial y} \\ \frac{\partial \phi_{00}}{\partial z} &= -\frac{\partial T_2^{(32)}}{\partial z} + \frac{\partial T_3^{(32)}}{\partial z} + \frac{\partial T_1^{(41)}}{\partial z} - \frac{\partial T_4^{(41)}}{\partial z} \end{aligned} \tag{D.10}$$

$$\frac{\partial \phi_{01}}{\partial x} = -z \frac{\partial v_y^{(0)}}{\partial x} + y \frac{\partial \phi_{00}}{\partial x}$$

$$\frac{\partial \phi_{01}}{\partial y} = -z \frac{\partial v_y^{(0)}}{\partial y} + y \frac{\partial \phi_{00}}{\partial y} + V_z(\text{source}) \quad (\text{D.11})$$

$$\frac{\partial \phi_{01}}{\partial z} = -z \frac{\partial v_y^{(0)}}{\partial z} + y \frac{\partial \phi_{00}}{\partial z} - V_y(\text{source})$$

$$\frac{\partial \phi_{10}}{\partial x} = -z \frac{\partial v_x^{(0)}}{\partial x} + x \frac{\partial \phi_{00}}{\partial x} + V_z(\text{source})$$

$$\frac{\partial \phi_{10}}{\partial y} = -z \frac{\partial v_x^{(0)}}{\partial y} + x \frac{\partial \phi_{00}}{\partial y} \quad (\text{D.12})$$

$$\frac{\partial \phi_{10}}{\partial z} = -z \frac{\partial v_x^{(0)}}{\partial z} + x \frac{\partial \phi_{00}}{\partial z} - V_x(\text{source})$$

Now define

$$J_{11} = \frac{r_3 - r_2}{S_{32}^2} + \frac{r_1 - r_4}{S_{41}^2} + \frac{m_{32}}{S_{32}^3} (x - m_{32}y - b_{32})L \quad (32)$$

$$- \frac{m_{41}}{S_{41}^3} (x - m_{41}y - b_{41})L \quad (41) \quad (\text{D.13})$$

$$\frac{\partial J_{11}}{\partial x} = \frac{\alpha_3 - \alpha_2}{S_{32}^2} + \frac{m_{32}}{S_{32}^3} L \quad (32) + \frac{m_{32}}{S_{32}^3} (x - m_{32}y - b_{32}) \frac{\partial L \quad (32)}{\partial x}$$

$$+ \frac{\alpha_1 - \alpha_4}{S_{41}^2} - \frac{m_{41}}{S_{41}^3} L \quad (41) - \frac{m_{41}}{S_{41}^3} (x - m_{41}y - b_{41}) \frac{\partial L \quad (41)}{\partial x}$$

$$\frac{\partial J_{11}}{\partial y} = \frac{\beta_3 - \beta_2}{S_{32}^2} - \frac{m_{32}}{S_{32}^3} L \quad (32) + \frac{m_{32}}{S_{32}^3} (x - m_{32}y - b_{32}) \frac{\partial L \quad (32)}{\partial y}$$

$$+ \frac{\beta_1 - \beta_4}{S_{41}^2} + \frac{m_{41}}{S_{41}^3} L \quad (41) - \frac{m_{41}}{S_{41}^3} (x - m_{41}y - b_{41}) \frac{\partial L \quad (41)}{\partial y} \quad (\text{D.14})$$

$$\begin{aligned} \frac{\partial J_{11}}{\partial z} &= \frac{\gamma_3 - \gamma_2}{S_{32}^2} + \frac{m_{32}}{S_{32}^3} (x - m_{32}y - b_{32}) \frac{\partial L}{\partial z} \quad (32) \\ &+ \frac{\gamma_1 - \gamma_4}{S_{41}^2} - \frac{m_{41}}{S_{41}^3} (x - m_{41}y - b_{41}) \frac{\partial L}{\partial z} \quad (41) \end{aligned}$$

Using the above

$$\begin{aligned} V_x^{(Q)} &= - \left[z \frac{\partial J_{11}}{\partial x} + x \frac{\partial \phi_{01}}{\partial x} + y \frac{\partial \phi_{10}}{\partial x} - xy \frac{\partial \phi_{00}}{\partial x} - z V_y^{(0)} \right] \\ V_y^{(Q)} &= - \left[z \frac{\partial J_{11}}{\partial y} + x \frac{\partial \phi_{01}}{\partial y} + y \frac{\partial \phi_{10}}{\partial y} - xy \frac{\partial \phi_{00}}{\partial y} - z V_x^{(0)} \right] \quad (D.15) \\ V_z^{(Q)} &= - \left[z \frac{\partial J_{11}}{\partial z} + x \frac{\partial \phi_{01}}{\partial z} + y \frac{\partial \phi_{10}}{\partial z} - xy \frac{\partial \phi_{00}}{\partial z} + J_{11} \right] \end{aligned}$$

Also define

$$\begin{aligned} H_{02} &= m_{32} \frac{r_2 - r_3}{S_{32}^2} + m_{41} \frac{r_4 - r_1}{S_{41}^2} + \frac{1}{S_{32}^3} (x - m_{32}y - b_{32}) L \quad (32) \\ &- \frac{1}{S_{41}^3} (x - m_{41}y - b_{41}) L \quad (41) \quad (D.16) \end{aligned}$$

$$\begin{aligned} \frac{\partial H_{02}}{\partial x} &= \frac{m_{32}}{S_{32}^2} (\alpha_2 - \alpha_3) + \frac{1}{S_{32}^3} L \quad (32) + \frac{(x - m_{32}y - b_{32})}{S_{32}^3} \frac{\partial L}{\partial x} \quad (32) \\ &+ \frac{m_{41}}{S_{41}^2} (\alpha_4 - \alpha_1) - \frac{1}{S_{41}^3} L \quad (41) - \frac{(x - m_{41}y - b_{41})}{S_{41}^3} \frac{\partial L}{\partial x} \quad (41) \end{aligned}$$

$$\begin{aligned} \frac{\partial H_{02}}{\partial y} &= \frac{m_{32}}{S_{32}^2} (\beta_2 - \beta_3) - \frac{m_{32}}{S_{32}^3} L \quad (32) + \frac{(x - m_{32}y - b_{32})}{S_{32}^3} \frac{\partial L}{\partial y} \quad (32) \\ &+ \frac{m_{41}}{S_{41}^2} (\beta_4 - \beta_1) + \frac{m_{41}}{S_{41}^3} L \quad (41) + \frac{(x - m_{41}y - b_{41})}{S_{41}^3} \frac{\partial L}{\partial y} \quad (41) \quad (D.17) \end{aligned}$$

$$\begin{aligned} \frac{\partial H_{02}}{\partial z} &= \frac{m_{32}}{S_{32}^2} (\gamma_2 - \gamma_3) + \frac{(x - m_{32}y - b_{32})}{S_{32}^3} \frac{\partial L^{(32)}}{\partial z} \\ &+ \frac{m_{41}}{S_{41}^2} (\gamma_4 - \gamma_1) - \frac{(x - m_{41}y - b_{41})}{S_{41}^3} \frac{\partial L^{(41)}}{\partial z} \end{aligned}$$

Using the above

$$\begin{aligned} V_x^{(R)} &= - \left[z \frac{\partial H_{02}}{\partial x} + 2y \frac{\partial \phi_{01}}{\partial x} - (y^2 + z^2) \frac{\partial \phi_{00}}{\partial x} \right] \\ V_y^{(R)} &= - \left[z \frac{\partial H_{02}}{\partial y} + 2y \frac{\partial \phi_{01}}{\partial y} - (y^2 + z^2) \frac{\partial \phi_{00}}{\partial y} - 2zV_y^{(0)} \right] \\ V_z^{(R)} &= - \left[z \frac{\partial H_{02}}{\partial z} + 2y \frac{\partial \phi_{01}}{\partial z} - (y^2 + z^2) \frac{\partial \phi_{00}}{\partial z} - 2zV_z^{(0)} \right] \end{aligned} \quad (D.18)$$

Finally, define

$$\begin{aligned} J_{02} &= H_{02} - zV_z^{(0)} \\ J_{20} &= \phi^{(0)} - H_{02} \end{aligned} \quad (D.19)$$

$$\begin{aligned} \frac{\partial J_{20}}{\partial x} &= -V_x^{(0)} - \frac{\partial H_{02}}{\partial x}, & \frac{\partial J_{20}}{\partial y} &= -V_y^{(0)} - \frac{\partial H_{02}}{\partial y} \\ \frac{\partial J_{20}}{\partial z} &= -V_z^{(0)} - \frac{\partial H_{02}}{\partial z}, \end{aligned} \quad (D.20)$$

where

$$\begin{aligned} \phi^{(0)} &= (y - \eta_1)L^{(12)} + \frac{(x - \xi_2) - m_{32}(y - \eta_2)}{S_{32}} L^{(32)} \\ &- (y - \eta_3)L^{(34)} - \frac{(x - \xi_4) - m_{41}(y - \eta_4)}{S_{41}} L^{(41)} - zV_z^{(0)} \end{aligned} \quad (D.21)$$

Using the above

$$V_x^{(P)} = - \left[z \frac{\partial J_{20}}{\partial x} + 2x \frac{\partial \phi_{10}}{\partial x} - x^2 \frac{\partial \phi_{00}}{\partial x} - 2zV_x^{(0)} \right]$$

$$V_y^{(P)} = - \left[z \frac{\partial J_{20}}{\partial y} + 2x \frac{\partial \phi_{10}}{\partial y} - x^2 \frac{\partial \phi_{00}}{\partial y} \right] \quad (D.22)$$

$$V_z^{(P)} = - \left[z \frac{\partial J_{20}}{\partial z} + 2x \frac{\partial \phi_{10}}{\partial z} - x^2 \frac{\partial \phi_{00}}{\partial z} + J_{20} \right]$$

$$V_x^{(1x)} = xV_x^{(0)} - J_{20}$$

$$V_y^{(1x)} = xV_y^{(0)} - J_{11} \quad (D.22)$$

$$V_z^{(1x)} = xV_z^{(0)} - zV_x^{(0)}$$

$$V_x^{(1y)} = yV_x^{(0)} - J_{11}$$

$$V_y^{(1y)} = yV_y^{(0)} - J_{02} \quad (D.23)$$

$$V_z^{(1y)} = yV_z^{(0)} - zV_y^{(0)}$$

APPENDIX E
INTERMEDIATE-FIELD SOURCE FORMULAS

If

$$\rho_1 > r_0/t > \rho_2 \quad (E.1)$$

the intermediate-field formulas are used.

First define direction cosines

$$\alpha = \frac{x}{r_0}, \quad \beta = \frac{y}{r_0}, \quad \gamma = \frac{z}{r_0} \quad (E.2)$$

Next define certain "derivative functions" as follows:

First Order:

$$u_x = -\alpha, \quad u_y = -\beta, \quad u_z = -\gamma \quad (E.3)$$

Second Order:

$$\begin{aligned} u_{xx} &= 3\alpha^2 - 1, & u_{xy} &= 3\alpha\beta, & u_{yy} &= 3\beta^2 - 1 \\ u_{xz} &= 3\alpha\gamma, & u_{yz} &= 3\beta\gamma, & u_{zz} &= 3\gamma^2 - 1 \end{aligned} \quad (E.4)$$

Third Order:

$$\begin{aligned} u_{xxx} &= 3\alpha(3 - 5\alpha^2), & u_{xxy} &= 3\beta(1 - 5\alpha^2), & u_{xxz} &= 3\gamma(1 - 5\alpha^2) \\ u_{xyy} &= 3\alpha(1 - 5\beta^2), & u_{xyz} &= -15\alpha\beta\gamma, & u_{xzz} &= 3\alpha(1 - 5\gamma^2) \\ u_{yyy} &= 3\beta(3 - 5\beta^2), & u_{yyz} &= 3\beta(1 - 5\beta^2), & u_{yzz} &= 3\beta(1 - 5\gamma^2) \end{aligned} \quad (E.5)$$

Fourth Order:

$$u_{xxxx} = 9 - 90\alpha^2 + 105\alpha^4$$

$$u_{xxxxy} = 15\alpha\beta(7\alpha^2 - 3)$$

$$\begin{aligned}
u_{xxxx} &= 15\alpha\gamma(7\alpha^2 - 3) \\
u_{xxyy} &= 3 - 15(\alpha^2 + \beta^2) + 105\alpha^2\beta^2 \\
u_{xxyz} &= 15\beta\gamma(7\alpha^2 - 1) \\
u_{xxzz} &= 3 - 15(\alpha^2 + \gamma^2) + 105\alpha^2\gamma^2 & (E.6) \\
u_{xyyy} &= 15\alpha\beta(7\beta^2 - 3) \\
u_{xyyz} &= 15\alpha\gamma(7\beta^2 - 1) \\
u_{xyzz} &= 15\alpha\beta(7\gamma^2 - 1) \\
u_{yyyy} &= 9 - 90\beta^2 + 105\beta^4 \\
u_{yyyz} &= 15\beta\gamma(7\beta^2 - 3) \\
u_{yyzz} &= 3 - 15(\beta^2 + \gamma^2) + 105\beta^2\gamma^2
\end{aligned}$$

The source velocity components are:

$$\begin{aligned}
v_x^{(0)} &= \frac{t^2}{r_0^2} \left\{ -I_{00}u_x + \left(\frac{t}{r_0}\right) [I_{10}u_{xx} - \frac{1}{2} I_{01}u_{xy}] - \frac{1}{2} \left(\frac{t}{r_0}\right)^2 [I_{20}u_{xxx} + 2I_{11}u_{xxy} \right. \\
&\qquad\qquad\qquad \left. + I_{02}u_{xyy}] \right\} \\
v_y^{(0)} &= \frac{t^2}{r_0^2} \left\{ -I_{00}u_y + \left(\frac{t}{r_0}\right) [I_{10}u_{xy} + I_{01}u_{yy}] - \frac{1}{2} \left(\frac{t}{r_0}\right)^2 [I_{20}u_{xxy} + 2I_{11}u_{xyy} \right. \\
&\qquad\qquad\qquad \left. + I_{02}u_{yyy}] \right\} & (E.7) \\
v_z^{(0)} &= \frac{t^2}{r_0^2} \left\{ -I_{00}u_z + \left(\frac{t}{r_0}\right) [I_{10}u_{xz} + I_{01}u_{yz}] - \frac{1}{2} \left(\frac{t}{r_0}\right)^2 [I_{20}u_{xxz} + 2I_{11}u_{xyz} \right. \\
&\qquad\qquad\qquad \left. + I_{02}u_{yyz}] \right\}
\end{aligned}$$

	Far-Field	1st Order	2nd Order
$V_x^{(Q)}$	$= \frac{t^4}{r_0^3} \{I_{11}u_{xz} - (\frac{t}{r_0})[I_{21}u_{xxz} + I_{12}u_{xyz}] + \frac{1}{2} (\frac{t}{r_0})^2 [I_{31}u_{xxxz} + 2I_{22}u_{xxyz} + I_{13}u_{xyyz}]\}$		
$V_y^{(Q)}$	$= \frac{t^4}{r_0^3} \{I_{11}u_{yz} - (\frac{t}{r_0})[I_{21}u_{xyz} + I_{12}u_{yyz}] + \frac{1}{2} (\frac{t}{r_0})^2 [I_{31}u_{xxyz} + 2I_{22}u_{xyyz} + I_{13}u_{yyyz}]\}$		(E.8)
$V_z^{(Q)}$	$= \frac{t^4}{r_0^3} \{I_{11}u_{zz} - (\frac{t}{r_0})[I_{21}u_{xzz} + I_{12}u_{yzz}] + \frac{1}{2} (\frac{t}{r_0})^2 [I_{31}u_{xxzz} + 2I_{22}u_{xyzz} + I_{13}u_{yyzz}]\}$		

$V_x^{(R)}$	$= \frac{t^4}{r_0^3} \{I_{02}u_{xz} - (\frac{t}{r_0})[I_{12}u_{xxz} + I_{03}u_{xyz}] + \frac{1}{2} (\frac{t}{r_0})^2 [I_{22}u_{xxxz} + 2I_{13}u_{xxyz} + I_{04}u_{xyyz}]\}$		
$V_y^{(R)}$	$= \frac{t^4}{r_0^3} \{I_{02}u_{yz} - (\frac{t}{r_0})[I_{12}u_{xyz} + I_{03}u_{yyz}] + \frac{1}{2} (\frac{t}{r_0})^2 [I_{22}u_{xxyz} + 2I_{13}u_{xyyz} + I_{04}u_{yyyz}]\}$		(E.9)
$V_z^{(R)}$	$= \frac{t^4}{r_0^3} \{I_{02}u_{zz} - (\frac{t}{r_0})[I_{12}u_{xzz} + I_{03}u_{yzz}] + \frac{1}{2} (\frac{t}{r_0})^2 [I_{22}u_{xxzz} + 2I_{13}u_{xyzz} + I_{04}u_{yyzz}]\}$		

$V_x^{(P)}$	$= \frac{t^4}{r_0^3} \{I_{20}u_{xz} - (\frac{t}{r_0}) [I_{30}u_{xxz} + I_{21}u_{xyz}] + \frac{1}{2} (\frac{t}{r_0})^2 [I_{40}u_{xxxz} + 2I_{31}u_{xxyz} + I_{22}u_{xyyz}]\}$		
$V_y^{(P)}$	$= \frac{t^4}{r_0^3} \{I_{20}u_{yz} - (\frac{t}{r_0}) [I_{30}u_{xyz} + I_{21}u_{yyz}] + \frac{1}{2} (\frac{t}{r_0})^2 [I_{40}u_{xxyz} + 2I_{31}u_{xyyz} + I_{22}u_{yyyz}]\}$		(E.10)
$V_z^{(P)}$	$= \frac{t^4}{r_0^3} \{I_{20}u_{zz} - (\frac{t}{r_0}) [I_{30}u_{xzz} + I_{21}u_{yzz}] + \frac{1}{2} (\frac{t}{r_0})^2 [I_{40}u_{xxzz} + 2I_{31}u_{xyzz} + I_{22}u_{yyzz}]\}$		

$V_x^{(IX)}$	$= \frac{t^3}{r_0^2} \{I_{10}u_x - (\frac{t}{r_0})[I_{20}u_{xx} + I_{11}u_{xy}] + \frac{1}{2} (\frac{t}{r_0})^2 [I_{30}u_{xxx} + 2I_{21}u_{xxy} + I_{12}u_{xyy}]\}$		
--------------	---	--	--

$$v_y^{(1x)} = \frac{t^3}{r_0^2} \{I_{10}u_y - (\frac{t}{r_0})[I_{20}u_{xy} + I_{11}u_{yy}] + \frac{1}{2} (\frac{t}{r_0})^2 [I_{30}u_{xxy} + 2I_{21}u_{xyy} + I_{12}u_{yyy}]\} \quad (E.11)$$

$$v_z^{(1x)} = \frac{t^3}{r_0^2} \{I_{10}u_z - (\frac{t}{r_0})[I_{20}u_{xz} + I_{11}u_{yz}] + \frac{1}{2} (\frac{t}{r_0})^2 [I_{30}u_{xxz} + 2I_{21}u_{xyz} + I_{12}u_{yyz}]\}$$

$$v_x^{(1y)} = \frac{t^3}{r_0^2} \{I_{01}u_x - (\frac{t}{r_0})[I_{11}u_{xx} + I_{02}u_{xy}] + \frac{1}{2} (\frac{t}{r_0})^2 [I_{21}u_{xxx} + 2I_{12}u_{xxy} + I_{03}u_{xyy}]\}$$

$$v_y^{(1y)} = \frac{t^3}{r_0^2} \{I_{01}u_y - (\frac{t}{r_0})[I_{11}u_{xy} + I_{02}u_{yy}] + \frac{1}{2} (\frac{t}{r_0})^2 [I_{21}u_{xxy} + 2I_{12}u_{xyy} + I_{03}u_{yyy}]\} \quad (E.12)$$

$$v_z^{(1y)} = \frac{t^3}{r_0^2} \{I_{01}u_z - (\frac{t}{r_0})[I_{11}u_{xz} + I_{02}u_{yz}] + \frac{1}{2} (\frac{t}{r_0})^2 [I_{21}u_{xxz} + 2I_{12}u_{xyz} + I_{03}u_{yyz}]\}$$

APPENDIX F
FAR-FIELD SOURCE FORMULAS

As usual \vec{n} denotes the unit normal vector to a projected flat panel and \vec{i}_E and \vec{j}_E are, respectively, unit vectors along the x- and y-axis of the panel coordinate system (Appendix B). Define \vec{r}_0 as the vector from the origin of panel coordinates to the point where velocity is being evaluated and r_0 as its magnitude. Certain auxiliary vectors are needed:

$$\begin{aligned}\vec{D} &= - \left[3 \left(\frac{\vec{n} \cdot \vec{r}_0}{r_0} \right) \frac{\vec{r}_0}{r_0} - \vec{n} \right] \\ \vec{D}_i &= - \left[3 \left(\frac{\vec{i}_E \cdot \vec{r}_0}{r_0} \right) \frac{\vec{r}_0}{r_0} - \vec{i}_E \right] \\ \vec{D}_j &= - \left[3 \left(\frac{\vec{j}_E \cdot \vec{r}_0}{r_0} \right) \frac{\vec{r}_0}{r_0} - \vec{j}_E \right]\end{aligned}\tag{F.1}$$

The far-field expressions for the source velocities are

$$\begin{aligned}\vec{v}(0) &= \frac{t^2 I_{00}}{r_0^2} \frac{\vec{r}_0}{r_0} \\ \vec{v}(P) &= - \frac{t^4}{r_0^3} I_{20} \vec{D} \\ \vec{v}(Q) &= - \frac{t^4}{r_0^3} I_{11} \vec{D} \\ \vec{v}(R) &= - \frac{t^4}{r_0^3} I_{02} \vec{D}\end{aligned}\tag{F.3}$$

$$\vec{v}(1x) = \frac{t^3}{r_0^2} I_{10} \frac{\vec{r}_0}{r_0} - \frac{t^4}{r_0^3} [I_{20} \hat{D}_i + I_{11} \hat{D}_j] \quad (\text{F.4})$$

$$\vec{v}(1y) = \frac{t^3}{r_0^2} I_{01} \frac{\vec{r}_0}{r_0} - \frac{t^4}{r_0^3} [I_{11} \hat{D}_i + I_{02} \hat{D}_j]$$

The fact that three auxiliary vectors (F.1) are required means that in effect a transformation into panel coordinates has been performed. It appears to be somewhat faster computationally to use the vector far-field forms above rather than simply truncate the intermediate field formulas in panel coordinates.

APPENDIX G
SOME SPECIAL NEAR-FIELD FORMULAS

The near-field formulas of Appendices D and I can have numerical difficulties under certain circumstances. Some of these are inherent in the formulas, while others are due to extremes in panel dimensions - particularly very long thin panels. Special formulas have been developed to deal with these situations.

"Small Logs" (Long Thin Panels)

First consider side 32. If

$$\frac{r_3 + r_2 - d_{32}}{r_3 + r_2 + d_{32}} < \epsilon_3 = 10^{-3} \quad (G.1)$$

Then define

$$\epsilon^2 = \frac{h_{32}^2}{1 + m_{32}^2} + z^2$$

$$d_3 = \left| \frac{m_{32}}{\sqrt{1 + m_{32}^2}} (x - \xi_3) + \frac{1}{\sqrt{1 + m_{32}^2}} (y - r_3) \right| \quad (G.2)$$

$$d_2 = d_{32} - d_3$$

In the argument of the logarithm L(32) set

$$r_3 + r_2 - d_{32} = \frac{1}{2} \left(\frac{1}{d_3} + \frac{1}{d_2} \right) \epsilon^2 - \frac{1}{8} \left(\frac{1}{d_3} + \frac{1}{d_2} \right) \epsilon^4 \quad (G.3)$$

For Side 41

A similar procedure is used for $r_1 + r_4 - d_{41}$. Define

$$\epsilon^2 = \frac{h_{41}^2}{1 + m_{41}^2} + z^2 \quad (G.4)$$

$$d_4 = \left| \frac{m_{41}}{\sqrt{1 + m_{41}^2}} (x - \xi_4) + \frac{1}{\sqrt{1 + m_{41}^2}} (y - \eta_3) \right| \quad (\text{G.4})$$

$$d_1 = d_{41} - d_4$$

Then if

$$\frac{r_4 + r_1 - d_{41}}{r_4 + r_1 + d_{41}} < \epsilon_3 \quad (\text{G.5})$$

set

$$r_4 + r_1 - d_{41} = \frac{1}{2} \left(\frac{1}{d_4} + \frac{1}{d_1} \right) \epsilon^2 - \frac{1}{8} \left(\frac{1}{d_4^3} + \frac{1}{d_1^3} \right) \epsilon^4 \quad (\text{G.6})$$

The formulas are slightly different for the other two sides. If

$$\frac{r_1 + r_2 - d_{12}}{r_1 + r_2 + d_{12}} < \epsilon_3 \quad (\text{G.7})$$

define

$$\begin{aligned} \epsilon^2 &= (y - \eta_1)^2 + z^2 \\ d_1 &= x - \xi_1 \\ d_2 &= d_{12} - d_1 \end{aligned} \quad (\text{G.8})$$

and set

$$r_1 + r_2 - d_{12} = \frac{1}{2} \left(\frac{1}{d_1} + \frac{1}{d_2} \right) \epsilon^2 - \frac{1}{8} \left(\frac{1}{d_1^3} + \frac{1}{d_2^3} \right) \epsilon^4 \quad (\text{G.9})$$

Finally, if

$$\frac{r_3 + r_4 - d_{34}}{r_3 + r_4 + d_{34}} < \epsilon_3 \quad (\text{G.10})$$

define

$$\begin{aligned} \epsilon^2 &= (y - \eta_3)^2 + z^2 \\ d_4 &= (x - \xi_4) \end{aligned} \quad (\text{G.11})$$

$$d_3 = d_{34} - d_4$$

and set

$$r_3 + r_4 - d_{34} = \frac{1}{2} \left(\frac{1}{d_3} + \frac{1}{d_4} \right) \epsilon^2 - \frac{1}{8} \left(\frac{1}{d_3} + \frac{1}{d_4} \right) \epsilon^4 \quad (\text{G.12})$$

"T-Derivatives"

The individual T-derivatives in Appendix D become indeterminate if the point (x,y,z) is on the extension of a side of the panel. The "fix" of Ref. 5 is designed to remedy this, but it is inadequate for two reasons if the panels are long enough. One is that if the point is near the side itself, the fix is inappropriate. The other is that the criterion is too stringent if the point is indeed near the side extension. The following appears to be a reasonable "fix of the fix."

1. Slanted sides

If $(y - \eta_1)(y - \eta_3) < 0$, skip this part. Otherwise calculate

$$\epsilon_{32}^2 = h_{32}^2 + z^2 \quad (\text{G.13})$$

$$\epsilon_{41}^2 = h_{41}^2 + z^2$$

If $\epsilon_{32}^2/y^2 < 0.0001$, use

$$-\frac{\partial T_2^{(32)}}{\partial x} + \frac{\partial T_3^{(32)}}{\partial x} = -\frac{\partial T_2^{(32)}}{\partial y} + \frac{\partial T_3^{(32)}}{\partial y} = 0 \quad (\text{G.14})$$

$$-\frac{\partial T_2^{(32)}}{\partial z} + \frac{\partial T_3^{(32)}}{\partial z} = \frac{m_{32}}{\sqrt{1 + m_{32}^2}} \left(\frac{1}{|y - \eta_3|} - \frac{1}{|y - \eta_1|} \right)$$

If $\epsilon_{41}^2/y^2 < 0.0001$, use

$$-\frac{\partial T_1^{(41)}}{\partial x} + \frac{\partial T_4^{(41)}}{\partial x} = -\frac{\partial T_1^{(41)}}{\partial y} + \frac{\partial T_4^{(41)}}{\partial y} = 0. \quad (\text{G.15})$$

$$-\frac{\partial T_1^{(41)}}{\partial z} + \frac{\partial T_4^{(41)}}{\partial z} = -\frac{m_{41}}{\sqrt{1+m_{41}^2}} \left(\frac{1}{|y-\eta_1|} - \frac{1}{|y-\eta_3|} \right)$$

2. Parallel sides

If $h_{32}h_{41} < 0$, skip this part. Otherwise calculate

$$\epsilon_{12}^2 = (h - \eta_1)^2 + z^2 \tag{G.16}$$

$$\epsilon_{34}^2 = (y - \eta_3)^2 + z^2$$

If

$$\frac{\epsilon_{12}^2}{\{x - (\xi_1 + \xi_2)/2\}^2} < 0.0001, \tag{G.17}$$

use

$$-\frac{\partial T_2^{(32)}}{\partial x} + \frac{\partial T_1^{(41)}}{\partial x} = -\frac{\partial T_2^{(32)}}{\partial y} + \frac{\partial T_1^{(41)}}{\partial y} = 0 \tag{G.18}$$

$$-\frac{\partial T_2^{(32)}}{\partial z} + \frac{\partial T_1^{(41)}}{\partial z} = \frac{m_{41}}{|x - \xi_1|} - \frac{m_{32}}{|x - \xi_2|}$$

If

$$\frac{\epsilon_{34}^2}{\{x - (\xi_3 + \xi_4)/2\}^2} < 0.0001, \tag{G.19}$$

use

$$-\frac{\partial T_3^{(32)}}{\partial x} + \frac{\partial T_4^{(41)}}{\partial x} = -\frac{\partial T_3^{(32)}}{\partial y} + \frac{\partial T_4^{(41)}}{\partial y} = 0 \tag{G.20}$$

$$\frac{\partial T_2^{(32)}}{\partial z} - \frac{\partial T_1^{(41)}}{\partial z} = \frac{m_{32}}{|x - \xi_3|} - \frac{m_{41}}{|x - \xi_4|}$$

Edge Vortex Formulas Near Extended Line

These are needed for small values of

$$q^2 = (y - \eta_1)^2 + z^2 \quad (G.21)$$

If

$$\frac{q^2}{[x - \xi_1 \text{ or } 2]^2} < 2.5 \cdot 10^{-2} \quad (G.22)$$

use the following formula for $J_{0n}(F)$

$$J_{0n}(F) = \frac{\text{sgn}(x - \xi_1)}{n - 1} \left\{ \left[\frac{1}{(\xi_2 - x)^{n-1}} - \frac{1}{(\xi_1 - x)^{n-1}} \right] \right. \\ \left. - \frac{n(n-1)}{2(n+1)} q^2 \left[\frac{1}{(\xi_2 - x)^{n+1}} - \frac{1}{(\xi_1 - x)^{n+1}} \right] \right\} \quad (G.23)$$

"Simpson's Rule"

Define R as the distance of (x, y, z) from the closest point of the line vortex and d as the length of the line vortex. Then if

$$R/d > 10 \quad (G.24)$$

do not use the recursion formulas of Appendix I, but calculate the J_{mn} by the three-point Simpson's rule

$$J_{mn} = \int_{\xi_1}^{\xi_2} F(\xi) d\xi = \frac{\xi_2 - \xi_1}{6} \left[F(\xi_1) + 4F\left(\frac{\xi_1 + \xi_2}{2}\right) + F(\xi_2) \right] \quad (G.25)$$

APPENDIX H
CALCULATION OF VORTICITY INDUCED VELOCITIES IN TERMS OF
SOURCE INDUCED VELOCITIES

The calculation of the vorticity influences can be made much more efficient by expressing them in terms of the corresponding source influence, which of course, must be calculated in any event. The use of this procedure was put forward in Ref. 21. The portion of the theory that is needed for the present purpose is quite easy to state.

Suppose there is a variable source density σ on a portion of a plane or curved surface S . The velocity due to this at a point (x,y,z) is

$$\vec{V} \text{ (source)} = \iint_S \frac{\vec{r}}{r^3} \sigma dS \quad (\text{H.1})$$

where \vec{r} and r have their usual meanings. If there is a vorticity distribution on S of strength

$$\vec{\omega} = \omega \vec{t} \quad (\text{H.2})$$

The Biot-Savart law gives the resulting induced velocity as

$$\vec{V} \text{ (vorticity)} = \iint_S \frac{\vec{t} \times \vec{r}}{r^3} \omega dS \quad (\text{H.3})$$

Then if \vec{t} is a constant vector and if ω has the same spatial variation as σ , the velocity due to the vorticity distribution may be expressed in terms of the velocity due to the source distribution as

$$\vec{V} \text{ (vorticity)} = \vec{t} \times \vec{V} \text{ (source)} \quad (\text{H.4})$$

since $\vec{\omega}$ can be resolved into components, each of which has a constant direction, the restriction to a constant \vec{t} is not serious. Although the above results apply to a curved surface S , it is far simpler to apply to a flat surface. In the present context the above is applied to the flat projected panel.

Figure 8 illustrates the projection of a curved panel S on the surface of a flat panel A in the tangent plane. In particular, Figure 8 illustrates \vec{r} from a point of S and the vector \vec{r}_f from a point of the projected flat panel to the point (x,y,z). Evidently

$$\vec{r}_f = (x - \xi)\vec{i}_e + (y - \eta)\vec{j}_e + z\vec{k}_e \quad (\text{H.5})$$

where $\vec{i}_e, \vec{j}_e, \vec{k}_e$ are unit vectors along the axes of the panel coordinate system. As in Appendix A, the vertical distance ζ between the curved panel and its projection is approximated by its leading term ζ_2 , which represents a surface of second degree

$$\zeta_2 = P\xi^2 + 2Q\xi\eta + R\eta^2 \quad (\text{H.6})$$

The aim is to obtain a consistent two-term expansion of Eq. (H.3) and express the results in terms of source effects. From Eq. (2.6.7) it is seen that a two-term expansion of the vector vorticity distribution is

$$\vec{\omega} = \vec{\omega}_0 + \vec{\omega}_1 \quad (\text{H.7})$$

where

$$\vec{\omega}_0 = \mu_y\vec{i}_e - \mu_x\vec{j}_e \quad (\text{H.8})$$

is zero order and

$$\vec{\omega}_1 = 2(\mu_{xy}\xi + \mu_{yy}\eta)\vec{i}_e - 2(\mu_{xx}\xi + \mu_{xy}\eta)\vec{j}_e + 2[-(Q\xi + R\eta)\mu_x + (P\xi + Q\eta)\mu_y]\vec{k}_e \quad (\text{H.9})$$

is first order. The constants μ_x, μ_{xx} , etc. are the derivatives of the equivalent dipole distribution as given by Eq. (2.6.4). From Fig. 8 it can be seen that

$$\vec{r} = \vec{r}_f - \zeta_2\vec{k}_e \quad (\text{H.10})$$

Thus a two-term expansion of the velocity at (x,y,z) due to the vorticity on the panel is

$$\vec{v}_\omega = \iint_S \frac{\vec{\omega} \times \vec{r}}{r^3} dS = \iint_A \left\{ \frac{\vec{\omega}_0 \times \vec{r}_f}{r_f^3} \left(1 + 3z \frac{\zeta_2}{r_f^2} \right) + \frac{\vec{\omega}_1 \times \vec{r}_f}{r_f^3} - \zeta_2 \frac{\vec{\omega}_0 \times \vec{k}_e}{r_f^3} \right\} dA \quad (\text{H.11})$$

$$= \vec{\omega}_0 \times \iint_A \left[\frac{\vec{r}_f}{r_f^3} \left(1 + 3z \frac{z_2}{r_f^2} \right) - z_2 \frac{\vec{k}_e}{r_f^3} \right] dA + \iint_A \frac{\vec{\omega}_1 \times \vec{r}_f}{r_f^3} dA$$

By taking the gradient of the $\phi^{(0)}$ and $\phi^{(c)}$ terms of the source expansion in Eqs. (A.33) and (A.34) of Appendix A, it can be seen that the integral multiplying $\vec{\omega}_0$ above is just the sum of superscript 0 and c source terms for unit source density. Specifically this combination is the velocity

$$\vec{V} = \vec{V}^{(0)} + [P\vec{V}^{(P)} + 2Q\vec{V}^{(Q)} + R\vec{V}^{(R)}] \quad (H.12)$$

This same combination appears in Eqs. (2.4.1). To analyze the last term of Eq. (H.11), collect terms in Eq. (H.9) to obtain

$$\vec{\omega}_1 = 2(\xi \vec{q}_x + \eta \vec{q}_y) \quad (H.13)$$

where the vectors

$$\vec{q}_x = \mu_{xy} \vec{i}_e - \mu_{xx} \vec{j}_e + (P\mu_y - Q\mu_x) \vec{k}_e \quad (H.14)$$

$$\vec{q}_y = \mu_{yy} \vec{i}_e - \mu_{xy} \vec{j}_e + (Q\mu_y - R\mu_x) \vec{k}_e$$

are constants in the integration. The integrals that result from using Eq. (H.13) in the last term of Eq. (H.11) are the velocities due to linearly varying source densities in the ξ and η directions having unit slope, i.e. $\vec{V}^{(1x)}$ and $\vec{V}^{(1y)}$ of Eq. (2.4.1).

Thus the velocity due to vorticity on the panel may be expressed in terms of source velocities as follows

$$\vec{V}_\omega = \vec{\omega}_0 \times \vec{V} + 2[\vec{q}_x \times \vec{V}^{(1x)} + \vec{q}_y \times \vec{V}^{(1y)}] \quad (H.15)$$

It is interesting to note that Eq. (H.15) can be evaluated directly in reference coordinates after the relevant source velocities have been calculated and put into this system. With regard to the velocities due to the vorticity, this not only means that no transformations between panel and reference coordinates are required, but it also means that the question of far-field calculation need never arise. If the source velocities have been computed by far-field

formulas, they simply are used in Eq. (H.15), so that in effect the vorticity calculation uses the source far-field procedure. The present code takes advantage of the second of these facts, the use of far-field source formulas, but performs the calculation in panel coordinates.

The implementation in panel coordinates proceeds as follows.

Define

$$\begin{aligned} \alpha_1 &= -\frac{\eta_3}{w} & \beta_1 &= \frac{h_F}{w} - c(\eta_1 + \eta_3) \\ \alpha_2 &= \frac{\eta_1}{w} & \beta_2 &= -\frac{h_S}{w} + c(\eta_1 + \eta_3) \end{aligned} \quad (\text{H.16})$$

then

$$\begin{aligned} \vec{\omega}_0 \times \vec{V}' &= B_F \{ \vec{i}_e [-V'_z \alpha_1] + \vec{j}_e [-V'_z \beta_1] + \vec{k}_e [\beta_1 V'_y + \alpha_1 V'_x] \} \\ &+ B_S \{ \vec{i}_e [-V'_z \alpha_2] + \vec{j}_e [-V'_z \beta_2] + \vec{k}_e [\beta_2 V'_y + \alpha_2 V'_x] \} \end{aligned} \quad (\text{H.17})$$

Define

$$\begin{aligned} \delta_1 &= \frac{1}{2w} & \epsilon_1 &= c \\ \delta_2 &= -\frac{1}{2w} & \epsilon_2 &= -c \end{aligned} \quad (\text{H.18})$$

then

$$\begin{aligned} \vec{q}_x \times \vec{V}^{(1x)} &= B_F \{ \vec{i}_e [V_y^{(1x)} (P\beta_1 - Q\alpha_1) + \vec{j}_e [V_x^{(1x)} (P\beta_1 - Q\alpha_1) - V_z^{(1x)} \delta_1] \\ &+ \vec{k}_e [V_y^{(1x)} \delta_1] \} \\ &+ B_S \{ \vec{i}_e [V_y^{(1x)} (P\beta_2 - Q\alpha_2) + \vec{j}_e [V_x^{(1x)} (P\beta_2 - Q\alpha_2) - V_z^{(1x)} \delta_2] \\ &+ \vec{k}_e [V_y^{(1x)} \delta_2] \} \end{aligned} \quad (\text{H.19})$$

$$\begin{aligned}
\vec{q}_y \times \vec{V}^{(1y)} &= B_F \{ \vec{i}_e [-v_z^{(1y)} \delta_1 - v_y^{(1y)} (Q\beta_1 - R\alpha_1) + \vec{j}_e [v_x^{(1y)} (Q\beta_1 - R\alpha_1) - v_z^{(1y)} \epsilon_1] \\
&\quad + \vec{k}_e [v_y^{(1y)} \epsilon_1 + v_x^{(1y)} \delta_1] \} \\
&\quad + B_S \{ \vec{i}_e [-v_z^{(1y)} \delta_2 - v_y^{(1y)} (Q\beta_2 - R\alpha_2) + \vec{j}_e [v_x^{(1y)} (Q\beta_2 - R\alpha_2) - v_z^{(1y)} \epsilon_2] \\
&\quad + \vec{k}_e [v_y^{(1y)} \epsilon_2 + v_x^{(1y)} \delta_2] \}
\end{aligned}
\tag{H.20}$$

APPENDIX I
FORMULAS FOR THE EFFECT OF NEAR-FIELD LINE VORTEX
ALONG A STREAMWISE EDGE OF A PANEL

Derivation of the Influence of an Edge Vortex

The equation of the curved panel is Eq. (H.6). For definiteness consider the case when the edge in question lies in the plane $\eta = \eta_1$, i.e. the first N-line (Fig. 3). The modifications for the case of the second N-line are obvious. Thus the curve c along which the vortex lies is

$$\zeta = \zeta(\xi) = P\xi^2 + 2Q\xi\eta_1 + R\eta_1^2 \quad (I.1)$$

The unit vector along this curve is

$$\vec{t} = \frac{1}{\sqrt{1+T^2}} [\vec{i}_e + T\vec{j}_e] \quad (I.2)$$

where

$$T = 2(P\xi + Q\eta_1) \quad (I.3)$$

The velocity due to the vortex is

$$\vec{V}_T = \int_c \frac{\vec{t} \times \vec{r}}{r^3} \mu ds \quad (I.4)$$

where μ is the edge value of the equivalent dipole strength. Arc length along the curve is related to distance in the tangent plane by

$$ds = \sqrt{1+T^2} d\xi \quad (I.5)$$

Thus with r expressed in panel coordinates (Fig. 8)

$$\begin{aligned} (\vec{t} \times \vec{r}) ds = & \{ [\quad 0 \quad -T(y - \eta_1) \quad] \vec{i}_e \\ & [\quad z \quad +T(x - \xi) + \zeta \quad] \vec{j}_e \\ & [(y - \eta_1) + \quad 0 \quad] \vec{k}_e \} d\xi \end{aligned} \quad (I.6)$$

where the terms in the first column of Eq. (I.6) are first order, and those in the second column are second order. This expression is exact except for the approximation $\zeta = \zeta_2$.

As shown in Appendix A, a three-term expansion of $1/r^3$ is

$$\frac{1}{r^3} = \frac{1}{r_f^3} [1 + 3c_1 + 3(c_1^2 + c_2)] \quad (I.7)$$

where r_f is distance from a point of the flat tangent panel and where

$$c_1 = \frac{z\zeta_2}{r_f^2} \quad (I.8)$$

$$c_2 = \frac{3}{2} c_1^2 - \frac{1}{2} \frac{\zeta_2^2}{r_f^2}$$

Along the N-line the equivalent dipole strength varies linearly

$$\mu = B(h + \xi) \quad (I.9)$$

where h is the total arc length along the N-line up to the η -axis of panel coordinates (see Section 9.2 of Ref. 2), and B is the unknown value of vorticity that is determined from the Kutta condition. The fundamental flow is obtained by setting B equal to unity in Eq. (I.9). Multiplying the above expansions gives the components of the vortex velocity as follows

$$\begin{aligned} V_{\Gamma_x} &= \int_{\xi_1}^{\xi_2} \frac{1}{r_f^3} \{0 - [T(y - \eta_1)h] - [T(y - \eta_1)(3c_1h + \xi)]\} d\xi \\ V_{\Gamma_y} &= \int_{\xi_1}^{\xi_2} \frac{1}{r_f^3} \{-zh + [-z(3c_1h + \xi) + h(T(x_1 - \xi)_1 + \zeta_2)] \\ &\quad + [-z\{3(c_1^2 + c_2)h + 3c_1\xi\} + (3c_1h + \xi)(T(x - \xi) + \zeta_2)]\} d\xi \\ V_{\Gamma_z} &= (y - h_1) \int_{\xi_1}^{\xi_2} \frac{1}{r_f^3} \{h + [3c_1h + \xi] + [3(c_1^2 + c_2)h + 3c_1\xi]\} d\xi \end{aligned} \quad (I.10)$$

The integrals in Eq. (I.10) have the form

$$J_{mn} = \int_{\xi_1}^{\xi_2} \frac{\xi^m}{r_f^n} d\xi \quad (I.11)$$

Once the J_{0n} and J_{1n} have been calculated the others are calculated from the recursion formulas

$$J_{mn} = J_{(m-2)(n-2)} + 2xJ_{(m-1)n} - p^2 J_{(m-2)n} \quad (I.12)$$

where

$$p^2 = x^2 + (y - \eta_1)^2 + z^2 \quad (I.13)$$

The required J_{0n} and J_{1n} are

$$\begin{aligned} J_{01} &= \log \frac{r_1 + r_2 + d_{12}}{r_1 + r_2 - d_{12}} = -L \quad (12) \\ J_{11} &= r_2 - r_1 + xJ_{01} \\ J_{03} &= \frac{1}{q^2} \left[\frac{\xi_2 - x}{r_2} - \frac{\xi_1 - x}{r_1} \right] \\ J_{13} &= \frac{1}{r_1} - \frac{1}{r_2} + xJ_{03} \\ J_{05} &= \frac{1}{3q^2} \left[\frac{\xi_2 - x}{r_2^3} - \frac{\xi_1 - x}{r_1^3} + 2J_{03} \right] \\ J_{15} &= -\frac{1}{3} \left(\frac{1}{r_2^3} - \frac{1}{r_1^3} \right) + xJ_{05} \\ J_{07} &= \frac{1}{5q^2} \left[\frac{\xi_2 - x}{r_2^5} - \frac{\xi_1 - x}{r_1^5} + 4J_{05} \right] \\ J_{17} &= -\frac{1}{5} \left(\frac{1}{r_2^5} - \frac{1}{r_1^5} \right) + xJ_{07} \end{aligned} \quad (I.14)$$

where

$$q^2 = (y - \eta_1)^2 + z^2 \quad (I.15)$$

and where r_1 and r_2 are, respectively, distances of the point (x,y,z) from the ends of the interval, i.e.,

$$r_k^2 = (x - \xi_k)^2 + (y - \eta_1)^2 + z^2 \quad (I.16)$$

In terms of certain auxiliary functions, F_n , the velocity components of Eq. (I.10) are

$$\begin{aligned} V_{\Gamma x} &= -(y - \eta_1)[hF_1 + F_5] \\ V_{\Gamma y} &= -zhJ_{03} + [-zF_2 + hF_3] - z[3hF_4 + F_6] + F_7 \\ V_{\Gamma z} &= +(y - \eta_1)[hJ_{03} + F_2 + 3hF_4 + F_6] \end{aligned} \quad (I.17)$$

The auxiliary functions for on-body panels are:

$$F_1 = 2PJ_{13} + 2Q\eta_1J_{03}$$

$$F_2 = 3zh[PJ_{25} + 2Q\eta_1J_{15} + R\eta_1^2J_{05}] + \{J_{13}\}$$

$$F_3 = 2PxJ_{13} + 2Q\eta_1xJ_{03} - PJ_{23} + R\eta_1^2J_{03}$$

$$F_4 = \frac{5}{2} z^2 Q_7 - \frac{1}{2} Q_5$$

$$Q_j = [P^2J_{4j} + 4PQ\eta_1J_{3j} + (2PR + 4Q^2)\eta_1^2J_{2j} + 4QR\eta_1^3J_{1j} + R^2\eta_1^4J_{0j}] \quad (I.18)$$

$$F_5 = 6zh[P^2J_{35} + 3PQ\eta_1J_{25} + PR\eta_1^2J_{15} + 2Q^2\eta_1^2J_{15} + QR\eta_1^3J_{05}] + \{2PJ_{23} + 2Q\eta_1J_{13}\}$$

$$F_6 = \{3z[PJ_{35} + 2Q\eta_1J_{25} + R\eta_1^2J_{15}]\}$$

$$\begin{aligned} F_7 &= 3zh[-P^2J_{45} + (2P^2x - 2PQ\eta_1)J_{35} + 6PQx\eta_1J_{25} + (4Q^2x\eta_1^2 + 2PRx\eta_1^2 + 2QR\eta_1^3)J_{15} \\ &\quad + (2QRx\eta_1^3 + R^2\eta_1^4)J_{05}] + \{-PJ_{33} + 2PxJ_{23} + (2Qx\eta_1 + R\eta_1^2)J_{13}\} \end{aligned}$$

The formulas for wake panels are obtained from Eq. (I.18) by deleting all terms in {} and replacing h by L (total).

For the semi-infinite last wake additional changes are made to the formulas (I.14) for the J_{mn} corresponding to

$$\xi_2 \rightarrow \infty \quad r_2 \rightarrow \infty \quad \xi_2/r_2 \rightarrow 1 \quad (I.19)$$

Furthermore, P and Q are set equal to zero.

APPENDIX J
FAR-FIELD EDGE VORTEX FORMULAS

Compute

$$r_F^2 = \left[x - \left(\frac{\xi_1 + \xi_2}{2} \right) \right]^2 + [y - \eta_1]^2 + z^2 \quad (J.1)$$

If

$$(\xi_2 - \xi_1)^2 / r_F^2 < 0.001,$$

use

$$\begin{aligned} V_{\Gamma x} &= -(y - \eta_1) T_0 I \\ V_{\Gamma y} &= \left[-z + T_0 \left(x - \frac{\xi_1 + \xi_2}{2} \right) + \xi_0 \right] I \\ V_{\Gamma z} &= (y - \eta_1) I \end{aligned} \quad (J.2)$$

where

$$\begin{aligned} I &= \frac{\xi_2 - \xi_1}{r_f^3} \left(h + \frac{\xi_1 + \xi_2}{2} \right) \\ T_0 &= 2 \left[P \frac{\xi_1 + \xi_2}{2} + Q \eta_1 \right] \\ \xi_0 &= \left(P \frac{\xi_1 + \xi_2}{2} \right)^2 + 2Q \eta_1 \left(\frac{\xi_1 + \xi_2}{2} \right) + R \eta_1^2 \end{aligned} \quad (J.3)$$

For the second N-line the obvious quantities are replaced by the corresponding ones. The above equations replace the elaborate formulas of Appendix I.

APPENDIX K
PARABOLIC CHORDWISE VORTICITY

The assumption of constant vorticity around a wing section (linear variation of the underlying dipole strength) can lead to numerical difficulties on certain wings with very thin trailing edges. Accordingly, a second chordwise variation option is required. The important consideration is to have the "bound" vorticity strength approach zero at the trailing edge on both upper and lower wing surfaces. This is accomplished by a quadratic global variation of vorticity as a function of arc length along an N-line. While only two global chordwise variations have been incorporated into the present method, many such variations are possible. As will be seen below, the required modifications to the program are quite minor. This flexibility is due to the use of vorticity as an auxiliary singularity.

To implement the parabolic vorticity option, the linear variation of the underlying dipole strength along an N-line is replaced by a cubic variation having zero derivative at the upper and lower trailing edge. Specifically,

$$\mu = Bs \left\{ 3 \frac{s}{L(\text{total})} - 2 \left[\frac{s}{L(\text{total})} \right]^2 \right\} \quad (\text{K.1})$$

where s is arc length along the N-line. The above is a global variation. The variation over an individual panel can be no higher a degree than quadratic, and in the present method has been taken as linear. It is assumed that the underlying dipole distribution on a panel agrees with Eq. (K.1) at the corners of the panel and varies linearly in between. Thus, the overall behavior is that of an inscribed-polygon approximation to Eq. (K.1).

For an individual panel the arc length measured along an N-line from the trailing edge to the lower corner of the panel is $h_F + \xi_1$ or $h_S + \xi_4$ while the arc length associated with the upper corner is $h_F + \xi_2$ or $h_S + \xi_3$. The linear function that agrees with Eq. (K.1) at these two values of arc length is

$$\mu = B(H + I\xi) \quad (\text{K.2})$$

where on the two N-lines the constants H and I have the values

$$H_F = \frac{3}{L_F (\text{total})} (h_F^2 - \epsilon_1 \epsilon_2) - \frac{2}{[L_F (\text{total})]^2} [h_F^3 - \epsilon_1 \epsilon_2 (3h_F + \epsilon_1 + \epsilon_2)]$$

$$I_F = \frac{3}{L_F (\text{total})} (2h_F - \epsilon_1 + \epsilon_2) - \frac{2}{[L_F (\text{total})]^2} [3h_F^2 + 3h_F(\epsilon_1 + \epsilon_2) + \epsilon_1^2 + \epsilon_2^2 + \epsilon_1 \epsilon_2] \quad (\text{K.3})$$

$$H_S = \frac{3}{L_S (\text{total})} (h_S^2 - \epsilon_3 \epsilon_4) - \frac{2}{[L_S (\text{total})]^2} [h_S^3 - \epsilon_3 \epsilon_4 (3h_S + \epsilon_3 + \epsilon_4)]$$

$$I_S = \frac{3}{L_S (\text{total})} (2h_S - \epsilon_3 + \epsilon_4) - \frac{2}{[L_S (\text{total})]^2} [3h_S^2 + 3h_S(\epsilon_3 + \epsilon_4) + \epsilon_3^2 + \epsilon_4^2 + \epsilon_3 \epsilon_4]$$

where all symbols have the same meaning as in Section 2.6.1. Thus the quadratic form (2.6.9) for the variation of dipole strength over a panel is replaced by

$$\mu = \frac{B_F I_F - B_S I_S}{w} \epsilon_\eta + \frac{B_F H_F - B_S H_S}{w} \eta + \frac{B_S I_S \eta_1 - B_F I_F \eta_3}{w} \xi + \frac{B_S H_S \eta_1 - B_F H_F \eta_3}{w} \xi + c(B_F - B_S)(\eta - \eta_3)(\eta - \eta_1) \quad (\text{K.4})$$

The dipole derivative formulas of Section 2.6.1 are modified in an obvious way, specifically

- a. Terms containing c are not changed.
- b. In terms containing h_F or h_S these quantities are replaced by H_F or H_S , respectively.
- c. All other terms are multiplied by I_F or I_S as appropriate.

The wake formulas are unchanged except for c . In the constant chordwise vorticity option, the parameter c is nonzero on wake panels if the "piecewise linear" spanwise variation of vorticity is used. However, if the parabolic chordwise vorticity option is used, c is taken as zero on all panels.

The near-field edge-vortex formulas (Appendix I) are modified as follows:

$F_1 =$ unchanged

$F_2 =$ replace h_F by H_F
multiply J_{13} by I_F

$F_3 =$ unchanged

$F_4 =$ unchanged

(K.5)

$F_5 =$ Replace h_F by H_F
multiply $[2PJ_{23} + 2Q\eta_1 J_{13}]$ by I_F

$F_6 =$ multiply entire term by I_F

$F_7 =$ replace h_F by H_F
multiply $[-PJ_{33} + 2P_x J_{23} + (2Q_x \eta_1 + R\eta_1^2)J_{13}]$ by I_F

The wake formulas are unchanged. Replace H by $L_F(\text{tot.})$ and set $I = 0$.

Note that the terms multiplied by I are exactly the terms neglected in the wake.

In the far field (Appendix J), the only change is that I becomes

$$I = \frac{d_F}{r_F^3} \left(H_F + \frac{\xi_1 + \xi_2}{2} I_F \right) \quad (\text{K.6})$$

APPENDIX L
B DERIVATIVES AT SECTION EDGES

If the k-th strip is last in a section, the square bracket in Eq. (2.6.30) of Section 2.6.5 is replaced by

$$[DB_{k-2} + EB_{k-1} + FB_k] \quad (L.1)$$

$$D = \frac{w_k}{w_{k-1} + 1/2(w_{k-2} + w_k)} \left(\frac{w_{k-1} + w_k}{w_{k-2} + w_{k-1}} \right)$$

$$E = -4w_k \frac{w_{k-1} + 1/2(w_{k-2} + w_k)}{(w_{k-2} + w_{k-1})(w_{k-1} + w_k)} \quad (L.2)$$

$$F = w_k \frac{w_{k-2} + 3w_{k-1} + 2w_k}{(w_{k-1} + w_k)[w_{k-1} + 1/2(w_{k-2} + w_k)]}$$

If the k-th strip is first in a section, the square bracket is replaced by

$$[DB_k + EB_{k+1} + FB_{k+2}] \quad (L.3)$$

$$D = -w_k \frac{2w_k + 3w_{k+1} + w_{k+2}}{(w_k + w_{k+1})[w_{k+1} + 1/2(w_k + w_{k+2})]}$$

$$E = 4w_k \frac{w_{k+1} + 1/2(w_k + w_{k+2})}{(w_k + w_{k+1})(w_{k+1} + w_{k+2})} \quad (L.4)$$

$$F = - \frac{w_k}{w_{k+1} + 1/2(w_k + w_{k+2})} \left(\frac{w_k + w_{k+1}}{w_{k+1} + w_{k+2}} \right)$$

If a section has only one strip, eliminate the square bracket, i.e.

$$D = E = F = 0 \quad (L.5)$$

If the section has two strips, use

$$D = 0$$

$$E = - \frac{2w_k}{w_{k+1} + w_k} \quad (\text{L.6})$$

$$F = -E$$

for the first strip, and

$$D = \frac{2w_k}{w_k + w_{k-1}} \quad (\text{L.7})$$

$$E = -D$$

$$F = 0$$

for the second strip.

APPENDIX M
CONVERGENCE ACCELERATION SCHEME

After each iteration, a convergence acceleration procedure is invoked in which a new solution is defined in terms of a linear combination of the previous solutions. This appendix will give the details of the calculation of the required linear combination.

Let X^0, X^1, \dots, X^k and $RES^0, RES^1, \dots, RES^k$ be $k + 1$ successive approximations, and their corresponding residual vectors. Since there are $N+L$ unknowns to be solved for, we define the $(N+L) \times (k+1)$ matrix whose columns are the solution vectors

$$[X] = [X^0, X^1, \dots, X^k] \quad (M.1)$$

Similarly, define the residual matrix

$$[RES] = [RES^0, RES^1, RES^2, \dots, RES^k] \quad (M.2)$$

Define the "linear combination vector"

$$\begin{bmatrix} f_0 \\ \cdot \\ \cdot \\ \cdot \\ f_k \end{bmatrix}$$

such that a new approximation X' is given by the matrix product

$$X' = [X] \begin{bmatrix} f_0 \\ \cdot \\ \cdot \\ \cdot \\ f_k \end{bmatrix} \quad (M.3)$$

and the corresponding residual is

$$RES' = [RES] \begin{bmatrix} f_0 \\ \cdot \\ \cdot \\ \cdot \\ f_k \end{bmatrix} \quad (M.4)$$

Note that we can write

$$RES' = R - AX'$$

$$= R - A[X] \begin{bmatrix} f_0 \\ \cdot \\ \cdot \\ \cdot \\ f_k \end{bmatrix}$$

$$= R(1 - \sum_{i=0}^k f_i) + [(R - AX^0), (R - AX^1), \dots, (R - AX^k)] \begin{bmatrix} f_0 \\ \cdot \\ \cdot \\ \cdot \\ f_k \end{bmatrix}$$

$$= R(1 - \sum_{i=0}^k f_i) + [RES^0, RES^1, \dots, RES^k] \begin{bmatrix} f_0 \\ \cdot \\ \cdot \\ \cdot \\ f_k \end{bmatrix} \tag{M.5}$$

Therefore, by choosing

$$f_k = (1 - \sum_{i=0}^{k-1} f_i) \tag{M.6}$$

the first term will disappear, and a new residual is given by

$$RES' = [RES] \begin{bmatrix} f_0 \\ \cdot \\ \cdot \\ \cdot \\ f_{k-1} \\ 1 - f_0 - \dots - f_{k-1} \end{bmatrix} \tag{M.7}$$

Define $(k+1) \times (k+1)$ "modified" unit matrix I_1 by

$$I_1 = \begin{bmatrix} 1 & & & & & & \\ & 1 & & & & & \\ & & 1 & & & & \\ & & & 1 & & & \\ & 0 & & & \cdot & & \\ & & & & & \cdot & \\ & & & & & & \vdots \\ -1 & -1 & -1 & \dots & -1 & & 1 \end{bmatrix} \quad (M.8)$$

from which the linear combination vector can be written:

$$\begin{bmatrix} f_0 \\ \vdots \\ f_k \end{bmatrix} = I_1 \begin{bmatrix} f_0 \\ \vdots \\ f_{k-1} \\ 1 \end{bmatrix} = I_1 \begin{bmatrix} F \\ 1 \end{bmatrix} \quad (M.9)$$

where F is the (k x 1) vector

$$F = \begin{bmatrix} f_0 \\ \vdots \\ f_{k-1} \end{bmatrix}$$

The new residual vector RES' can now be written as a matrix product involving the old residual matrix and the unknown vector F in the form (using Eq. (M.4))

$$RES' = [RES][I_1] \begin{bmatrix} F \\ 1 \end{bmatrix} \quad (M.10)$$

Define the norm of this vector, ||RES'|| by

$$\begin{aligned} ||RES'||^2 &= RES'^T \cdot RES' \\ &= [F^T \ 1] [I_1]^T [RES]^T [RES] [I_1] \begin{bmatrix} F \\ 1 \end{bmatrix} \quad (M.11) \end{aligned}$$

The right-hand side of this equation is a quadratic non-negative (scalar) function of the k unknowns $f_0, f_1 \dots f_{k-1}$. The minimum value must therefore occur at the point at which

$$\frac{\partial}{\partial f_i} ||RES'||^2 = 0 \quad \text{for} \quad i = 0, \dots, k-1.$$

This will therefore provide k linear equations which can be solved to minimize Eq. (M.11).

Calculation of Partial Derivatives of $||RES'||^2$

First define the symmetric matrix P by

$$P = [RES]^T [RES]$$

i.e. $P = [P_{ij}]$, where $P_{ij} = RES^i \cdot RES^j$ (M.12)

(scalar product of i^{th} and j^{th} residual vectors). Now partition the matrix P in the following manner:

$$P = \begin{bmatrix} P_{11} & P_{12} \\ (k \times k) & (k \times 1) \\ P_{12}^T & P_{22} \\ (1 \times k) & (1 \times 1) \end{bmatrix} \quad (M.13)$$

so that P_{11} = scalar products between all of the residuals $RES^0 \dots RES^{k-1}$, while P_{12} consists of scalar products between latest residual RES^k , and all of earlier residuals, $RES^0 \dots RES^{k-1}$, and P_{22} is scalar $||RES^k||^2$.

Next define the symmetric matrix Q by

$$Q = [I_1]^T [P] [I_1], \quad (M.14)$$

and again partition the matrix Q to separate the last row and column:

$$Q = \begin{bmatrix} Q_{11} & Q_{12} \\ (k \times k) & (k \times 1) \\ Q_{12}^T & Q_{22} \\ (1 \times k) & (1 \times 1) \end{bmatrix} = \begin{bmatrix} & -1 \\ & \vdots \\ & -1 \\ [0 \dots 0] & 1 \end{bmatrix} \begin{bmatrix} P_{11} & P_{12} \\ P_{12}^T & P_{22} \end{bmatrix} \begin{bmatrix} & 0 \\ & \vdots \\ & 0 \\ [-1 \dots -1] & 1 \end{bmatrix} \quad (M.15)$$

Straightforward matrix multiplication can show that:

$$Q_{11} = P_{11} + P_{12}[-1]^T + [-1]P_{12}^T + P_{22}[-1][-1]^T \quad (M.16)$$

or $q_{11_{ij}} = p_{11_{ij}} - p_{12_i} - p_{12_j} + p_{22}$

and

$$Q_{12} = P_{12} + P_{22}[-1] \quad (M.17)$$

or

$$q_{12_i} = p_{12_i} - p_{22}$$

and

$$Q_{22} = P_{22}$$

Eq. (M.11) now can be written

$$\|RES'\|^2 = [F^T \quad 1] \begin{bmatrix} Q_{11} & Q_{12} \\ Q_{12}^T & Q_{22} \end{bmatrix} \begin{bmatrix} F \\ 1 \end{bmatrix} \quad (M.18)$$

and partial differentiation of this expression with respect to f_0, f_1, \dots, f_{k-1} provides a set of k linear equations:

$$Q_{11}F + Q_{12} = 0 \quad (M.19)$$

or

$$Q_{11}F = -Q_{12}$$

the solution of which provides the unknown k acceleration coefficients.

Given this solution, we can define the acceleration vector

$$F' = \begin{bmatrix} f_0 \\ \vdots \\ f_{k-1} \\ 1 - f_0 \cdots -f_{k-1} \end{bmatrix} \quad (\text{M.20})$$

from which the new solution X' is given by

$$\begin{aligned} X' &= [X]F' \\ \text{and} \\ \text{RES}' &= [\text{RES}]F' \end{aligned} \quad (\text{M.21})$$

APPENDIX N
THE COMPRESSIBILITY CORRECTION

The user inputs the average incompressible velocity \bar{V}_i , which should correspond to physical conditions in the region of interest. If $\bar{V}_i > a_*'$, \bar{V}_i is set equal to a_*' and the average density ratio ϵ is

$$\epsilon = \frac{\bar{\rho}}{\rho_t} = 0.6339 \quad (\text{N.1})$$

If this occurs the point is labeled "choked" on the output.

If $\bar{V}_i < a_*'$, it is used as it stands to compute $(\bar{\rho}/\rho_t)$ by an iterative procedure. The iterative equation is

$$\epsilon = \left[1 - \frac{1}{5} \left(\frac{\bar{V}_i}{a_t} \right)^2 \frac{1}{\epsilon} \right]^{2.5} \quad (\text{N.2})$$

with initial value $\epsilon = 1$.

Finally, the compressible velocity magnitude V is calculated from

$$V = V_i' \left(\frac{1}{\epsilon} \right)^m, \quad m = \frac{V_i'}{\bar{V}_i} \quad (\text{N.3})$$

where V_i' is the magnitude of the local equivalent incompressible velocity (Section 3.3). The direction of local velocity is not changed.

It will be seen in Appendix O, Eq. (O.20), that an equivalent incompressible average velocity V_c' is computed at the control station. For compatibility at the control station, the input should insure that

$$\bar{V}_i = V_c' \quad (\text{N.4})$$

or the computed surface Mach number will not agree with that input for the control station. (This is also the default.) This seemingly contradictory flexibility is allowed to improve results if the region of interest is far from the control station..

APPENDIX O
OPTIONS OF THE COMBINATION PROGRAM

0.1 Incompressible Option

If the flow is incompressible, this option is selected and only the following quantities are input:

- V_{∞} freestream velocity
- V_c average velocity at the control station
- V_{ref} reference velocity used in computing pressure coefficient
- α angle of attack
- β angle of yaw

0.2 Freestream Conditions

For compressible flow the freestream conditions are defined by inputting angle of attack α , angle of yaw β , and three additional quantities:

- either velocity V_{∞} or Mach number M_{∞}
- either total pressure P_t or static pressure P_s
- either total temperature T_t or static temperature T_s

Then the preliminary calculations are as follows:

0.2.1 M_{∞} Input

(a) If P_t is input, P_s is given by

$$P_s = P_t \left(1 + \frac{1}{5} M_{\infty}^2\right)^{-3/5} \quad (0.1)$$

If P_s is input, P_t is given by

$$P_t = P_s \left(1 + \frac{1}{5} M_\infty^2\right)^{3/5} \quad (0.2)$$

If neither is input, the default is

$$P_t = 2116.23 \quad (0.3)$$

and P_s is as above.

(b) If T_t is input, T_s is given by

$$T_s = T_t \left(1 + \frac{1}{5} M_\infty^2\right)^{-1} \quad (0.4)$$

If T_s is input, T_t is given by

$$T_t = T_s \left(1 + \frac{1}{5} M_\infty^2\right) \quad (0.5)$$

If neither is input, the default is

$$T_t = 518.67 \quad (0.6)$$

and T_s is as above.

In either case stagnation and freestream sound speeds a_t and a_s are calculated from

$$a_t = 49 \sqrt{T_t}, \quad a_s = 49 \sqrt{T_s} \quad (0.7)$$

and V_∞ from

$$V_\infty = a_t M_\infty \left(1 + \frac{1}{5} M_\infty^2\right)^{-1/2} \quad (0.8)$$

0.2.2 V_∞ Input

(a) If T_t is input, a_t is given by

$$a_t = 49 \sqrt{T_t} \quad (0.9)$$

M_∞ is then calculated from

$$M_\infty = \frac{V_\infty}{a_t} \left[1 - \frac{1}{5} \left(\frac{V_\infty}{a_t}\right)^2 \right]^{-1/2} \quad (0.10)$$

The remainder of the calculation proceeds as in 0.2.1 above.

(b) If T_s is input, a_s is given by

$$a_s = 49 \sqrt{T_s} \quad (0.11)$$

and M_∞ by

$$M_\infty = V_\infty / a_s \quad (0.12)$$

The remainder of the calculation proceeds as in 0.2.1 above.

0.2.3 Additional Freestream Quantities

Built into the program are constants

$$g = 32.174$$

$$R = 1715.63$$

The following quantities are calculated:

Total density:	$\rho_t = \frac{P_t}{RT_t}$	
Static density:	$\rho_s = \frac{P_s}{RT_s}$	(0.13)
Dynamic pressure:	$q_\infty = 0.7 P_t \left(\frac{P_s}{P_t}\right) M_\infty^2$	
Pressure ratio:	P_s / P_t	
Density ratio:	ρ_s / ρ_t	
Temperature/sea-level ratio:	$\theta = \frac{T_t}{518.67}$	(0.13)
Pressure/sea-level ratio:	$\delta = \frac{P_t}{2116.23}$	

Critical speed: $a_* = a_t / \sqrt{1.2}$

Maximum velocity: $V_{\max} = \sqrt{5} a_t$

Equivalent incompressible freestream velocity: $V'_\infty = V_\infty \left(\frac{\rho_s}{\rho_t} \right)$

Equivalent incompressible critical velocity: $a'_* = 0.6339 a_*$

0.2.4 Summary

Three freestream conditions are input: V_∞ or M_∞ , P_t or P_s , T_t or T_s (or default values). Calculated and saved are

$$\begin{aligned} &V_\infty, M_\infty, P_t, P_s, T_t, T_s, a_t, a_s \\ &\rho_t, \rho_s, q_\infty, P_s/P_t, \rho_s/\rho_t, \theta, \delta \\ &a_*, V_{\max}, V'_\infty, a'_* \end{aligned} \tag{0.14}$$

Nineteen quantities all together.

0.3 Control Station Conditions

Input consists of one of the following three quantities:

\dot{W} inlet mass flow rate

V_c average velocity

M_c average Mach number

The remaining two must be calculated plus some additional quantities.

0.3.1 V_c Input

ρ_c is given by

$$\rho_c = \rho_t \left[1 - \frac{1}{5} \left(\frac{V_c}{a_t} \right)^2 \right]^{2/5} \quad (0.15)$$

\dot{w} by

$$\dot{w} = g \rho_c V_c \frac{A_{FP}(k)}{144} \quad (0.16)$$

and M_c by

$$M_c = \frac{V_c}{a_t} \left[1 - \frac{1}{5} \left(\frac{V_c}{a_t} \right)^2 \right]^{-1/2} \quad (0.17)$$

0.3.2 M_c Input

V_c is given by

$$V_c = a_t M_c \left(1 + \frac{1}{5} M_c^2 \right)^{-1/2} \quad (0.18)$$

Then ρ_c and \dot{w} are obtained as in 0.3.1 above.

0.3.3 \dot{w} Input

Here V_c must be calculated iteratively by solving the equation

$$V_c = \frac{\dot{w}}{g(A_{FP}(k)/144)\rho_t \left[1 - 1/2(V_c/a_t)^2 \right]^{2.5}} \quad (0.19)$$

starting with $V_c = 0$.

Once V_c is known, M_c and ρ_c are obtained as in 0.3.1 above.

0.3.4 Additional Control Station Quantities.

These are calculated as follows:

$$\begin{aligned} \text{Pressure ratio:} & \quad (P_c/P_t) = \left[1 - \frac{1}{5} \left(\frac{V_c}{a_t} \right)^2 \right]^{3.5} \\ \text{Density ratio:} & \quad \rho_c/\rho_t \\ \text{Dynamic pressure:} & \quad q_c = 0.7 P_t \left(\frac{P_c}{P_t} \right) M_c^2 \\ \text{Velocity ratio:} & \quad V_\infty/V_c \\ \text{Corrected mass flow:} & \quad \dot{w}_{cor} = \dot{w} \frac{\sqrt{\theta}}{\delta} \\ \text{Equivalent incompressible average velocity:} & \quad V'_c = V_c \left(\frac{\rho_c}{\rho_t} \right) \end{aligned} \tag{0.20}$$

0.3.5 Summary

One quantity, \dot{w} , V_c , or M_c is input. Quantities saved are

$$\dot{w}, V_c, M_c, \rho_c, (P_c/P_t), (\rho_c/\rho_t), q_c, (V_\infty/V_c), \dot{w}_{cor}, V'_c \tag{0.21}$$

a total of ten quantities.

APPENDIX P
ORGANIZATION OF THE INPUT POINTS

The input to this program consists of the coordinates of a number of points. These points define the surface of the three-dimensional inlet around which the flow is to be computed. For the purpose of organizing these points for computation, each point is assigned a pair of integers, m and n . These integers need not be input, but their use must be understood to insure the correctness of the input and to facilitate the interpretation of the output.

For each point, n identifies the "column" of points to which it belongs, while m identifies its position in the "column," i.e., the "row." The first point of a "column" always has $m = 1$. To insure that the program will compute outward normal vectors, the following condition must be satisfied by the input points. If an observer is located in the flow and is oriented so that locally he sees points on the surface with m values increasing upward, he must also see n values increasing toward the right. Examples of correct and incorrect input are shown in Fig. 34(a). In this figure the flowfield lies about the paper, while the interior of the body lies below the paper. Occasionally, it happens that despite all care a body is input incorrectly. If the entire body is input incorrectly - not some sections correctly and some incorrectly - the difficulty can be remedied by changing the sign of one coordinate of all the input points. This trick will give a correctly input body of the proper shape at perhaps a peculiar location. Otherwise, the input will have to be done over. If the inlet is input correctly (Step 2), but a cross-section (Step 4) is input so that its normal vector points upstream, the combined flow will be correct, but the flux at the cross section will be negative. Clearly a control station with the wrong normal vector invalidates the calculation (Step 4).

The body surface is imagined divided into sections, which may be actual physical divisions or may be selected for convenience. A section is defined as consisting of a group of at least two n -lines. Within each section the n -lines are input in order to increasing n . On each n -line the points are input in order of increasing m . All n -lines in a section must have the same number of points, but this may vary from section to section. The first n -line of the first section is $n = 1$. From then on the n -lines may be thought of as numbered

continuously through all sections, i.e., the numbering is not begun over at the beginning of each section. Elements will be formed that are associated with points on every n-line except those that are last in their respective sections. Points on these latter n-lines are used only to form elements associated with points on the next lowest n-lines.

To illustrate this procedure, consider the plan view of a body shown in Fig. 34(b). This body has been divided into four sections, as shown in the figure. The first section contains four n-lines, $n = 1, 2, 3, 4$; the second, five n-lines, $n = 5, 6, 7, 8, 9$; the third three n-lines, $n = 10, 11, 12$; and the fourth three n-lines; $n = 13, 14, 15$. The number of points on each n-line are:

$$\begin{aligned} \text{Section} &= 1 \ 2 \ 3 \ 4 \\ M &= 4 \ 7 \ 4 \ 2 \end{aligned}$$

Notice that the line $n = 4$ has only four points, the points $m = 1, 2, 3, 4$ and the m-grid of Section 1, which is listed in the figure along the $n = 1$ line. The lines $n = 4$ and $n = 5$ are physically identical. Some of the points on the two lines are physically identical but correspond to different values of m . This is of no consequence. In this scheme sections are completely independent. No elements are computed corresponding to points on lines $n = 4, 9, 12, 15$.

There is no restriction that the m and n lines of different sections have to be roughly parallel. The arrangement shown in Fig. 34(c) is permissible.

1. Report No. NASA CR-174975		2. Government Accession No.		3. Recipient's Catalog No.	
4. Title and Subtitle CALCULATION OF COMPRESSIBLE FLOW ABOUT THREE-DIMENSIONAL INLETS WITH AUXILIARY INLETS, SLATS AND VANES BY MEANS OF A PANEL METHOD				5. Report Date June 1985	
				6. Performing Organization Code	
7. Author(s) J.L. Hess, D. M. Friedman and R. W. Clark				8. Performing Organization Report No. MDC J3789	
9. Performing Organization Name and Address Douglas Aircraft Company McDonnell Douglas Corporation 3855 Lakewood Blvd., Long Beach, CA 90845				10. Work Unit No.	
				11. Contract or Grant No. NAS3-22250	
12. Sponsoring Agency Name and Address National Aeronautics and Space Administration Lewis Research Center Cleveland, Ohio 44135				13. Type of Report and Period Covered Final Contractor Report 2/17/83 - 8/15/85	
				14. Sponsor. Agency Code	
15. Supplementary Notes Final Report. Project Manager: Danny P. Hwang, Propulsion Aerodynamics Division NASA Lewis Research Center, Cleveland, OH 44135					
16. Abstract An efficient and user-oriented method has been constructed for calculating flow in and about complex inlet configurations. Efficiency is attained by: the use of a panel method, a technique of superposition for obtaining solutions at any inlet operating condition, and employment of an advanced matrix-iteration technique for solving large full systems of equations, including the nonlinear equations for the Kutta condition. User concerns are addressed by the provision of several novel graphical output options that, taken together, yield a more complete comprehension of the flowfield than had been possible previously. Examples of these features are presented for some complicated configurations.					
17. Key Words (Suggested by Author(s)) Aerodynamics Graphical Display Auxiliary Inlets Inlets Compressible Flow Panel Method Computer Program Potential Flow Flowfield Lifting				18. Distribution Statement Unclassified - Distribution Unlimited	
19. Security Classif. (of this report) Unclassified		20. Security Classif. (of this page) Unclassified		21. No. of Pages 197	22. Price*

* For sale by the National Technical Information Service, Springfield, Virginia 22151

**END
DATE
FILMED**

NOV 19 1985